Functionality of solid-contact ISEs with physically damaged ion-selective membranes:

a comparison between potentiometric, coulometric and amperometric methods

Åbo Akademi University

Faculty of Science and Engineering

Rustem Rustem

Master's programme in Excellence in Analytical Chemistry

Degree project in Analytical Chemistry, 30 credits

Student number: 2002156

Supervisor: Zekra Mousavi (Åbo Akademi University)

Cosupervisors: Johan Bobacka (Åbo Akademi University)

Agnes Heering (University of Tartu)

August 2021

Abstract

In this thesis, a novel ion-to-electron signal transduction method was applied for checking the functionality of chloride and potassium solid-contact ISEs with physically damaged ion-selective membranes (ISMs). The potentiometric response was compared with amperometric and coulometric methods before and after damaging the ISMs. Poly(3,4-ethylenedioxythiophene) (PEDOT) were used as solid-contact doped with chloride anions (Cl^-), *i.e.,* PEDOT(Cl) and PEDOT doped with poly(styrene sulfonate) (PSS), *i.e.,* PEDOT(PSS). Sequential addition/dilution in concentration was recorded by using potentiometric, amperometric and coulometric signal transduction methods.

Potentiometric measurements carried out before and after damaging the ISM demonstrated the functionality of chloride ISEs, i.e., the potentiometric calibration curve showed acceptable slopes before and after damaging of ISMs. The coulometric measurement results showed a very similar response for every increase/decrease in concentration, showing stable accumulation of charge but with steady perceptible drift in the response. This drift was also noticed in potentiometry. The amperometric results depicted a significant increase in baseline noise, after the ISM had been damaged, thereby clearly proving that chloride ISEs are not functioning properly.

In the case of potassium SC-ISEs, all (potentiometric, coulometric and amperometric) measurements with and without BGE after damaging the ISM demonstrated inadequate and not comprehensible responses, proving that the ISEs were not functioning after damaging the ISM. However, some response was still observed for every stepwise addition in concentration when measured without any background electrolyte (BGE). The non-functionality was also proven by potentiometric calibration curves clearly showing non-Nernstian responses after electrodes had been damaged both with/without BGE. Based on the above results it can be concluded that the amperometric method is a reliable and suitable method for examining the SC-ISEs for their functionality.

The electrochemical impedance spectra for chloride and potassium SC-ISEs showed a high-frequency semicircle originating from the ISM. After damaging the ISM, the high-frequency semicircle in both chloride and potassium SC-ISEs disappeared. Thus, impedance measurements could also be used to prove that ISMs were damaged.

Keywords: Amperometry, coulometry, potentiometry, ion-to-electron signal transduction, solid-contact ion-selective electrodes, ion-selective membrane, impedance spectra.

Preface

This master's thesis was performed at the Åbo Akademi University, under the Erasmus Mundus joint master's degree programme – Excellence in Analytical Chemistry.

My first gratitudes to Professor Johan Bobacka for offering me such an interesting at the same time challenging topic. Thank you very much for your helpful supervision. Special thanks to my supervisor Dr Zekra Mousavi for your truly extended guidance throughout the whole project. Your effort and contribution are highly appreciated. I am very grateful to my co-supervisor Dr Agnes Heering for your thoughtful comments on my thesis.

Many thanks to Professor Ivo Leito, you truly care about your students and your classes were very helpful and fascinating. Many thanks to Anu Teearu, I sincerely appreciate the time you spent backing us during our studies.

I am also grateful to my parents and friends who gave support when I most needed it. None of it would have been possible today if you hadn't been so helpful and encouraging.

Contents

Abbreviation list

AD – after damaging

BD – before damaging

CV – cyclic voltammetry

Cl^--SC-ISE – chloride-selective solid-contact ion-selective electrode

CP – conducting polymer

DOS – bis(2-ethylhexyl) sebacate

EDOT – 3,4–ethyledioxythiophene

ETH 500 – Tetradodecylammonium tetrakis (4-chlorophenyl)borate

EIS – electrochemical impedance spectroscopy

GC – glassy carbon

ISM – ion-selective membrane

ISE – ion-selective electrode

K^+-SC-ISE – potassium-selective solid-contact ion-selective electrode

KCl – potassium chloride

KTFPB – potassium tetrakis [3.5-bis(trifluoromethyl)phenyl)]borate

NaCl – sodium chloride

NaPSS – poly(sodium 4-styrenesulfonate)

o-NPOE – 2-nitrophenyloctyl ether

PEDOT – Poly(3,4-ethylenedioxythiophene)

PEDOT(PSS) – Poly(3,4-ethylenedioxythiophene) doped with PSS

PEDOT(Cl) – Poly(3,4-ethylenedioxythiophene) doped with chloride

PVC – poly(vinylchloride)

SC-ISE – solid-contact ion-selective electrode

TDMACl – tridodecylmethylammonium chloride

THF – tetrahydrofuran

Introduction

The field of use of ion-selective electrodes (ISEs) is tremendously wide, especially in clinical diagnostics, environmental monitoring, process control and many other branches. The use of ISEs is highly beneficial in comparison with other conventional analytical techniques because they can provide a relatively cheap, accurate, fast and selective determination of a wide range of ionic species [1, 2].

For instance, the identification and quantification of physiologically important ions in the blood (K^+, Na^+, Mg^{2+}, Cl^- and Ca^{2+}) play an essential role in medicine. The goal of analytical chemists is to meet the needs, develop and refine new low-cost, rapid and accurate ISEs [3]. Advantages of the miniaturized, reliable, robust and maintenance-free sensors led to the manufacturing of a solid-state ISE based on conducting polymer as the ion-to-electron transducer [4].

The key element in a potentiometric ion sensor or ISE is the ion-recognition element, i.e. the ion-selective membrane (ISM). The main parameter determining the response of the ISE is the interaction between the ion-recognition element and target ions. This response is converted into a potential signal which is measured under zero current condition [5].

While conducting measurements with remotely controlled ISEs in real use, one might not be aware that an electrode is damaged and demonstrates not precise or even ambiguous results. The key point is to gather the information about the state of the electrode as much as possible, so one could draw a more reliable and adequate conclusion from the analysis. Such information can be very useful for evaluating the performance of sensors used in remotely controlled measurements as any deterioration in the response of the sensors can be easily recognized and fixed in time.

Chloride and potassium solid-contact ion-selective electrodes (SC-ISEs) were prepared using, as solid contact, the conducting polymer poly(3,4-ethylenedioxythiophene) doped with chloride (Cl^-) and polystyrene sulfonate, respectively. The sensors were characterized and mainly studied using potentiometric, chronocoulometric and chronoamperometric methods before and after damaging the ion-selective membranes of the sensors. Results from the potentiometric, amperometric and coulometric measurements before and after damaging of the membrane are compared to see whether these analysis methods can be used to evaluate the condition of the SC-ISE.

1 Theoretical background

1.1 Chemical sensors

A chemical sensor is a special tool that converts chemical information, i.e. total concentration or defined analyte concentration in the sample into an electronic signal. The whole process consists of two main steps: molecular recognition and signal transduction. The molecular recognition part is the part where the chemical reaction takes place, producing a specific signal such as a mass change, increase in temperature or color etc. The signal transduction element converts the obtained information into a measurable signal. The latter corresponds to the quantity present in the sample [6]. The signal transducers can be divided into four types (Figure **1**): optical, electrochemical, mass, and thermal [7].

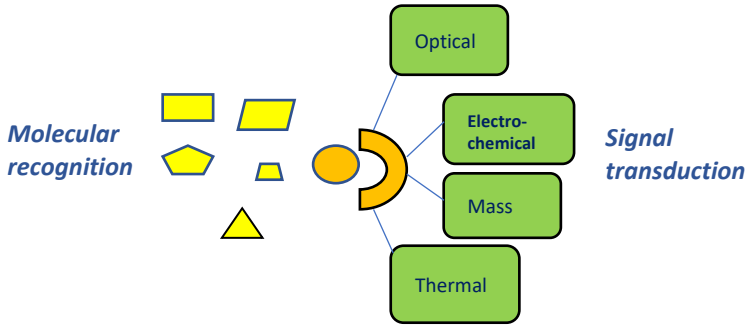

Figure 1. Schematic illustration of the components of chemical sensor and signal transduction type.

The molecular recognition part is in charge of being selective towards a certain analyte. In ideal cases, one molecular recognition part is specific for only one molecular species. Unfortunately, this is not the case in reality; rather, certain molecular recognition parts can be more selective to a given molecular species in comparison to others. The latter ones are called interfering molecular species [6].

1.2 Solid Contact Ion Selective electrodes

In the group of electrochemical sensors, there is an important subgroup called potentiometric sensors or they can also be called ISEs [8]. The practical application of ISEs is broad for several reasons such as low cost, low energy consumption, portability, and small size. The working principle of an ISE is based on a polymeric membrane containing an ionophore, which is selective to the defined inorganic or organic ions, and the ability to transduce the information from the recognition process into an electrical signal [2].

Solid-contact ion-selective electrodes (SC-ISEs) have exceptionally huge advantages when compared to conventional ion-selective electrodes where a liquid solution is used for ion-to-electron transduction. In SC-ISEs, a conducting polymer (CP) is often used as an ion-to-

electron transducer, which makes them maintenance-free, and easy to miniaturize [7], [9]. The conventional ISE is schematically illustrated in Figure 2a, where poly (vinyl chloride) (PVC)-based ion-selective membrane (ISM) is attached to the end of the electrode which is in its turn filled with an internal filling solution. The solution should contain an ion that is going to be measured and acts as a charge carrier between the membrane and the inner reference electrode.

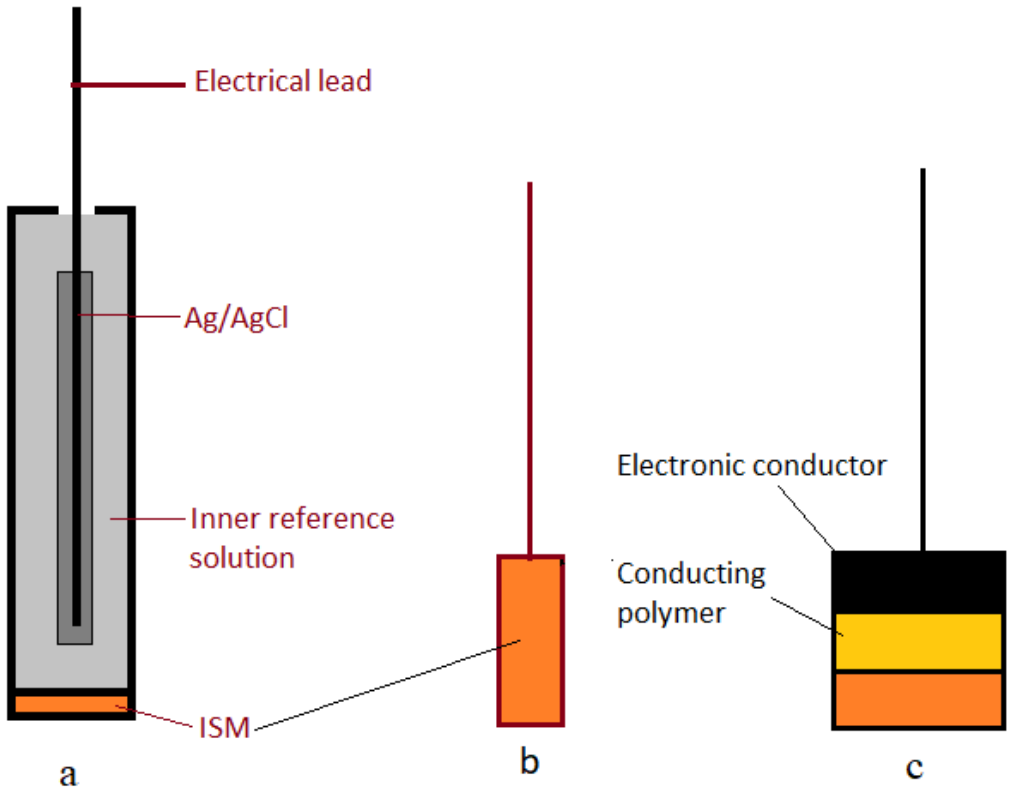

Figure 2. Schematic illustration of a) conventional ion selective electrode (ISE); b) coated wire electrode (CWE); c) Solid-contact ion selective electrode (SC-ISE)

A new generation of electrodes is the coated-wire electrode (CWE) invented by Catrall and Freiser [10]. Since this invention, the development in the construction of all-solid-state ion-selective electrodes is constantly evolving. The CWE is schematically demonstrated in Figure *2*b, where the ISM is deposited on a solid conductor, such as glassy carbon, silver, copper, or platinum wire, etc. However, along with advantages such as low cost, simplicity of the design, flexibility and miniaturization, there were some prominent drawbacks related to this structure such as poor adhesion of ISM onto the solid conductor and low potential stability of the electrode. The use of CP (discussed more in detail in chapter 1.4) in the preparation of ISEs has led to the creation of a maintenance-free all-solid-state ion-selective electrode. The conducting polymer functions as an ion-to-electron transducer between the ion-selective membrane and electronic conductor as shown in equation 1 below:

$$P^+A^- + e^- \leftrightarrow P + A^- \quad (1)$$

where: P^+ and P are the conducting polymer's oxidized and neutral forms, respectively and A^- is an anion.

The conducting polymer can be deposited either physically or electrochemically onto a solid electronic conductor. Then, an ISM is applied on top of the conducting polymer; the resulted electrode is called solid-contact ion-selective electrode (SC-ISE) (Figure 2c). The whole process of selectivity is due to the interaction between the analyte and the ISM (ion recognition part). This type of electrode shows high potential stability in comparison with CWEs and similar results in comparison with conventional electrodes. Different types of conducting polymers can be used in the fabrication of SC-ISEs. Some of the most prominent representatives are poly(3,4-ethylenedioxythiophene) (PEDOT) [11], polypyrrole [12] and polyaniline [13].

1.3 Polyvinyl chloride-based membrane and its components

PVC–based ISM is one of the most popular ISMs which has many advantageous physico-chemical properties. PVC allows the integration of different types of ionophores [14, 15]. In general, a PVC-based ISM mostly consists of four main components: plasticizer, PVC, ionophore and/or a small amount of lipophilic salts. Everything is dissolved in an organic solvent such as tetrahydrofuran [16].

PVC holds all components of the membrane together. Plasticizers increase the dielectric constant as well as the membrane's homogeneity, flexibility and mechanical properties. Plasticizers likewise provide the ISM with liquid properties, thereby alleviating an ion exchange through the membrane and decreasing the hydrophobic properties [6]. Broadly used representatives among plasticizers are bis(2-ethylhexyl)sebacate (DOS) and 2-nitrophenyl octyl ether (o-NPOE) [6], [17].

Lipophilic salts reduce the interference from counter ions in the sample. Additionally, they reduce the electrical resistance, thereby increasing the sensitivity of ISEs with the ionophore [18]. Widely used lipophilic salts for neutral ionophore-based cation-selective ISEs are: potassium tetrakis[3,5-bis(trifluoromethyl)phenyl)]borate and potassium tetrakis(4-chlorophenyl)borate [19, 20].

The ionophore plays a role as molecular recognition part in the membrane. Due to its physicochemical properties and ability to interact with the target ion, such as ionic interaction and size exclusion, the membrane-based ISE selectively binds a specific ion in the sample solution. The ionophore can be charged or neutral. The neutral ionophores do not have any

charge and by creating ion-to-ionophore complexes they selectively bind to ions of interest [16]. In this work, the neutral ionophore Valinomycin (Figure 3a) was used for preparing potassium-ion selective electrodes [21]. In the composition of the chloride ion-selective electrodes (Cl^--ISEs) studied in this thesis, the ion-exchanger – tri-dodecyl methylammonium chloride (Figure 3b) is used instead of the ionophore [20], [22].

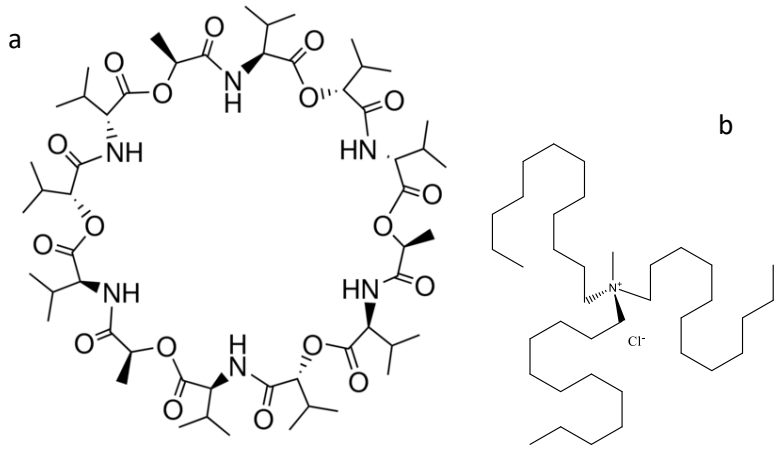

Figure 3. Molecular structure of the neutral ionophore – valinomycin [23] **(a) and tridodecylmethylammonium chloride (ion-exchanger used in Cl^- ISEs) (b).**

1.4 Electrically conducting polymers

1.4.1 General overview

The discovery of polyacetylene's electrical conductivity properties is considered to be the starting point of the development of semiconducting polymers. Some conducting polymers that attracted high attention from the both scientific and practical point of view are polythiophene, polypyrrole, poly(paraphenylene) and poly(3,4-ethylenedioxythiophene) are shown in Figure ***4***.

Conducting polymers exhibit excellent and tunable properties, making them a great alternative as an ion-to-electron transducer in the sensor technology sector. The simplicity in fabrication as well as being relatively low-cost material made conducting polymers suitable candidates to be used for the mass production of disposable miniaturized electrodes [24]

.

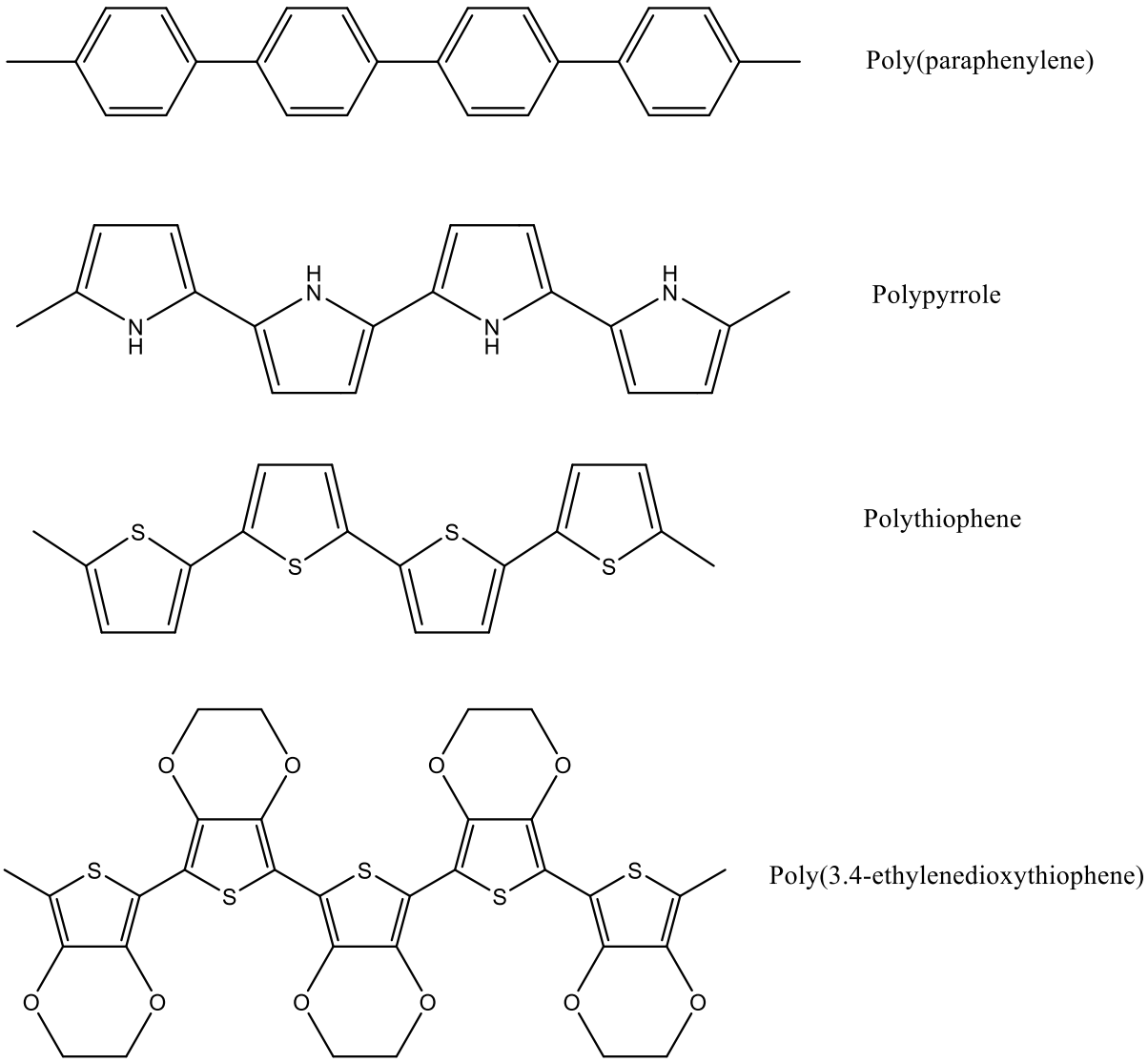

Figure 4. The molecular structure of common conjugated polymers

1.4.2 Synthesis of conducting polymers

Polymerization of conducting polymers is divided into chemical and electrochemical polymerization. Chemical polymerization is suitable for mass production and is much cheaper. However, chemical polymerization is not the right choice to produce a thin film.

Electrochemical methods have many advantages due to the simplicity and reproducibility of the process and therefore is the preferred method in various applications [25]. In electrochemical polymerization two or three electrodes are used, auxiliary and working or auxiliary, working and reference electrodes, respectively. The electrodes are mounted in an electrochemical cell containing electrolyte and the monomer dissolved in a solvent. When the polymerization starts, the conducting polymer film is deposited gradually on the surface of the working electrode to produce a polymer layer with the proper thickness [26].

The polymerization reaction takes place at the working electrode surface and the thickness of the film is controlled by the polymerization time. The electrochemical polymerization is performed using three main modes: galvanostatic, potentiostatic and potentiodynamic polymerization. The most common method is galvanostatic electrochemical polymerization where a constant current is applied. In potentiostatic polymerization, a constant potential is used. In potentiodynamic polymerization, the applied potential is varied, and, as a result of this, a more stable and homogeneous polymer film is obtained [25], [27].

1.4.3 Doping of conducting polymers

The term band gap (energy gap) is the energy difference between the conduction and valence bands. In conductors, the valence and conduction bands overlap, and that is why the conductivity of these materials is so high and only a little energy is required to move the electron between two bands. Semiconductors and insulators have an energy gap as demonstrated in Figure 5 [28].

In conducting polymers, the valence band is filled but conduction bands are empty. The energy gap is too high for the electron to be thermally excited from the valence band to the conduction band and, as a consequence, the conductivity is low. Doping is the process to increase the conductivity of the conjugated polymers by creating new energy levels to make the electron transfer possible. It means that electrons should be either removed from or inserted in the material; these processes are called p-doping or n-doping, respectively [29].

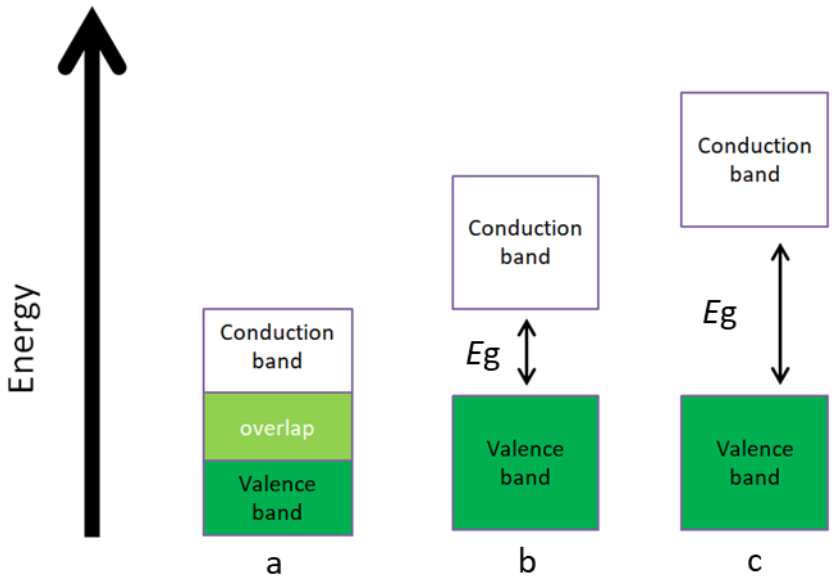

Figure 5. Overview of the bandgap (E_g) in a) metals; b) semiconductors; c) insulators

The range of conductivities of conjugated polymers is comparable with the range of semiconductors locating between the insulators and metals, ranging from 10^{-10} to 10^{6} Sm^{-1}. The range of conductivity depends on the doping level of conjugated polymers as well as the type of polymer used. Both chemical and electrochemical doping methods are used. The level of doping can be controlled in the electrochemical method by the voltage applied. By applying a determined potential, the polymer is oxidized (p-doping, equation 2) or reduced (n-doping, equation 3) accompanied by insertion of charge-compensating anions and cations, respectively:

$$P + A^- \rightarrow P^+A^- + e^- \qquad \text{p-doping} \qquad (2)$$

$$P + e^- + C^+ \rightarrow P^-C^+ \qquad \text{n-doping} \qquad (3)$$

P is the neutral form of the polymer, P^+ is the oxidized form and P^- is the reduced form. A^- and C^+ are the counter ions [30].

1.4.4 Poly(3,4-ethylenedioxythiophene) (PEDOT)

Many research works have been done on thiophene-based conducting polymers such as poly(3,4-ethylenedioxythiophene) (Figure 4). PEDOT can be synthesized from the monomer 3,4-ethylendioxythiophene (EDOT) with the chemical and electrochemical polymerization methods. The electrochemical method is more beneficial both in terms of time and the required amount of monomer. PEDOT is synthesized electrochemically using electrolyte salts by galvanostatic, potentiostatic and cyclic voltammetric methods.

Due to its fascinating properties, PEDOT (Figure 4) is considered one of the most important polythiophene derivative. It has high conductivity (in the p-doped state), low oxidation potential and energy gap, as well as good environmental stability. Above mentioned properties of PEDOT make it attractive to use as semiconducting material in SC-ISEs.

However, PEDOT itself is insoluble in water and to make it soluble during polymerization poly(styrene sulfonic acid) (PSS) was utilized as a charge-balancing dopant. Eventually, dark blue PEDOT(PSS) is obtained, which is soluble in water [31]. PEDOT(PSS) polymer, which is also called Baytron P, has a wide range of manufacturing fields such as electrode material for capacitors [32], rechargeable batteries [33], photovoltaic devices [32], and many other applications.

1.5 Potentiometry

An ISE is an example of an electrochemical sensor using the principles of potentiometry. The potential of an indicator electrode (ISE) cannot be measured directly by itself. It is measured against the reference electrode at equilibrium conditions. The working principle of the ISE is

that when the membrane comes into contact with the analyte it converts the activity of the target ion into an electrical potential. As stated by the Nernst equation this potential is linearly dependent on the logarithm of the ionic activity [6], [34]. The set-up for a potentiometric measurement using a conventional ISE is depicted in Figure 6.

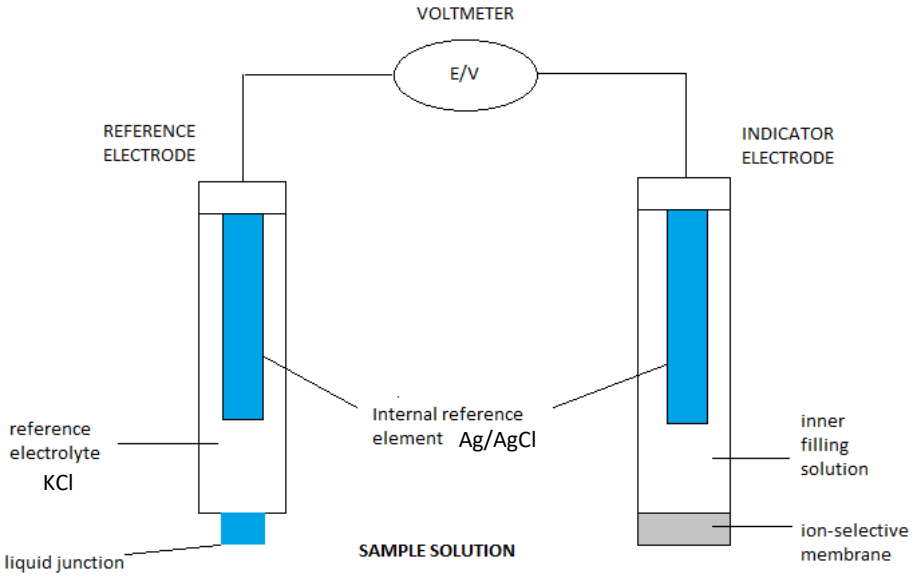

Figure 6. Schematic illustration of an electrochemical cell for potentiometric measurements.

A reference electrode such as Ag/AgCl electrode consists of the metal wire electrode sheeted with the same salt of that metal submerged into the concentrated solution with the same anion of this salt. This is kind of structure procures the potential stability of the reference electrode [34].

The resulted cell potential (E_{ind}) is governed by Nernst equation (5) [17], [34] shown below:

$$E = const + \frac{RT}{n_i F} lna_i + E_j \qquad (5)$$

where:

- *const* includes all potential contributions other than ISM, e.g., reference electrode potential and standard potential of indicator electrode,
- T is the temperature (K),
- R and F are the universal gas constant and the Faraday constant, respectively,
- a_i is an activity of the target ion,
- n_i is the charge of the target ion,
- E_j is the liquid junction potential.

The liquid junction potential is the potential that develops at the interface between two different solutions and can be calculated with the Henderson formula if the solvent is the same. In most cases, liquid junction potential at the reference electrode can be sufficiently eliminated if the junction potential is kept constant during calibration and measurement [30, 31].
The slope of the calibration curve where potential is plotted versus the logarithm of the activity of the ion for a single charged cation would be 59.2 mV or $59.2/n_i$ mV for others at 25 °C and negative for anions. Another issue to be considered is the determination of the ion activity using equation (6) below:

$$a_i = \gamma_i c_i \tag{6}$$

where,

- c_i is the concentration of the target ion,
- γ_i is the activity coefficient of the ion.

The activity coefficient, which strongly depends on the ionic strength of the solution, can be calculated using the Debye–Hückel [35] equation at low ionic strength (J < 0.1 mol kg^{-1}) (7):

$$log\gamma_i = \frac{An_i^2\sqrt{J}}{1+a_{Kjel}B\sqrt{J}} \tag{7}$$

where:

- J is the ionic strength,
- A and B are constants where in the case of aqueous solutions at 25 °C; A= 0.512 and B= 0.328,
- a_{Kjel} is the Kjelland parameter (hydrated ion radius),
- n_i is the charge of ion i.

The selectivity, or the response of an ISE to a certain ion (primary ion) in the presence of interfering ions, can be determined using the Nikolsky-Eisenman equation (8) [36] shown below:

$$E = const + \frac{RT}{n_iF}\ln\left(a_i + \sum_j K_{i,j}a_j^{n_{i/n_j}}\right) \tag{8}$$

where:

- $K_{i,j}$ is the selectivity coefficient
- i is the primary ion

- j is the interfering ion
- a is the activity of ion
- n_i & n_j are the charge of the primary and interfering ion, respectively
- E is the measured potential
- *const* combines all other potentials in the cell.

1.6 Coulometric signal transduction method

As it was mentioned earlier, in classical potentiometry the equilibrium potential between an indicator electrode (ISE) and a reference electrode is measured. In this case, the flowing current is close to zero due to the high input impedance of the voltmeter used for measuring the potential [34], [37].

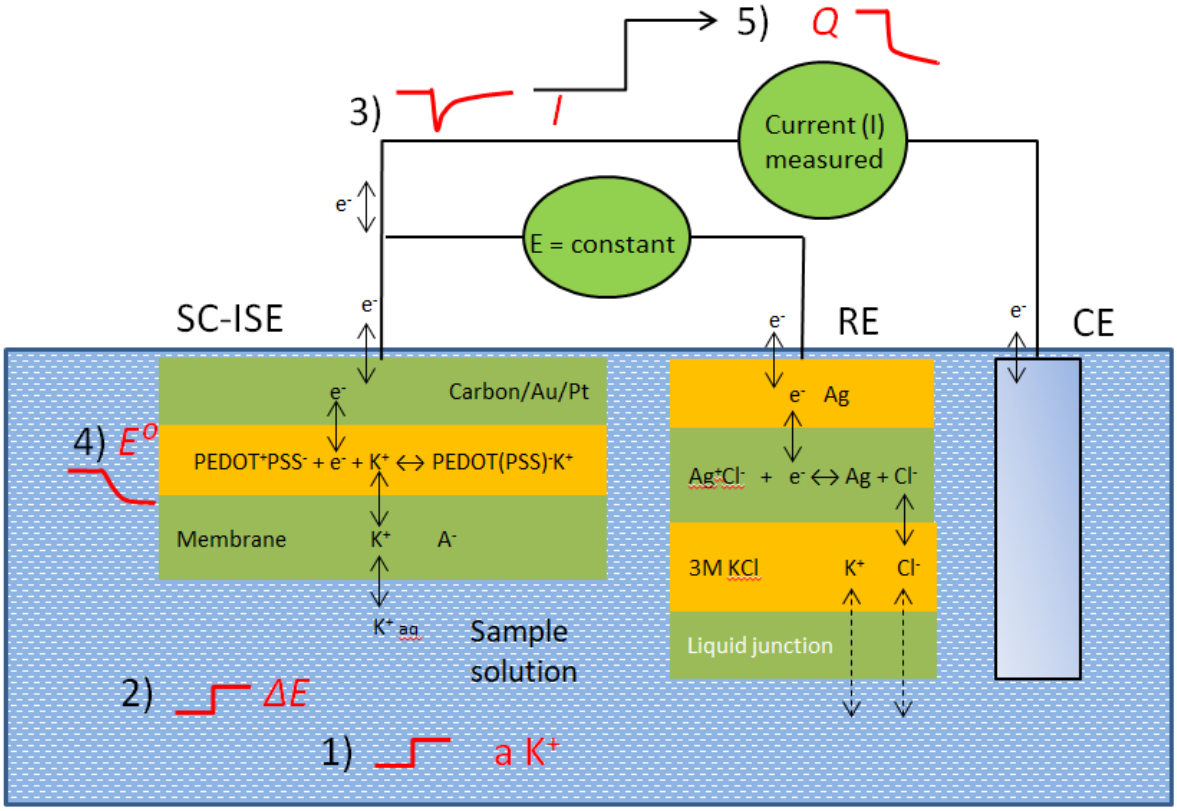

Figure 7. Illustration of the novel ion-to-electron transduction principle in a three-electrode cell. Scheme adapted from [37].

A novel ion-to-electron transduction method for SC-ISEs was introduced by J. Bobacka et al. in 2015 which is based on constant potential coulometry [37]. As illustrated in Figure 7, in this approach the potential between the SC-ISE and the reference electrode in a three-electrode cell is kept constant by using a potentiostat. Since the potential of the SC-ISE is held constant, any change in the concentration (activity) of the primary ion in the sample solution (Figure 7, 1)

will cause a potential difference at the membrane/solution interface (Figure 7, 2) and subsequently a rise in the potential difference between reference and working electrodes.

Since the potential of SC-ISE is forced to remain constant, the potential change at the membrane/solution interface will cause the flow of a transient current between the SC-ISE and the counter electrode (CE) (Figure 7, 3). This current will cause the oxidation/reduction of the conducting polymer PEDOT(PSS) until the potential change at the membrane/solution interface is compensated by an equal but opposite change in the potential of the conducting polymer (Figure 7, 4). When the equilibrium is reached, the current will stop flowing and the resulting current vs. time profile can be integrated to obtain the total charge (Figure 7, 5) [37, 38].

Ionophore-based SC-ISEs require recalibration before they can be used. It is always better to eliminate the recalibration procedure as long as the method allows it [39, 40]. Another advantage of the novel method is that the amount of volume introduced can be neglected as the novel method is more focused on counting the charge consumed within the solid-contact layer of the SC-ISE. The current is obtained from integration that will flow until the new equilibrium is reached with every change in the activity of ions [40].

Some new methods of application have been introduced in practical application such as detection of small changes in pH in seawater as well as studies in the determination of activity changes in potassium ion in serum [41]. Studies on how the electrode geometry influences measurements proved that with an increase of the area of the SC-ISEs the response time shortened [42].

The novel signal transduction method can be utilized to amplify the analytical signal by increasing the film thickness (redox capacitance) of the solid contact while keeping the Nernstian response (linear dependence of potential to the log of activity of ions) [38].

1.7 Other characterization techniques

1.7.1 Cyclic voltammetry

Cyclic voltammetry (CV) is one of the most broadly used electrochemical techniques to examine the oxidation and reduction processes of chemical species. CV is performed in a three-electrode electrochemical cell where the potential between the reference and working electrodes is controlled and current between the working and the counter electrode is measured. A linear potential sweep vs. time is applied to the cell in the form of a triangle [43].

The obtained current is recorded and plotted vs. the applied potential to acquire the so-called cyclic voltammogram. In other words, cyclic voltammetry is performed by sweeping the potential of the working electrode and measuring the resulted current. The anodic and cathodic current peaks found in a cyclic voltammogram indicate the existence of oxidation or a reduction reaction of a redox couple [44].

When the scan rate increases, the current will also increase allowing more ions to be oxidized or reduced (within a given time) leading to the increase in the anodic and cathodic currents. The experiments are done in a non-stirred solution. CV is a popular technique for both the synthesis and characterization of conducting polymers [45, 46].

1.7.2 Chronoamperometry and chronocoulometry

Amperometry measures a current that flows in the electrochemical system. The measured current is proportional to the concentration of the analyte under diffusion-controlled conditions. Hence, based on the obtained information, the concentration of the analyte can be determined. Chronoamperometry is the amperometry measured versus time at a constant applied potential in a three-electrode setup.

The Clark oxygen electrode can be one of the examples, where chronoamperometry is used. Measurement of the oxygen concentration in biological samples is of help in the medical diagnostics field [47]. A novel ion-to-electron transduction principle for SC-ISEs used in this work is another example where chronoamperometry is used for characterisation of conducting polymers in ISEs [38], [41].

Coulometry measures the amount of charge passed in the electrochemical system. There are two coulometric methods – controlled potential coulometry and constant current coulometry. The first one, also known as chronocoulometry, is applied in a three-electrode cell, where the potential of the indicator electrode is kept stable. Thus, the current is decreased with the concentration of analyte in the solution. Integration of the current over time gives the information of the total charge consumed. In constant-current coulometry as the name states for itself, the current is kept constant during a certain time that is beforehand known by the length of reaction. The accumulated charge can be computed by multiplying current versus time [41].

1.7.3 Electrochemical Impedance Spectroscopy (EIS)

Electrochemical impedance spectroscopy (EIS) [48] is an electrochemical technique used to measure the impedance of a system in dependence on the alternating current (AC) frequency. EIS gives information about the kinetics and mechanisms of electrochemical processes. The

EIS is a non-destructive technique and can provide various information about complex samples such as batteries, fuel cells and conducting polymers coated with a membrane [43], [49].
EIS is based on examining the response of an electrochemical system when the alternating sinusoidal excitation signal is applied, and the obtained sinusoidal alternating current is measured. The phase shift gives information about the behaviour of the electrochemical system. So, that phase shift values of 0°, 45°, and 90° correspond to a resistor, Warburg impedance, and a capacitor, respectively [34], [43], [48].
The impedance of a system Z is a vector quantity consisting of a real (Z') and an imaginary (−Z'') part. |Z| is presented in the complex plane, −Z'' and Z' as the components of a vector in the so-called "Nyquist plot". To put it in another way, the Nyquist plot is the plot of the imaginary impedance component versus the real impedance component [43], [49].

Sometimes it is difficult to understand what electrochemical processes occur on the electrode's surface. An equivalent circuit can help to grasp this information in a simplified way by breaking it down into electrical compounds such as double-layer capacitance, solution resistance and the charge-transfer resistance, etc. The EIS measurement data can help to reconstruct the model of the equivalent circuit as well as, inversely, based on equivalent circuit summarize the electrochemical process happening in the system [43], [49].

2 Experimental work

2.1 Materials

Tetrahydrofuran (THF, ≥ 99.9 %), 3,4-ethylenedioxythiophene (EDOT, ≥ 97.0 %), 2-nitrophenyloctyl ether (o-NPOE, ≥ 99.0 %) poly(sodium 4-styrenesulfonate) (NaPSS; MW~70.000) and sodium chloride (NaCl, ≥ 99 %), were obtained from Sigma-Aldrich. Tetradodecylammonium tetrakis(4-chlorophenyl)borate (ETH 500), bis(2-ethylhexyl) sebacate (DOS), potassium ionophore I (valinomycin), high molecular weight poly(vinyl chloride) (PVC, ≥ 97.0 %), tridodecylmethylammonium chloride (TDMACl, ≥ 98.0 %), potassium tetrakis[3.5-bis(trifluoromethyl)phenyl)]borate (KTFPB), were obtained from Fluka. Potassium chloride (KCl, ≥ 99.5 %) was obtained from Merck. Distilled and deionized water (ELGA Purelab Ultra; resistivity 18.2 MΩcm) was used in the preparation of all aqueous solutions.
Glassy carbon (GC) disk electrodes (SIGRADUR® G, Germany) were used as working (indicator) electrodes. Metrohm single-junction (6.0733.100) Ag/AgCl/3M KCl and Metrohm double-junction (6.0726.100) Ag/AgCl/3M KCl/1M LiOAc were used as reference electrodes.

2.2 Preparation of the ISEs

2.2.1 Polishing and cleaning the electrodes

GC disk electrodes, with the area 0.07 cm^2 (3 mm in diameter) and surrounded by PVC body, were polished using sandpapers with various coarseness: 180, 400, 600, 800, 1000, 1400, 2000 and the last one is 4000. The second step was polishing the electrodes using diamond paste with different particle size. Polishing the electrodes with alumina slurry and clean cloth in water was the final step in the polishing sequence. The sequence was from top to bottom and from left to right for approximately 1 minute for each step. After the polishing procedure, all electrodes were cleaned by sonication in ethanol, and then in deionized water each for 15 minutes. Every step included rinsing with deionized water and examining the quality of the smooth polishing with the naked eye.

2.2.2 Cyclic voltammetry

The CV technique was used to check that the electrodes were properly cleaned as well as checking the formation of the conducting polymer films deposited on the electrode surfaces by the electrochemical polymerization. The measurements were carried out in 0.1 M KCl solution in a three-electrode electrochemical cell connected to the Autolab General Purpose Electrochemical System (AUT30.FRA2-Autolab Eco Chemie, B.V., The Netherlands). The working electrode was either a polished GC electrode or a GC electrode with the conducting polymer deposited on it. The auxiliary electrode was a GC rod and as a reference electrode, a Metrohm single-junction Ag/AgCl/3M KCl electrode was used. The deaeration of the 0.1 KCl solution with nitrogen gas was conducted for 15 minutes before measurement and the gas flow was kept above the solution during the measurements to eliminate any chances for secondary redox reactions such as the oxygen in the solution, which may cause interference in the measurements. Cyclic voltammograms were recorded for two cycles in the potential range −0.5 V to 0.5 V with 0.2 V as the starting potential, and a scan rate of 0.1 V/s [50, 51].

2.2.3 Electrosynthesis of PEDOT(Cl) and PEDOT(PSS)

The galvanostatic polymerisation method was used for electrochemical deposition of the conducting polymer PEDOT doped with chloride (Cl^-), *i.e.,* PEDOT(Cl), and PEDOT doped with PSS, *i.e.,* PEDOT(PSS), from a deaerated aqueous solution containing 0.1 M KCl with 0.01 M EDOT (the monomer) in the case of PEDOT(Cl) and 0.1 M NaPSS with 0.01 M EDOT in the case of PEDOT(PSS). The prepared solutions were stirred overnight to ensure the dissolution of the monomer. The electrochemical polymerization was carried out in a one-

compartment three-electrode (or two-electrodes in the case of PEDOT(PSS) electrochemical cell connected to the Autolab general purpose electrochemical system (AUT30.FRA2-Autolab Eco Chemie, B.V., The Netherlands). The polished GC electrodes were used as working electrodes, a Metrohm single-junction Ag/AgCl/3M KCl was used as the reference electrode and a GC rod was used as the counter electrode in the case of PEDOT(Cl). The reference electrode was not used in the case of PEDOT(PSS) polymerization to avoid contamination. A constant current of 0.0141 mA was applied for 142 seconds to obtain a polymerization charge of 2 mC. When the polymerization was done, the resulting GC/PEDOT(Cl) and GC/PEDOT(PSS) electrodes were rinsed thoroughly with distilled water and conditioned in 0.01 M KCl solution. After being conditioned for 24 hours, the recorded cyclic voltammograms (2^{nd} cycle) as proof of the formation of the conducting polymer films (PEDOT(Cl) and PEDOT(PSS)) deposited on the electrode surfaces by the electrochemical polymerization, is illustrated in Appendix A. As can be seen, the close to the rectangular capacitor-like shape of the cyclic voltammograms proves that the formation of PEDOT(Cl) and PEDOT(PSS) films were successful.

2.2.4 Preparation of the ion-selective membrane cocktails

All the components for preparing the cocktails were weighed and dissolved in THF. All cocktail components for chloride or potassium ion-selective membrane were poured into a glass vial (5 ml) and vortexed until the dissolution of most of the compounds and then kept overnight on a slowly shaking rocker for a complete dissolution of the components. All membrane cocktails had the final dry mass content of 15 %. The latter was defined as the proportion of the sum of all membrane elements masses, excluding THF, to the sum of all membrane elements masses including THF (Table 1).

Table 1. The composition of ion-selective membranes.

Chloride-ISM			**Potassium-ISM**		
Content	m/mg	ω/%	Content	m/mg	ω/%
o-NPOE	120.20	51.00	DOS	152.80	64.93
PVC	81.40	34.00	ETH 500	2.40	1.02
TDMACl	35.30	15.00	KTFPB	1.18	0.50
THF	1333.5	-	PVC	76.60	32.55
			Valinomycin	2.35	1.00
			THF	1333.5	-

2.2.5 Preparation of SC-ISEs

The preparation of the chloride and potassium solid contact ion-selective electrodes (Cl^--SC-ISEs, K^+-SC-ISEs) was done by drop-casting 50 µl of the corresponding membrane cocktail on top of each of the GC/PEDOT(Cl) ctrode was covered with a membrane cocktail. Before applying the membrane cocktail, the electrodes were fixed face up on top of the plastic cell. While applying the cocktail on top of the electrode one must make sure that there is no bubble left on the surface (a needle was used for removing bubbles). After drop-casting the membrane, the electrodes were left to dry for 24–48 hours under a glass cover to protect the membrane from dust and other contaminations. Electrodes with dried membrane were immersed in 0.01 M KCl solution for at least 24 hours of conditioning before further measurements.

2.3 Potentiometric response of the prepared electrodes

The performance of the prepared electrodes was checked by carrying out conventional potentiometric calibrations. Automatic calibration was performed using a 16-channel millivoltmeter (Lawson Labs EMF16 Interface system) with a high input impedance of 10^{15} Ω and L-EMF DAQ 3.0 software. The prepared chloride and potassium SC-ISEs were used as the indicator electrodes and Metrohm double-junction Ag/AgCl/3M KCl/1M LiOAc was used as a reference electrode. Additionally, a commercial solid-state chloride-ion-selective electrode (Cl-ISE, Thermo Scientific Orion 9417BN) was used as the indicator electrode for comparative purposes when calibrating the Cl^--SC-ISEs. Sequential automatic dilutions were performed using two Metrohm Dosino 700 instruments equipped with burets of 50 mL capacity (Herisau, Switzerland). The burets were first rinsed twice to eliminate any air bubbles. The pumps were programmed to dilute the sample solution either with fresh deionized water or with 0.1 M NaCl as background electrolyte (BGE) (only in the case of potassium SC-ISEs). The starting solution was 50 ml of 0.1M KCl or 0.1 M KCl with 0.1 M NaCl as BGE (only in the case of potassium SC-ISEs) that was pipetted into an electrochemical cell and corresponding ISE was immersed into the solution. Six dilutions were conducted until the concentration reached 10^{-7} M KCl. The time between each dilution step was 5 minutes for potential stabilization and at the end of each step, the final potential value was noted. The average of the last 5 potential values (points) from each dilution was used for plotting the calibration curves. Instead of concentration, the activity values calculated using the Debye-Hückel equation (equation 7) was applied. The calculation of the slopes was performed for the linear part of the calibration curves.

2.4 Electrochemical Impedance spectroscopy

Electrochemical impedance spectroscopy (EIS) measurements were carried out using the Autolab Frequency Response Analyser System (AUT30.FRA2-Autolab Eco Chemie, B.V., The Netherlands). The measurements for all of the prepared electrodes were conducted at the open circuit potential in deaerated 0.1 M KCl solution. Deaeration of the solution was made for 15 minutes with nitrogen gas before the experiments and then the gas inlet was kept above the solution during the measurement. The prepared SC-ISE connected to a one-compartment three-electrode electrochemical cell. The auxiliary electrode was a GC rod and the reference electrode was Ag/AgCl/3M KCl. The frequency range under which spectra were recorded was 100 kHz to 10 mHz and using an AC excitation amplitude of 10 mV.

2.5 Chronopotentiometry and chronoamperometry (chronocoulometry)

Chronopotentiometric and chronoamperometric measurements were performed using a conventional three-electrode cell with GC rod as a counter electrode (for chronoamperometry), chloride SC-ISEs as the working electrode and Metrohm Ag/AgCl/3M KCl/1M LiOAc as the reference electrode connected to an Ivium CompactStat instrument (Ivium Technologies, The Netherland). The starting solution was 50 ml of 0.1 KCl solution. In all measurements, the time for one analysis was 10 min with a stepwise increase in the concentration for every 2 min, starting from either 1 mM or 10 mM KCl electrolyte solution. The amount of stepwise increase in the concentration was for 5 % and 10 % or stepwise decrease in the concentration in 100 mM KCl electrolyte for only 10 %. A 100 mM KCl solution was used to increase the concentration and deionized water was used to decrease (dilution) the concentration. The required volumes were calculated and are summarized in Tables 1a, 1b and 1c (Appendix B).

The same set-up was used in the case of potassium SC-ISEs. The volume of starting solution was 50 ml of 1mM or 10 mM KCl (in deionized water or 100 mM NaCl as BGE). In all measurements, the time for one analysis was 61 min with a stepwise 10 % increase in the concentration of 1 mM or 10 mM KCl electrolyte (in deionized water or 100 mM NaCl as BGE). The required volumes were calculated and are shown in Table 2 (Appendix B). The first alteration in concentration was done after 1 min and the other every 10 min. These time ranges were fixed for the electrodes before damaging the ISM. After damaging the ISM, the amperometric response increased and in order to save time, it was decided to shorten the time ranges down to 10 min (with a stepwise increase every 2 min) for both amperometric and potentiometric measurements.

The electrodes were immersed in the solution, which was stirred using a magnetic stirrer, and the chronoamperograms and chronopotentiograms were recorded. The potential was measured and noted after waiting from 1 min to 2 min for signal stabilization in the chronopotentiometric measurements. In chronoamperometry, the measured stable potential was applied.

2.6 Damaging the ISM in SC-ISEs

After completing all the tests such as checking the potentiometric response, carrying out chronopotentiometric, chronoamperometric (coulometric) and EIS measurements, the ISM of the chloride and potassium SC-ISEs were physically damaged using a blade. The commercial Cl^--ISE was not damaged but measured with damaged Cl^--SC-ISEs for comparison reason. The blade was applied 3-4 times from the top to the bottom of the surface of ISM to cause damage to the membrane. The applied effort was subjectively equal to the whole electrodes. The comparison of the ISMs of the chloride and potassium SC-ISEs before and after damaging is illustrated in Appendix C. The photos are taken using a USB microscope: Veho discovery VMS-004 Deluxe.

3 Results and discussion

Six Cl^--SC-ISE and six K^+-SC-ISEs electrodes were prepared. ISM of three chloride SC-ISEs and four potassium SC-ISEs were damaged. Results for only one representative for each type of electrode before and after damaging are demonstrated, whereas the results for the rest of the electrodes are shown in the Appendices.

3.1 Cl^--SC-ISE: characterisation and comparison of the obtained sensors before and after physical damaging of the ISM

3.1.1 Potentiometric calibration

The calibration curves were obtained in the concentration range 10^{-1} to 10^{-7} M KCl solution (Figure 8a before damaging the ISM). The slopes for these electrodes were approaching to Nernstian and can be considered reasonable for further chronopotentiometric and chronoamperometric measurements. The slopes were found in the linear range 10^{-1} M to 10^{-4} M KCl with the calibration values shown in Table 2. Based on the EIS spectra obtained on the chloride SC-ISEs (Appendix D) the Replicates 2, 5 and 6 were chosen as the most suitable (with the closest resistance) for onward damaging ISM and conducting the measurements (Figure 8b calibration curve after damaging the ISM).

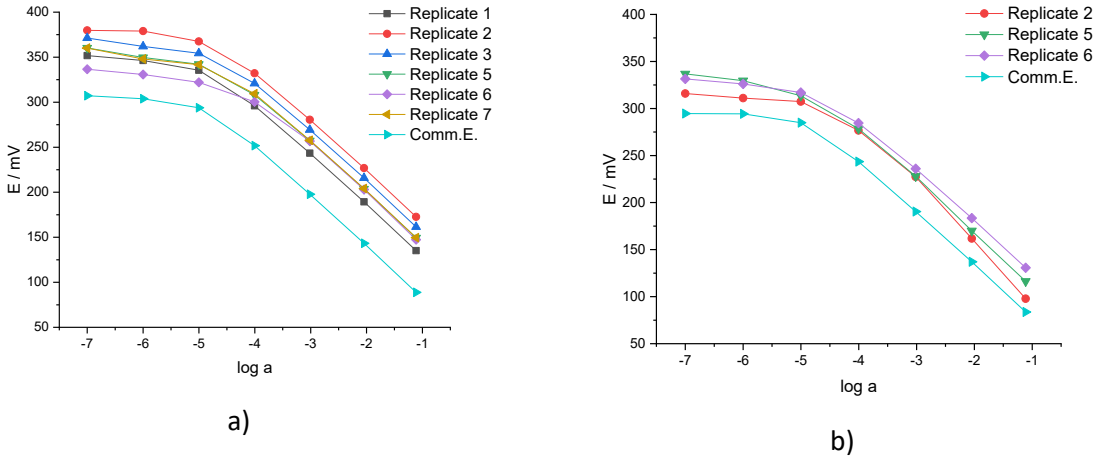

Figure 8. Potentiometric calibration curves of the commercial Cl^--ISE (Comm E.) and the GC/PEDOT(Cl)/Cl-ISM electrodes before damaging the ISM (a) and after damaging the ISM (b).

As can be observed from Table 2, the slope of the commercial electrode is −56.3 mV and for the rest of the electrodes, the slope was in the range of (–54.9 ± 0.9) mV (mean ± s_d, n=6). After damaging the ISM of chosen electrodes the slope was calculated and found to be in the range (−57.4 ± 4.6) mV (mean ± s_d, n=3). Interestingly, replicate 2 after damaging the ISM showed a distinct slope value in comparison with the rest electrodes. The reason for that is unknown. The slope of the commercial electrode was also measured for comparison reason and showed a similar slope value as shown in Table 2**.** The results show that the electrodes even after damaging the ISM were approaching the Nernstian slopes. The linearity range including that of the commercial electrode was found to be 10^{-1} M to 10^{-4} M, further dilution led to gradual levelling-off of the potential changes both before and after damaging of ISM.

Table 2. Potentiometric calibration values for the commercial electrode (Comm. E.) and for Cl^--SC-ISEs before (BD) and after damaging (AD) the ISM.

Electrode	Intercept/mV		Slope/mV	
	BD	AD	BD	AD
Replicate 1	74.5	-	-55.6	-
Replicate 2	112.7	32.2	-55.2	-62.4
Replicate 3	101.7	-	-55.1	-
Replicate 5	90.0	54.7	-55.2	-56.4
Replicate 6	91.7	73.2	-53.1	-53.3
Replicate 7	89.6	-	-55.2	-
Comm. E.	27.2	23.2	-56.3	-55.2

3.1.2 Chronopotentiometric and chronoamperometric (chronocoulometric) measurements

Before conducting the addition/dilution chronopotentiometric measurements, approximately 1 min to 2 min was given for potential stabilization. In Figure 9 the addition of 5 % and 10 %

in a 10^{-2} M KCl starting solution before damaging the ISM (a) and after damaging the ISM (b) of chloride SC-ISE (Replicate 2) is demonstrated. As can be observed from both graphs, *e.g.,* for 5 % or 10 % increase (*addition*) in the concentration of Cl^- anions led to an approximately proportional decrease in potentials (−2.5 mV for 10 % and −1.3 mV for 5 % additions) throughout the measurement either conducted with damaged or undamaged membrane. However, after damaging the ISM a potential drift was noted, where between the additions more time was required for the stabilization of the reading. The addition for the rest of the replicates and dilution with deionized water before and after damaging the ISM is depicted in Appendix E where a similar trend is also observed.

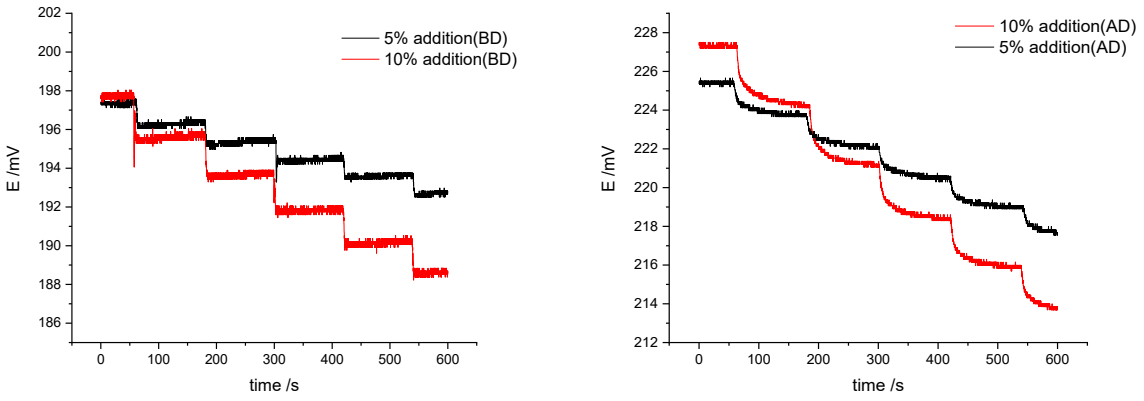

a) b)

Figure 9. Chronopotentiometric response recorded for Cl^--SC-ISE (Replicate 2) in starting solution 0.01 M KCl during stepwise 5 % and 10 % addition in concentration before damaging the ISM (a) and after damaging the ISM (b). See also Appendix E.

Similar to potentiometry, chronocoulometric responses (integration of the current peaks) demonstrated stable accumulation of charge *(Q)* transferred in the process during the addition. The coulometric response of chloride SC-ISE (Replicate 2) during the stepwise addition in concentration is presented in Figure 10a before damaging and in Figure 10b after damaging the ISM, where 10^{-2} M KCl was used as starting solution (see also Appendix F for other replicates).

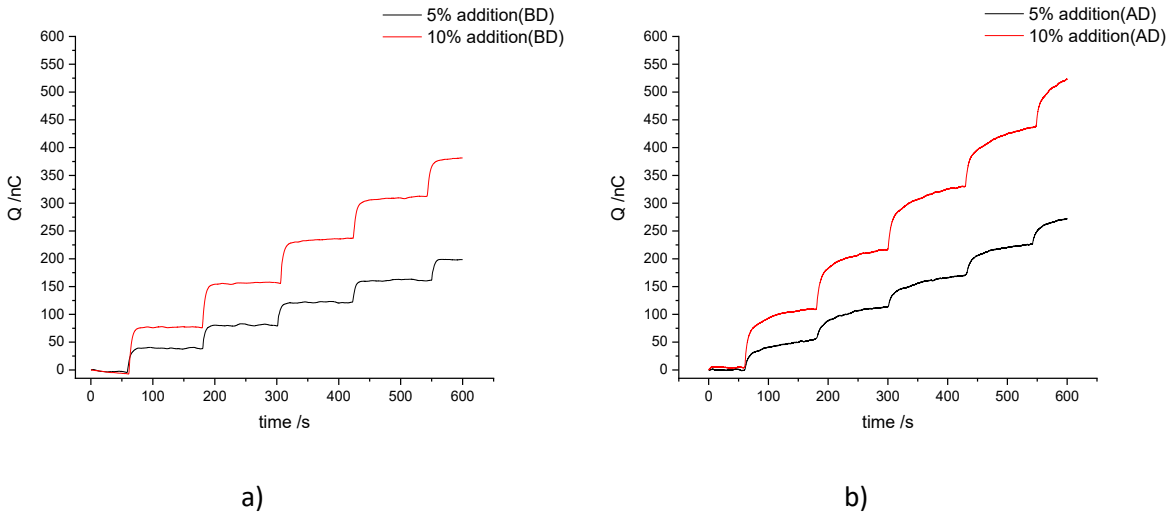

Figure 10. Chronocoulometric response recorded for Cl^--SC-ISE (Replicate 2) in starting solution 0.01 M KCl during stepwise 5 % and 10 % addition in concentration before damaging the ISM (a) and after damaging the ISM (b) See also Appendix F

In Figure 10a in both 5 % and 10 % stepwise additions the higher the concentration of KCl added the more charge was accumulated or in other words, the larger changes in the activity of the primary ion in the solution the larger charges were measured. However, in Figure 10b a drift in the response was observed for both 5 % and 10 % stepwise additions. This can be related to the potential instability (Figure 9b) and/or damages on the membrane surface which could also influence the overall accumulation of charge throughout the time measured. The cumulative charge appeared to be slightly increased (5 % addition) from 200 nC to 250 nC before and after damaging the ISM, respectively. In this case, the accumulated charge for 10 % stepwise additions was approximately twice that of 5 % additions in both before and after damaging the ISM.

In chronoamperometric measurements before and after damaging the ISM (Figure 11a and Figure 11b), the responses showed dissimilar results. Before damaging the membrane (Figure ***11***a) every increase in concentration both for 5 % and 10 % gave a reproducible current peak with little noise, whereas damaging the membrane surface of ISE led to a significant increase in baseline noise. The noise levels increased by more than ca 20 times after damaging the ISM. Nevertheless, after damaging the ISM, the current peaks were still visible. One can claim that this tremendous baseline noise effect is due to damage of the ISM and that the SC-ISE is not properly functioning. Interestingly, the high noise level in the amperometric response (Figure 11b) was not visible in the coulometric response (Figure 10b) that was obtained by the integration of the amperometric signal. See Appendix G for other replicates in addition/dilution of concentration.

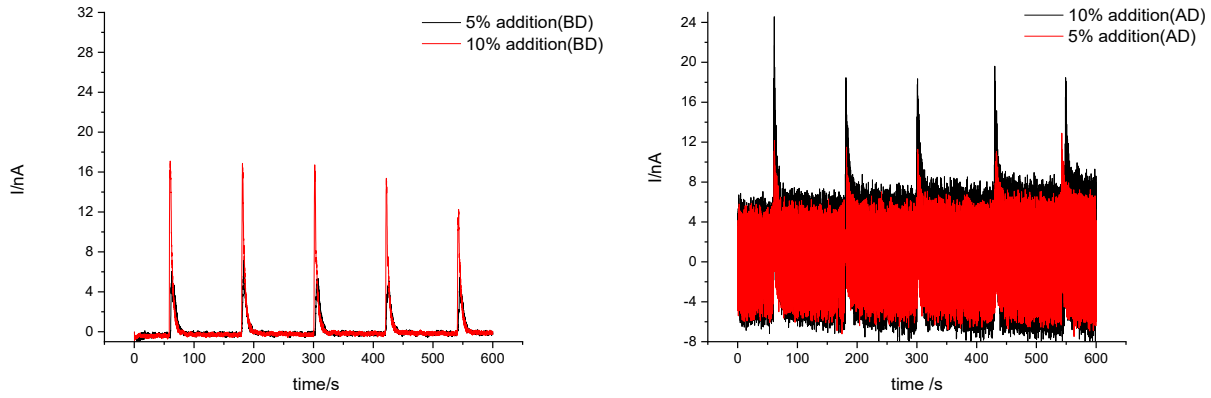

a) b)

Figure 11. Chronoamperometric response recorded for Cl^--SC-ISE (Replicate 2) in starting solution 0.01 M KCl during stepwise 5 % and 10 % addition in concentration before damaging the ISM (a) and after damaging the ISM (b) See also Appendix G.

3.1.3 Electrochemical Impedance spectroscopy

The electrochemical characteristics of the prepared SC-ISEs were studied by EIS to gain more information about the electrochemical processes that take place at the interface of the chloride SC-ISE and bulk solution (0.1 M KCl). The impedance spectra of SC-ISE, before damaging the ISM (a) and after damaging the ISM (b), are demonstrated in Figure 12 (Appendix H for other replicates). Before membrane damaging the impedance spectra of the Cl^--SC-ISE (Replicate 2) showed a high-frequency semicircle (indicating the formation of the ISM) originating from the bulk resistance and of the membrane together with its geometric capacitance. The bulk resistance which is equal to the diameter of the semicircle was equal to 100 kΩ. The low-frequency tail was an almost ideal capacitor showing an angle of ca 90°, which can be related to the bulk redox capacitance of the solid contact PEDOT(Cl). The low-frequency capacitance (C_L) was estimated from the imaginary impedance value ($-Z'' = 410$ kΩ) at $f = 0.01$ Hz, as follows: $C_L = (2\pi \times 0.01\ \text{Hz} \times 410000\ \Omega)^{-1}\ \text{F} = 39\ \mu\text{F}$.

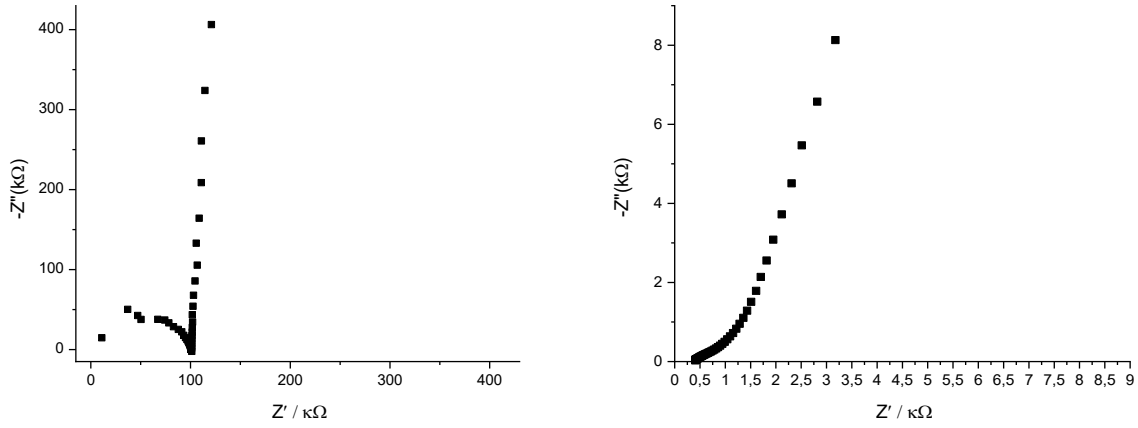

a) b)

Figure 12. EIS recorded for Cl^--SC-ISE (Replicate 2) before (a) and after damaging the ISM (b). The direct current potential is open circuit potential (0.13 V). The frequency range is 100 kHz to 10 mHz. The electrolyte is 0.1M KCl. See also Appendix H.

However, the impedance spectrum of the damaged electrode showed an approximately 45° Warburg diffusion line at high frequencies, that was gradually approaching towards 70° line at low frequencies. Furthermore, the high-frequency semicircle was absent, and the overall impedance was much lower for the damaged electrode. This behaviour can be explained when considering that damaging of the ISM exposes part of the PEDOT(Cl) film to the electrolyte solution. This facilitates the reversible oxidation of PEDOT. Estimating the low-frequency capacitance (C_L) from the imaginary impedance value ($-Z'' = 8.2$ kΩ) at $f = 0.01$ Hz, resulted in $C_L = 1.9$ mF, which is higher than expected for a 2 mC film of PEDOT(Cl).

3.2 K^+-SC-ISE: characterisation and comparison of the obtained sensors before and after physical damaging of the ISM

3.2.1 Potentiometric calibration

The calibration curves without BGE were obtained in the concentration range 10^{-1} M to 10^{-7} M KCl solution (Figure 13a before damaging the ISM). The slopes were determined from the linear range 10^{-1} M to 10^{-5} M KCl, resulting in the calibration values shown in Table 3a. The slopes for these electrodes can be considered as near-Nernstian and may be deemed reasonable for further chronopotentiometric and chronoamperometric measurements.

Based on the impedance spectra (Appendix H**,** in more detail, will be discussed section 3.2.3) obtained on the K^+-SC-ISEs the replicates with the two smallest (Replicates 1 and 2) and with two highest resistance (Replicates 5 and 6) were chosen for onward damaging electrodes' ISMs and conducting the measurements. Calibration curves for the chosen electrodes without BGE after damaging the ISM are demonstrated in Figure 13b.

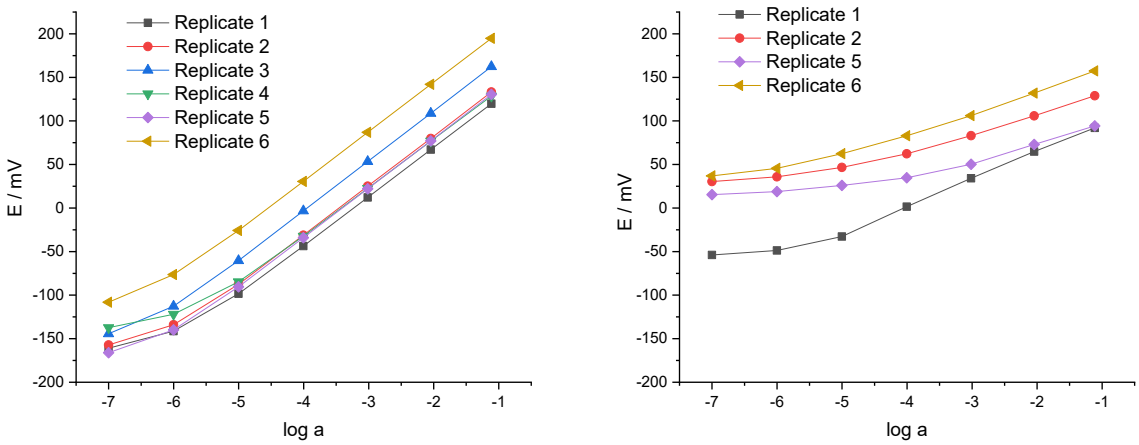

Figure 13. Potentiometric calibration curves of the K+-SC-ISE electrodes in the concentration range 10^{-1} M to 10^{-7} M KCl before (a) and after damaging the ISM (b) without BGE.

The slopes of electrodes were calculated and found to be in the range of (56.5 ± 0.8) mV (mean ± s_d, n=6). After damaging the ISM of chosen electrodes the slopes were calculated and found to be non-Nernstian, having slope values in the range (24.0 ± 6.1) mV (mean ± s_d, n=4) (Table 3a).

Table 3a. Potentiometric calibration values for K^+-SCI-SEs without BGE before (BD) and after damaging (AD) the ISM.

Electrode	Intercept/mV		Slope/mV	
	without BGE			
	BD	AD	BD	AD
Replicate 1	182.0	129.5	56.2	32.1
Replicate 2	196.2	150.2	56.8	21.3
Replicate 3	226.0	-	57.3	-
Replicate 4	189.2	-	55.0	-
Replicate 5	193.5	110.1	56.8	17.9
Replicate 6	258.0	182.6	56.8	24.5

The calibration curves with 0.1 M NaCl as BGE were obtained in the concentration range 10^{-1} M to 10^{-7} M KCl solution (Figure 14a before damaging the ISM). The slopes determined in the linear range 10^{-1} to 10^{-5} M KCl were (49.5 ± 0.7) mV (mean ± s_d, n=6) as shown in Table 3b. The slopes for this electrode had some interference from BGE but can be considered as approaching to near-Nernstian and may be deemed reasonable for further chronopotentiometric and chronoamperometric measurements. After damaging the ISM of chosen electrodes the slopes were calculated and found to be as previously non-Nernstian, having extremely low slope values in the range (4.4 ± 0.9) mV (mean ± s_d, n=4) (Table 3b). As

was foreseeable, the calibration curves for the chosen electrodes with 0.1 M NaCl as BGE after damaging the ISM demonstrated inadequate potential response which is shown in Figure 14b.

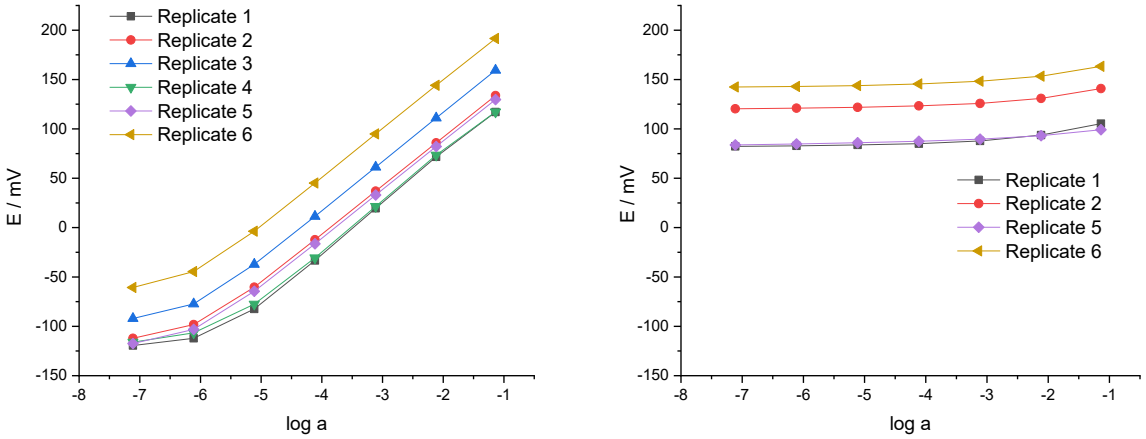

Figure 14. Potentiometric calibration curves of the K^+-SC-ISE electrodes in the concentration range 10^{-1} M to 10^{-7} M KCl before (a) and after damaging the ISM (b) with 0.1 M NaCl as BGE.

Table 3b. Potentiometric calibration values for K^+-SC-ISEs with BGE before and after damaging ISM.

Electrode	Intercept/mV		Slope/mV	
	with BGE (0.1 M NaCl)			
	BD	AD	BD	AD
Replicate 1	176.5	107.3	50.7	5.2
Replicate 2	189.3	142.8	48.9	4.6
Replicate 3	215.7	-	49.6	-
Replicate 4	175.6	-	49.4	-
Replicate 5	185.5	101.1	48.9	3.2
Replicate 6	247.9	165.5	49.2	4.7

3.2.2 Chronopotentiometric and chronoamperometric (chronocoulometric) measurements

Conducting chronopotentiometric measurements for potassium SC-ISEs took a long time for potential stabilization and it varied from 5 min to 10 min, but for some electrodes, it took even longer. In Figure 15 stepwise increase for 10 % in a 10^{-2} M KCl starting solution before damaging the ISM (a) and after damaging the ISM (b) of K^+-SC-ISE (Replicate 1) is illustrated. As can be seen from Figure 15a, a steady stepwise potential increase of 2 mV was observed for every step concentration addition. However, a significant potential drift was noted towards a steep decrease in Figure 15b after ISM had been damaged. Nevertheless, despite the damage in the ISM for every stepwise addition, the potential growth was estimated at ~0.3 mV. The rest

of the replicates before and after damaging the ISM are depicted in Appendix I, where a similar trend was also observed.

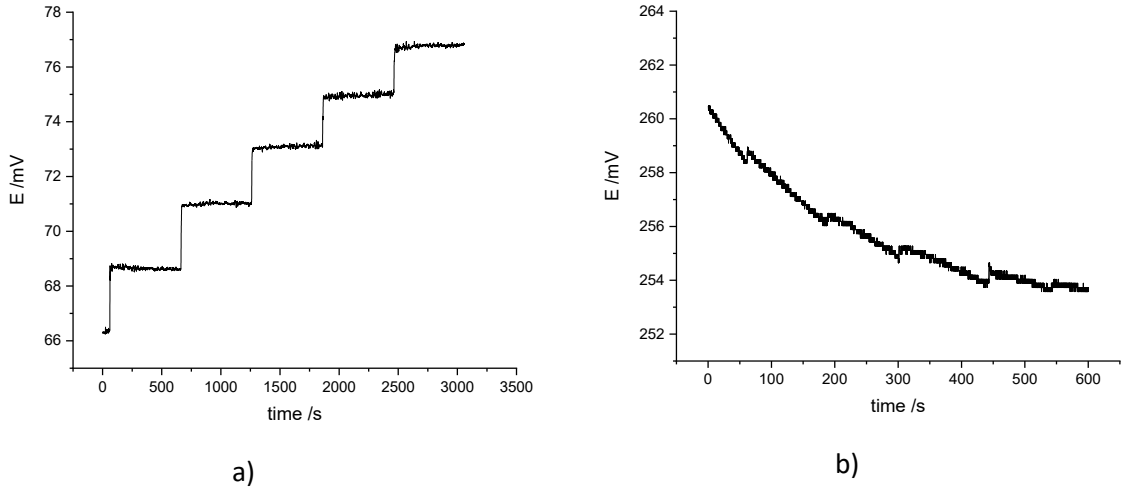

Figure 15. Chronopotentiometric response recorded for K^+-SC-ISE (Replicate 1) in starting solution 0.01 M KCl during stepwise 10 % concentration addition of 0.1 M KCl without BGE (a) before damaging the ISM and (b) after damaging the ISM. See also Appendix I.

In Figure 16 stepwise increase for 10 % in a 10^{-2} M KCl starting solution with BGE before damaging the ISM (a) and after damaging the ISM (b) of potassium SC-ISE (Replicate 1) is shown. As one can notice from Figure 16a, in the presence of BGE a steady stepwise potential increase of 2 mV was also observed for every step of 10 % concentration addition but superimposed on a potential drift. This can be due to interference from BGE.

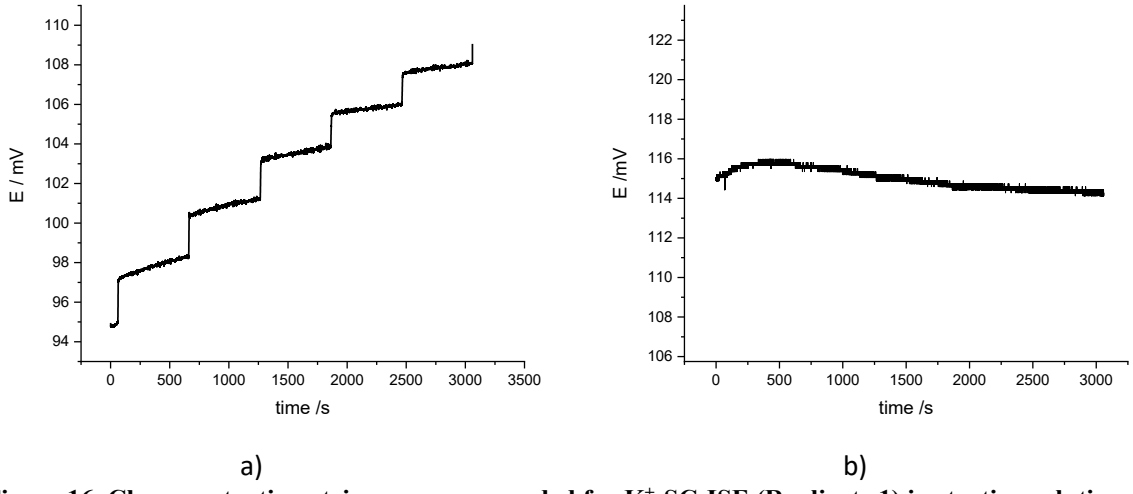

Figure 16. Chronopotentiometric response recorded for K^+-SC-ISE (Replicate 1) in starting solution 0.01 M KCl with 0.1 M NaCl as BGE during stepwise 10 % concentration addition of 0.1 M KCl with 0.1 M NaCl as BGE (a) before damaging the ISM and (b) after damaging the ISM. See also Appendix I.

The damaged SC-ISE measured in presence of interfering ions from BGE demonstrated inadequate response in the potential (Figure 16b). This was also proved by the potential calibration curve illustrated in Figure 14b. Overall, the interference from the BGE was

significant as one can compare Figure 15b without BGE and Figure 16b with BGE. Although significant potential drift exists in both cases, without BGE there was some increase in potential response for every 10 % increase in concentration, which cannot be seen with BGE. The rest of the replicates before and after damaging the ISM with interfering ions are also displayed in Appendix I.

Both with and without 0.1 M NaCl as BGE before damaging the ISM (Figure 17a and Figure ***18***a) the K^+-SC-ISE showed almost identical responses in terms of the accumulated charge (−0.2 µC) for every stepwise increase in concentration.

After damaging the ISM without BGE a significant decrease of the coulometric response of K^+-SC-ISE was seen. It can be due to damage to the membrane surface and potential instability (Figure 17b).

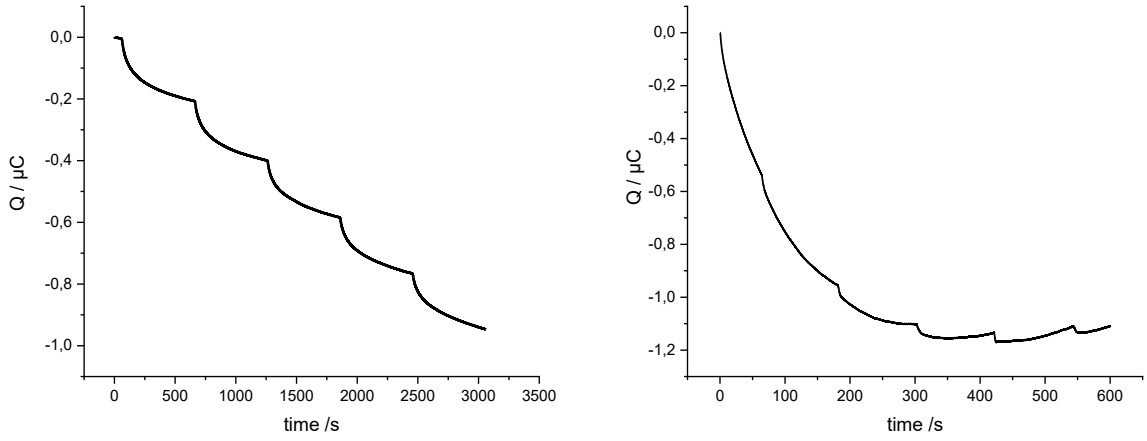

Figure 17 Chronocoulometric response recorded for K^+-SC-ISE (Replicate 1) in starting solution 0.01 M KCl during stepwise 10 % concentration addition of 0.1 M KCl (a) before damaging the ISM and (b) after damaging the ISM without BGE. See also Appendix J.

Despite the damage in ISM about ~0.02 µC accumulation of charge for every stepwise addition is noticeable. The corresponding measurements with interfering ions from BGE (Figure 18b) showed an almost straight line that was opposite in the direction to the response measured before damaging the ISM (Figure 18a). Overall, the interference from BGE was significant as one can compare Figure 17b and Figure 18b.

In general, Figure 17b and Figure 18b confirm the non-functionality of K^+-SC-ISE after its ISM is damaged. It is also illustrated by calibration curves (Figure 13b and Figure 14b) and non-Nernstian slope values (Tables 3a and 3b). The rest of the replicates are displayed in Appendix J where a similar trend is also observed.

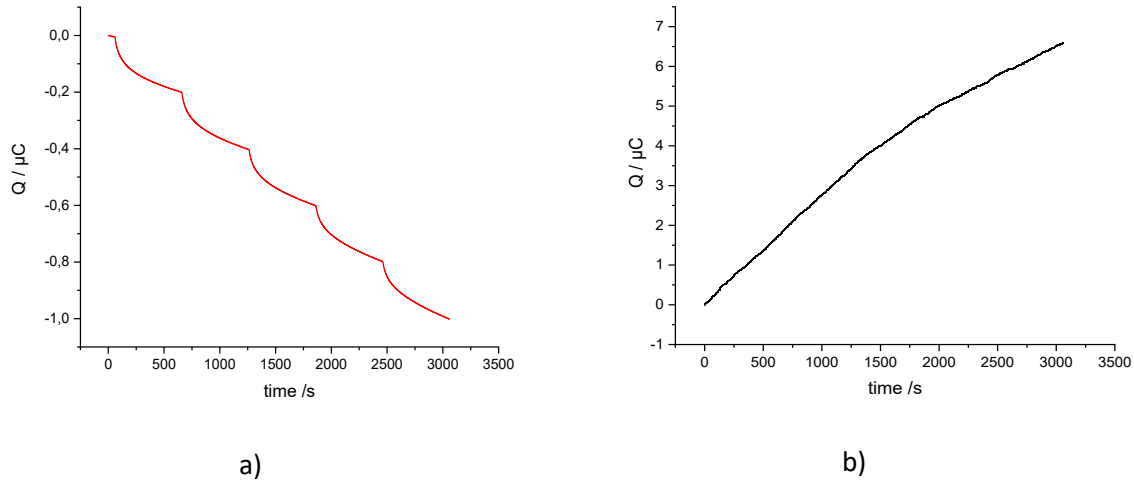

a) b)

Figure 18. Chronocoulometric response recorded for K^+-SC-ISE (Replicate 1) in starting solution of 0.01 M KCl with 0.1 M NaCl as BGE during stepwise 10 % concentration addition of 0.1 M KCl (a) before damaging the ISM and (b) after damaging the ISM. See also Appendix J

Similar to the potentiometric and coulometric responses, the chronoamperometric measurements before damaging of the ISM either with or without BGE exhibited similar current responses for every stepwise 10 % addition in concentration. However, the baseline noise effect in both concentrations was more pronounced in solutions measured without BGE. The rational explanation for this phenomenon is unclear.

Damaging the membrane surface of the ISE led to a significant increase in baseline noise. One can argue that this tremendous baseline noise effect is due to the compromised integrity of the ISM. The noise level indeed increased more than 80 times after damaging the ISM in the case of 0.01 M KCl without BGE (Figure 19a and Figure 19b), and more than 200 times in presence of the BGE (Figure 20a and Figure 20b). Nevertheless, after damaging the ISM, a barely seen current response still exists in the case of measurement without BGE (as it was shown in previous measurements above).

However, interference from the BGE has a tremendous impact on the current response of the damaged K^+-SC-ISE (Figure 20b) where zero signal is found throughout the stepwise increase in concentration (See Appendix K for other replicates). Not surprisingly, the calibration curves (Figure 13b and Figure 14b), as well as slope values (Tables 3a and 3b), clearly confirm the non-functionality of the K^+-SC-ISE after damaging the ISM. Comparison among potentiometric, coulometric and amperometric responses after damaging the ISM in both chloride and potassium SC-ISEs give clear comprehension that electrodes do not give a proper response for every stepwise addition in concentrations.

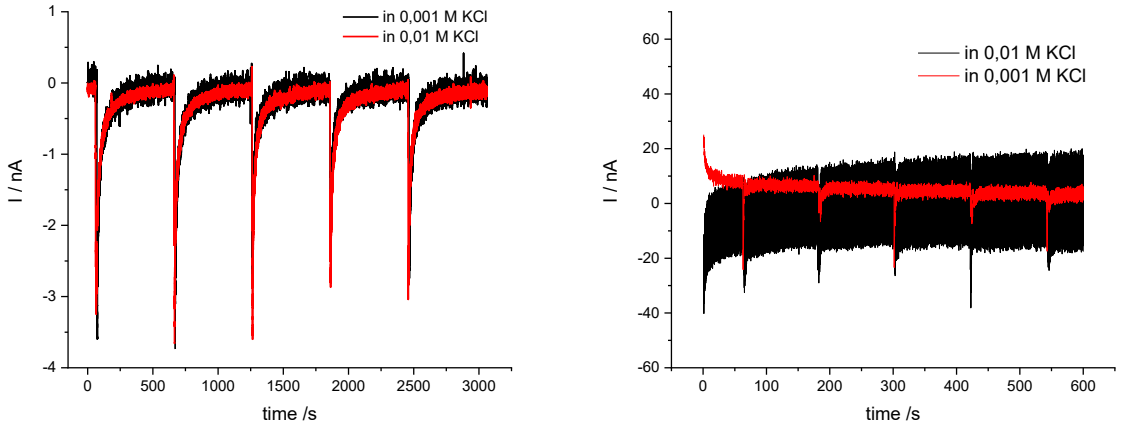

Figure 19. Chronoamperometric response recorded for K^+-SC-ISE (Replicate 1) in starting solution 0.01 M and 0.001 M KCl during stepwise 10 % concentration addition of 0.1 M KCl before damaging the ISM (a) and after damaging the ISM (b) without BGE. See also Appendix K

One might have a misleading ambiguous feeling that chronopotentiometric measurements after damaging the electrode's membrane are still functioning and give adequate response for addition in concentration as it is illustrated for the chloride ISE, where PEDOT(Cl) itself can give a response for Cl^-, as a consequence functioning even after damaging the ISM (Figure 9b). This is not valid for the K^+-SC-ISEs (Figure 15b and Figure 16b). However, it is visible from the chronoamperometric responses in all above-mentioned cases, that after damaging the ISM of the SC-ISE, it is no longer functioning properly (Figure 11b, Figure 19b and Figure 20b).

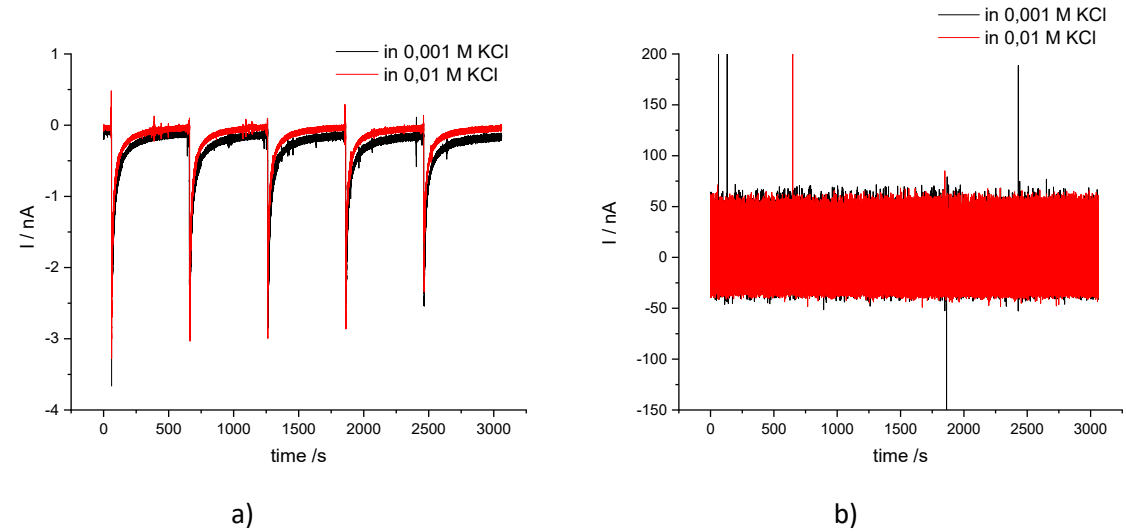

Figure 20. Chronoamperometric response recorded for K^+-SC-ISE (Replicate 1) in starting solution 0.01 M and 0.001 M KCl during stepwise 10 % concentration addition of 0.1 M KCl before damaging the ISM (a) and after damaging the ISM (b) with 0.1 M NaCl as BGE See also Appendix K

3.2.3 Electrochemical Impedance spectroscopy

The impedance spectra of K^+-SC-ISEs are demonstrated in Figure 21. Before membrane damaging the impedance spectrum of the K^+-SC-ISE (Replicate 1) is very similar to the spectrum of Cl^--SC-ISE. Both demonstrated a high-frequency semicircle (indicating the formation of the ISM) originating from the bulk resistance and of the membrane together with its geometric capacitance.

The bulk resistance which was equal to the diameter of the semicircle was 500 kΩ, which is 5 times larger than it was in Cl^--SC-ISE, considering that Replicate 1 was with the smallest resistance value (Figure 21 and Appendix D). The low-frequency tail showed a 40° angle, which is very close to the 45° Warburg impedance. This is because potassium ions diffuse to and from the solid-contact ISE. The low-frequency capacitance (C_L) was estimated from the imaginary impedance value ($-Z'' = 50$ kΩ) at $f = 0.01$ Hz, as follows: $C_L = (2\pi \times 0.01\text{Hz} \times 50000\ \Omega)^{-1}$ F = 318 μF.

However, the impedance spectrum of the damaged electrode shows the beginning of a semicircle that gradually tends towards a capacitive line. This behaviour can be explained when considering that damaging of the ISM exposes part of the PEDOT(PSS) film to the electrolyte solution. This facilitates the reversible oxidation of PEDOT. Estimating the low-frequency capacitance (C_L) from the imaginary impedance value ($-Z'' = 3.5$ kΩ) at $f = 0.01$ Hz, resulted in $C_L = 4.5$ mF, which is higher than expected for a 2 mC film of PEDOT(PSS).

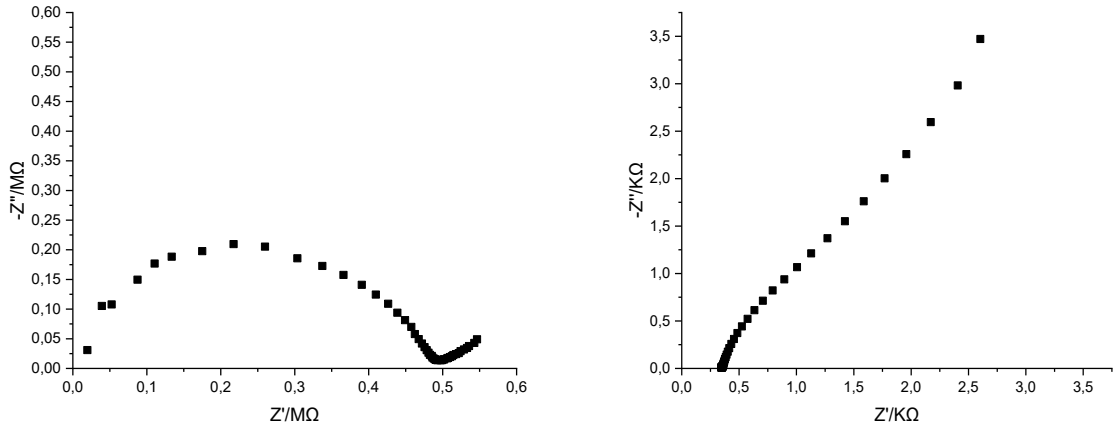

Figure 21. Electrochemical Impedance Spectrum recorded for potassium SC-ISEs before (a) and after damaging the ISM (b). The direct current potential is open circuit potential (0.13V). The frequency range is 100 kHz to 10 mHz. Electrolyte = 0.1M KCl.

Summary

In this thesis, the functionality of solid-contact ISEs with physically damaged ISMs was studied applying a novel ion-to-electron signal transduction method and a comparison between potentiometric, coulometric and amperometric methods was made. Two types of solid-contact ion-selective electrodes (SC-ISEs) were prepared: PEDOT doped with chloride anions (Cl^-), *i.e.,* PEDOT(Cl) and PEDOT doped with poly(styrene sulfonate) (PSS), *i.e.* PEDOT(PSS) were used as solid-contact in the fabrication of Cl^--SC-ISEs and K^+-SC-ISEs. Chronoamperometry, chronocoulometry, chronopotentiometry and electrochemical impedance spectroscopic measurements were carried out on the prepared electrodes. Then deliberate damage on the ion-selective membrane (ISM) of the electrode was done and the above-mentioned measurements were conducted again. The idea behind this was to compare the potentiometric, coulometric and amperometric response of the electrodes before and after damaging the ISM, to find out which of the methods was most sensitive to electrode damage.

The linearity ranges from potentiometric calibration curves before and after damaging the ISM was found to be 10^{-1} M to 10^{-4} M in the case of Cl^--SC-ISEs and 10^{-1} M to 10^{-5} M in the case of K^+-SC-ISEs with and without BGE. The linear slopes for chloride and potassium SC-ISEs demonstrated close to Nernstian values, with lower (close to near-Nernstian) values measured with BGE in the case of potassium SC-ISEs before damaging the ISM. However, chloride SC-ISEs demonstrated near-Nernstian behaviour (-57.4 ± 4.6 mV (mean $\pm$ $s_{d,}$ n=3)) even after damaging the ISM, stating that electrodes were still functioning, which was not the case for damaged potassium SC-ISEs.

Potentiometric measurements carried out before and after damaging the ISM demonstrated very similar responses for chloride ISEs, only a slight potential drift was noticed, and more time was required for potential stabilization. Similarly, coulometric results demonstrated stable accumulation of charge but a steady perceptible drift in response was also observed due to potential instability and/or damages of the ISM. However, the amperometric results revealed differences – after damaging the membrane the current response showed a significant increase in baseline noise (more than 20 times) that was not observed before damages on the ISM. This tremendous baseline noise in amperometric measurements proved that the chloride SC-ISE was not functioning properly. Hence, amperometry could be used to detect physical damage to an SC-ISE.

In the case of chloride SC-ISEs, the potentiometric and coulometric measurement results were reasonable even after damaging the ISM, which could falsely indicate that the electrode

functioned properly. The potentiometric calibration curves, after damaging the ISM, still showed adequate, near-Nernstian slope value. It can be because the exposed PEDOT(Cl) film can also give a response to Cl^-, and therefore the chloride SC-ISEs was functioning even after damaging the ISM. Nevertheless, chronoamperometric measurement results showed that the Cl^--SC-ISEs was not functioning properly due to the baseline noise effect, because of damages on the ISM.

Potentiometric measurements without BGE carried out before and after damaging the ISM demonstrated very dissimilar responses for potassium SC-ISEs. After damaging the ISM, a significant potential drift was noted and the response to K^+ has deteriorated. Similarly, coulometric measuring results demonstrated the same significant drift and only a minor accumulation of charge for about ~0.02 μC for every step of addition in concentration. The amperometric responses showed similar results as for chloride SC-ISEs – after damaging the membrane the current response showed a significant increase in baseline noise (around 80 times). All measurements taken for K^+-SC-ISEs with BGE showed inadequate responses. This can be related to interference from BGE due to the non-functionality of the electrode's ISM. The non-functionality of the damaged K^+-SC-ISEs was also clearly proven by the potentiometric calibration curve, showing non-Nernstian behaviour both with and without BGE. A significant potential drift existed in both cases (with and without BGE). However, without BGE there was still some attempt in responses for every 10 % increase in concentration that was not seen with BGE. Overall, the fact that K^+-SC-ISEs were non-functioning after damages on the surface of ISM was proven by all measurement methods used.

To sum up, which method would be more precise, accurate and suitable to examine the electrode functionality depends on the type of electrode used and the background electrolyte present. For instance, chloride SC-ISEs demonstrated near-Nernstian potentiometric response even after damaging the ISM. Most probably that PEDOT(Cl) itself responded to Cl^-, as stated above. However, the malfunctioning of the damaged potassium selective SC-ISEs was visible in all measurements. Nevertheless, it was clearly illustrated that the chronoamperometric method was more reliable and suitable for testing the functionality of SC-ISEs, where non-functionality after damaging the ISM was demonstrated in both types of electrodes.

Results from the electrochemical impedance spectroscopic measurements for chloride and potassium SC-ISEs demonstrated that, before membrane damage, the impedance spectra showed a high-frequency semicircle (indicating the formation of the ISM) coming from the bulk resistance of the ion-selective membrane. However, for chloride SC-ISEs, the low-frequency tail was estimated as an almost ideal capacitor with a phase angle close to 90°. In the

case of potassium SC-ISEs, the low-frequency tail showed 40° angle, which was very close to 45° Warburg impedance. This was related to the diffusion of potassium ions to and from the solid-contact ISE. However, the impedance spectra of the damaged electrodes showed a dramatic decrease in the overall impedance and the absence of a clear high-frequency semicircle for both chloride and potassium SC-ISEs. This behaviour can be explained when considering that damaging of the ISM exposes part of the PEDOT film to the electrolyte solution. This facilitates the reversible oxidation of PEDOT.

References

[1] E. Brauer, "J. Koryta: *Ions, Electrodes and Membranes* , John Wiley & Sons Ltd., Chichester, New York, Brisbane, Toronto, Singapore 1982. 197 Seiten, Preis: £ 7.90," *Berichte Bunsenges. Für Phys. Chem.*, vol. 86, no. 11, pp. 1090–1090, Nov. 1982, DOI: 10.1002/bbpc.198200043.

[2] E. Bakker, P. Bühlmann, and E. Pretsch, "Carrier-based ion-selective electrodes and bulk optodes. 1. General characteristics," *Chem. Rev.*, vol. 97, no. 8, pp. 3083–3132, 1997.

[3] J. Bobacka, "Conducting Polymer-Based Solid-State Ion-Selective Electrodes," *Electroanalysis*, vol. 18, pp. 7–18, Oct. 2005, DOI: 10.1002/elan.200503384.

[4] S. Anastasova *et al.*, "Development of miniature all-solid-state potentiometric sensing system," *Sens. Actuators B Chem.*, vol. 146, pp. 199–205, Apr. 2010, DOI: 10.1016/j.snb.2010.02.044.

[5] "Ion-Selective Electrode - an overview | ScienceDirect Topics." https://www.sciencedirect.com/topics/materials-science/ion-selective-electrode (accessed Apr. 22, 2021).

[6] J. Janata, *Principles of Chemical Sensors*. Springer Science & Business Media, 2010.

[7] Cattrall W.R., *Chemical Sensors*, 1st ed. Great Clarendon Street, Oxford OX2 6DP, Great Britain: Oxford University Press, 1997.

[8] E. Bakker and M. Telting-Diaz, "Electrochemical sensors," *Anal. Chem.*, vol. 74, no. 12, pp. 2781–2800, 2002.

[9] R. W. Cattrall and I. C. Hamilton, "Coated-Wire Ion-Selective Electrodes," in *Ion-Selective Electrode Reviews*, vol. 6, J. D. R. Thomas, Ed. Elsevier, 1984, pp. 125–172. DOI: 10.1016/B978-0-08-033201-7.50009-8.

[10] R. W. Cattrall and H. Freiser, "Coated wire ion-selective electrodes," p. 2.

[11] J. Bobacka, "Potential Stability of All-Solid-State Ion-Selective Electrodes Using Conducting Polymers as Ion-to-Electron Transducers," *Anal. Chem.*, vol. 71, no. 21, pp. 4932–4937, Nov. 1999, DOI: 10.1021/ac990497z.

[12] A. Michalska, A. Hulanicki, and A. Lewenstam, "All solid-state hydrogen ion-selective electrode based on a conducting poly(pyrrole) solid contact," *Analyst*, vol. 119, no. 11, pp. 2417–2420, Jan. 1994, DOI: 10.1039/AN9941902417.

[13] W.-S. Han, M.-Y. Park, K.-C. Chung, D.-H. Cho, and T.-K. Hong, "All Solid State Hydrogen Ion Selective Electrode Based on a Tribenzylamine Neutral Carrier in a Poly(vinyl chloride) Membrane with a Poly(aniline) Solid Contact," *Electroanalysis*, vol.

13, no. 11, pp. 955–959, 2001, DOI: https://doi.org/10.1002/1521-4109(200107)13:11<955::AID-ELAN955>3.0.CO;2-5.

[14] K. N. Mikhelson, "Ion-selective electrodes in PVC matrix," *Sens. Actuators B Chem.*, vol. 18, no. 1, pp. 31–37, Mar. 1994, DOI: 10.1016/0925-4005(94)87051-9.

[15] M. Imoto, T. Sakaki, and T. Osakai, "Sophisticated Design of PVC Membrane Ion-Selective Electrodes Based on the Mixed Potential Theory," *Anal. Chem.*, vol. 85, no. 9, pp. 4753–4760, May 2013, DOI: 10.1021/ac400427p.

[16] K. Mikhelson, "AC-Impedance Studies of Ion Transfer Across Ionophore-Based Ion-Selective Membranes," *Chem. Anal.*, vol. 51, Jan. 2006.

[17] J. Wang, *Analytical electrochemistry*, 3rd ed. Hoboken, N.J: Wiley-VCH, 2006.

[18] T. Lindfors, P. Sjöberg, J. Bobacka, A. Lewenstam, and A. Ivaska, "Characterization of a single-piece all-solid-state lithium-selective electrode based on soluble conducting polyaniline," *Anal. Chim. Acta*, vol. 385, no. 1, pp. 163–173, Apr. 1999, DOI: 10.1016/S0003-2670(98)00587-X.

[19] D. Ammann, E. Pretsch, W. Simon, E. Lindner, A. Bezegh, and E. Pungor, "Lipophilic salts as membrane additives and their influence on the properties of macro- and micro-electrodes based on neutral carriers," *Anal. Chim. Acta*, vol. 171, pp. 119–129, May 1985, DOI: 10.1016/S0003-2670(00)84189-6.

[20] R. D. Armstrong and G. Horvai, "Properties of PVC based membranes used in ion-selective electrodes," *Electrochimica Acta*, vol. 35, no. 1, pp. 1–7, Jan. 1990, DOI: 10.1016/0013-4686(90)85028-L.

[21] K. N. Mikhelson, "ISE Constructions," in *Ion-Selective Electrodes*, K. N. Mikhelson, Ed. Berlin, Heidelberg: Springer, 2013, pp. 135–148. DOI: 10.1007/978-3-642-36886-8_8.

[22] P. Bühlmann and L. D. Chen, "Ion-Selective Electrodes With Ionophore-Doped Sensing Membranes," in *Supramolecular Chemistry*, American Cancer Society, 2012. DOI: 10.1002/9780470661345.smc097.

[23] "Valinomycin | Sigma-Aldrich." https://www.sigmaaldrich.com/catalog/substance/valinomycin111132200195811?lang=en&region=CA&gclid=Cj0KCQjw78yFBhCZARIsAOxgSx3th5VdUEr_UcS2WaWzjyO2YGdamNGVVy5JcpjEI-9t-eeiuwyskSEaAp1TEALw_wcB (accessed May 30, 2021).

[24] J. Bobacka, A. Ivaska, and A. Lewenstam, "Potentiometric Ion Sensors Based on Conducting Polymers," *Electroanalysis*, vol. 15, no. 5–6, pp. 366–374, 2003, DOI: 10.1002/elan.200390042.

[25] "Electrical and Optical Polymer Systems: Fundamentals: Methods, and Applications," *Routledge & CRC Press*. https://www.routledge.com/Electrical-and-Optical-Polymer-Systems-Fundamentals-Methods-and-Applications/Wise/p/book/9780824701185 (accessed May 01, 2021).

[26] P. Chandrasekhar, *Conducting Polymers, Fundamentals and Applications: A Practical Approach*. Springer US, 1999. DOI: 10.1007/978-1-4615-5245-1.

[27] M. Gvozdenovic, B. Jugovic, J. Stevanovic, and B. Grgur, "Electrochemical synthesis of electroconducting polymers," *Hem. Ind.*, vol. 68, no. 6, pp. 673–684, 2014, DOI: 10.2298/HEMIND131122008G.

[28] P. Y. Yu and M. Cardona, *Fundamentals of Semiconductors*. Berlin, Heidelberg: Springer Berlin Heidelberg, 2010. DOI: 10.1007/978-3-642-00710-1.

[29] A. MacDiarmid, "Synthetic Metals: A Novel Role for Organic Polymers," *Synth. Met.*, vol. 125, pp. 11–22, Nov. 2001, DOI: 10.1016/S0379-6779(01)00508-2.

[30] A. J. Heeger, "Semiconducting and metallic polymers: the fourth generation of polymeric materials," *Synth. Met.*, vol. 125, no. 1, pp. 23–42, Nov. 2001, DOI: 10.1016/S0379-6779(01)00509-4.

[31] L. Groenendaal, F. Jonas, D. Freitag, H. Pielartzik, and J. R. Reynolds, "Poly(3,4-ethylenedioxythiophene) and Its Derivatives: Past, Present, and Future," *Adv. Mater.*, vol. 12, no. 7, pp. 481–494, 2000, DOI: https://doi.org/10.1002/(SICI)1521-4095(200004)12:7<481::AID-ADMA481>3.0.CO;2-C.

[32] G. Heywang and F. Jonas, "Poly(alkylenedioxythiophene)s—new, very stable conducting polymers," *Adv. Mater.*, vol. 4, no. 2, pp. 116–118, 1992, DOI: https://doi.org/10.1002/adma.19920040213.

[33] M. Av, Q. M, D. Mh, C. G, G. Cs, and V. K, "Exfoliation-induced nanoribbon formation of poly(3,4-ethylene dioxythiophene) PEDOT between MoS2 layers as cathode material for lithium batteries," *J. Power Sources*, vol. 156, no. 2, pp. 615–619, 2006.

[34] "Allen J. Bard and Larry R. Faulkner, Electrochemical Methods: Fundamentals and Applications, New York: Wiley, 2001, 2nd ed.," *Russ. J. Electrochem.*, vol. 38, no. 12, pp. 1364–1365, Dec. 2002, DOI: 10.1023/A:1021637209564.

[35] B. Dlamini, "Principles of Electrochemistry Wiley 1993 2", Accessed: May 08, 2021. [Online]. Available: https://www.academia.edu/4119906/Principles_of_Electrochemistry_Wiley_1993_2

[36] K. Ren, "Selectivity problems of membrane ion-selective electrodes," *Fresenius J. Anal. Chem.*, vol. 365, no. 5, pp. 389–397, Oct. 1999, DOI: 10.1007/s002160051629.

[37] E. Hupa, U. Vanamo (née Mattinen), and J. Bobacka, “Novel Ion-to-Electron Transduction Principle for Solid-Contact ISEs,” *Electroanalysis*, vol. 27, Jan. 2015, DOI: 10.1002/elan.201400596.

[38] U. Vanamo, E. Hupa, V. Yrjänä, and J. Bobacka, “New signal readout principle for solid-contact ion-selective electrodes,” *Anal. Chem.*, vol. 88, no. 8, 2016, DOI: 10.1021/acs.analchem.5b04800.

[39] G. Dimeski, T. Badrick, and A. S. John, “Ion Selective Electrodes (ISEs) and interferences—A review,” *Clin. Chim. Acta*, vol. 411, no. 5, pp. 309–317, Mar. 2010, DOI: 10.1016/j.cca.2009.12.005.

[40] E. Grygolowicz-Pawlak and E. Bakker, “Thin Layer Coulometry with Ionophore Based Ion-Selective Membranes,” *Anal. Chem.*, vol. 82, no. 11, pp. 4537–4542, Jun. 2010, DOI: 10.1021/ac100524z.

[41] T. Han, U. Mattinen, and J. Bobacka, “Improving the Sensitivity of Solid-Contact Ion-Selective Electrodes by Using Coulometric Signal Transduction,” *ACS Sens.*, vol. 4, no. 4, pp. 900–906, Apr. 2019, doi: 10.1021/acssensors.8b01649.

[42] T. Han, U. Vanamo, and J. Bobacka, “Influence of electrode geometry on the response of solid-contact ion-selective electrodes when utilizing a new coulometric signal readout method,” *ChemElectroChem*, vol. 3, no. 12, 2016, doi: 10.1002/celc.201600575.

[43] Southampton Electrochemistry Group and R. Greef, *Instrumental methods in electrochemistry.* London: Ellis Horwood, 1990.

[44] H. S. Crouch, *Principles of Instrumental Analysis 6th Edition*, 6th edition. Brooks Cole Pub., 2007.

[45] M. Mhammedi, K. Latifa, and C. Abdelilah, “Synthesis and Polymerization of Pyrole Characterization of Polypyrole,” *Leonardo Electron. J. Pract. Technol.*, vol. 6, Sep. 2007.

[46] M. Kesik *et al.*, “Synthesis and characterization of conducting polymers containing polypeptide and ferrocene side chains as ethanol biosensors,” *Polym. Chem.*, vol. 5, no. 21, pp. 6295–6306, Sep. 2014, DOI: 10.1039/C4PY00850B.

[47] “Electrochemical Methods: Fundamentals and Applications, 2nd Edition | Wiley,” *Wiley.com*. https://www.wiley.com/en-ir/Electrochemical+Methods%3A+Fundamentals+and+Applications%2C+2nd+Edition-p-9780471043720 (accessed May 10, 2021).

[48] J. R. Macdonald, “Impedance spectroscopy,” *Ann. Biomed. Eng.*, vol. 20, no. 3, pp. 289–305, May 1992, DOI: 10.1007/BF02368532.

[49] X. changjun and Q. shuhai, “Drawing impedance spectroscopy for Fuel Cell by EIS,” *Procedia Environ. Sci.*, vol. 11, pp. 589–596, Jan. 2011, DOI: 10.1016/j.proenv.2011.12.092.

[50] Z. Mousavi, J. Bobacka, A. Lewenstam, and A. Ivaska, “Response mechanism of potentiometric Ag+ sensor based on poly(3,4-ethylenedioxythiophene) doped with silver hexabromocarborane,” *J. Electroanal. Chem.*, vol. 593, no. 1, pp. 219–226, Aug. 2006, DOI: 10.1016/j.jelechem.2006.04.022.

[51] Z. Mousavi, J. Bobacka, A. Lewenstam, and A. Ivaska, “Poly(3,4-ethylenedioxythiophene) (PEDOT) doped with carbon nanotubes as ion-to-electron transducer in polymer membrane-based potassium ion-selective electrodes,” *J. Electroanal. Chem.*, vol. 633, no. 1, 2009, doi: 10.1016/j.jelechem.2009.06.005.

Appendices

Appendix A.

Cyclic voltammogram (2nd cycle) of GC/PEDOT(Cl) and GC/PEDOT(PSS) polymer films on SC-ISEs recorded in 0.1 M KCl electrolyte solution with 0.1 V/s scan rate

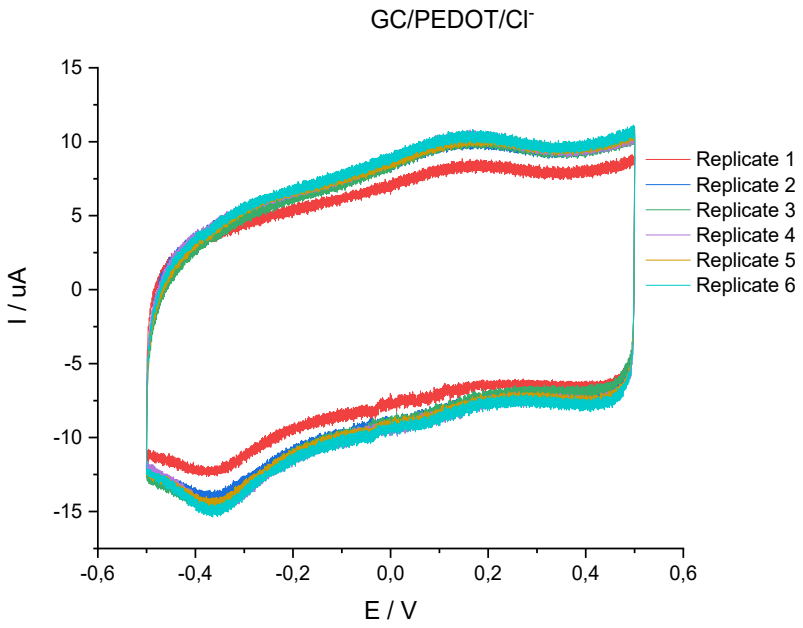

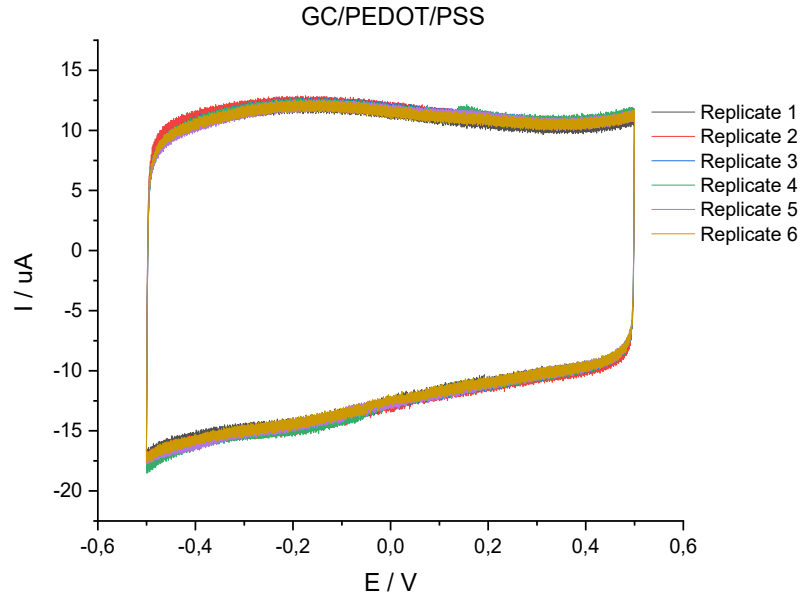

Appendix B

Table 1 a. The added volumes and change in concentration in 50 ml of 1 mM KCl starting solution using 5 % and 10 % addition.

Addition of volume of 100 mM KCl	Change in C_M of 1 mM KCl	Stepwise change in C_M	Addition of volume of 100 mM KCl	Change in C_M of 1 mM KCl	Stepwise change in C_M
25.3 µl	1.05 mM KCl	+5 %	50.6 µl	1.1 mM KCl	+10 %
25.3 µl	1.10 mM KCl	+5 %	50.7 µl	1.2 mM KCl	+10 %
25.4 µl	1.15 mM KCl	+5 %	50.8 µl	1.3 mM KCl	+10 %
25.4 µl	1.20 mM KCl	+5 %	50.9 µl	1.4 mM KCl	+10 %
25.5 µl	1.25 mM KCl	+5 %	51.0 µl	1.5 mM KCl	+10 %

Table 1 b. The added volumes and change in concentration in 50 ml of 10 mM KCl starting solution using 5 % and 10 % addition.

Addition of volume of 100 mM KCl	Change in C_M of 10 mM KCl	Stepwise change in C_M	Addition of volume of water	Change in C_M of 10 mM KCl	Stepwise change in C_M
279 µl	10.5 mM KCl	+5 %	562 µl	11.0 mM KCl	+10 %
283 µl	11.0 mM KCl	+5 %	575 µl	12.0 mM KCl	+10 %
286 µl	11.5 mM KCl	+5 %	587 µl	13.0 mM KCl	+10 %
289 µl	12.0 mM KCl	+5 %	601 µl	14.0 mM KCl	+10 %
292 µl	12.5 mM KCl	+5 %	616 µl	15.0 mM KCl	+10 %

Table 1 c. The added volumes and change in concentration in 50 ml of 100 mM KCl starting solution using 10 % dilution with deionized water.

Addition of volume of water	Change in C_M of 100 mM KCl	Stepwise change in C_M
5.6 ml	90 mM KCl	-10 %
6.9 ml	80 mM KCl	-10 %
8.9 ml	70 mM KCl	-10 %
11.9 ml	60 mM KCl	-10 %
16.7 ml	50 mM KCl	-10 %

Table 2. The added volumes and change in concentration of 50 ml of 1 mM and 10 mM KCl starting solution in deionized water or 100 mM NaCl as BGE using 10 % addition.

Addition of volume of 100 mM KCl*	Change in C_M of 1 mM KCl	Stepwise change in C_M	Addition of volume of 100 mM KCl*	Change in C_M of 10 mM KCl	Stepwise change in C_M
50.6 µl	1.1 mM KCl	+10 %	562 µl	11.0 mM KCl	+10 %
50.7 µl	1.2 mM KCl	+10 %	575 µl	12.0 mM KCl	+10 %
50.8 µl	1.3 mM KCl	+10 %	587 µl	13.0 mM KCl	+10 %
50.9 µl	1.4 mM KCl	+10 %	601 µl	14.0 mM KCl	+10 %
51.0 µl	1.5 mM KCl	+10 %	616 µl	15.0 mM KCl	+10 %

* In deionized water or 100 mM NaCl as BGE.

Appendix C

The surfaces of ISM of Cl^--SC-ISEs before and after physical damaging

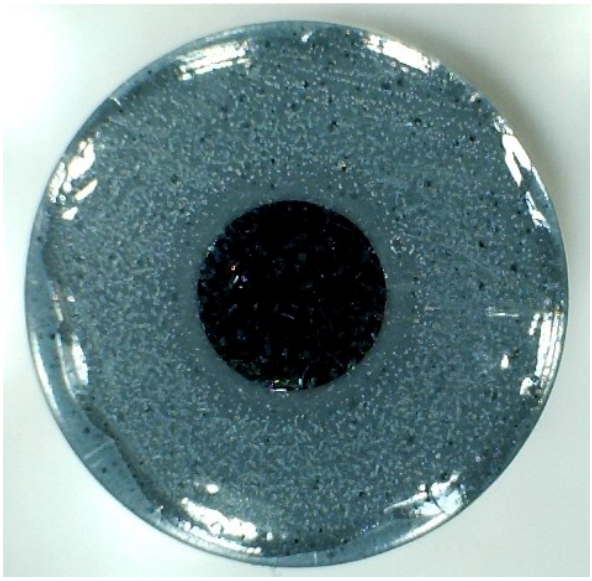

Replicate 2 before damaging ISM (control sample)

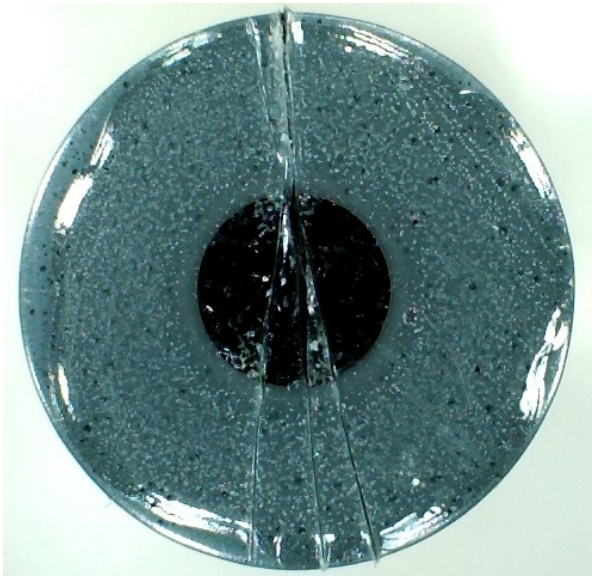

Replicate 2 after damaging ISM

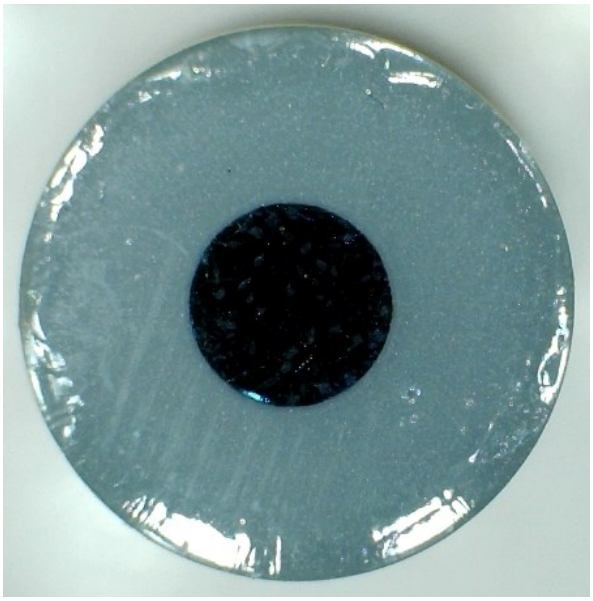

Replicate 5 before damaging ISM (control sample)

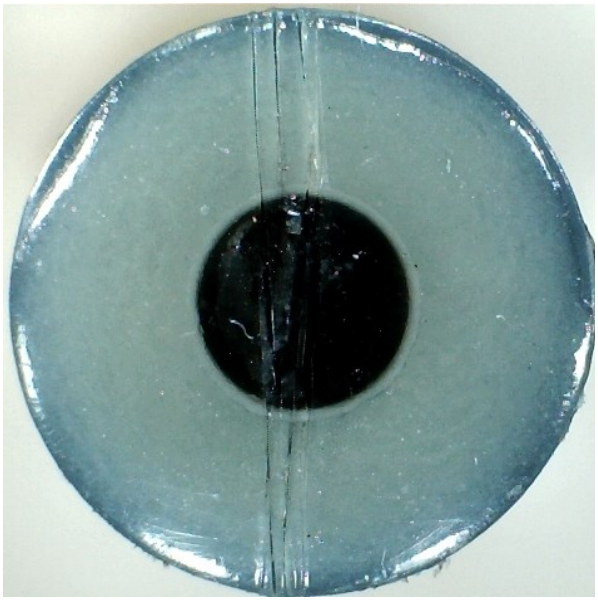

Replicate 5 after damaging ISM

NOT AVAILABLE

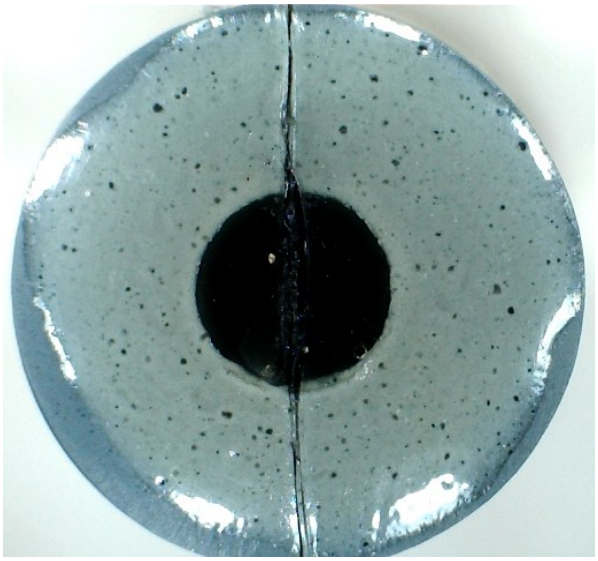

Replicate 6 before damaging ISM (control sample)

Replicate 6 after damaging ISM

The surfaces of ISM of K^+-SC-ISEs before and after physical damaging

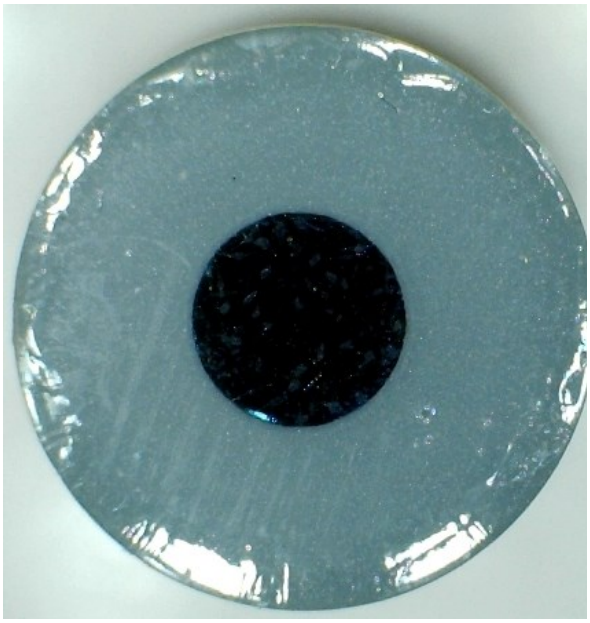

Replicate 1 before damaging ISM (control sample)

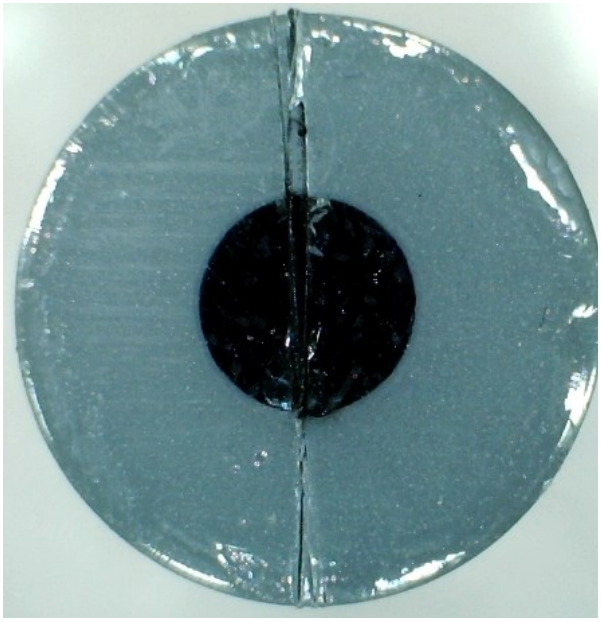

Replicate 1 after damaging ISM

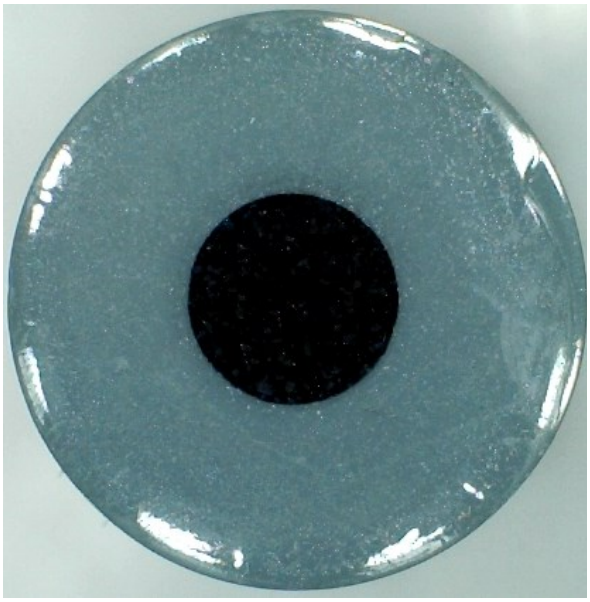

Replicate 2 before damaging ISM (control sample)

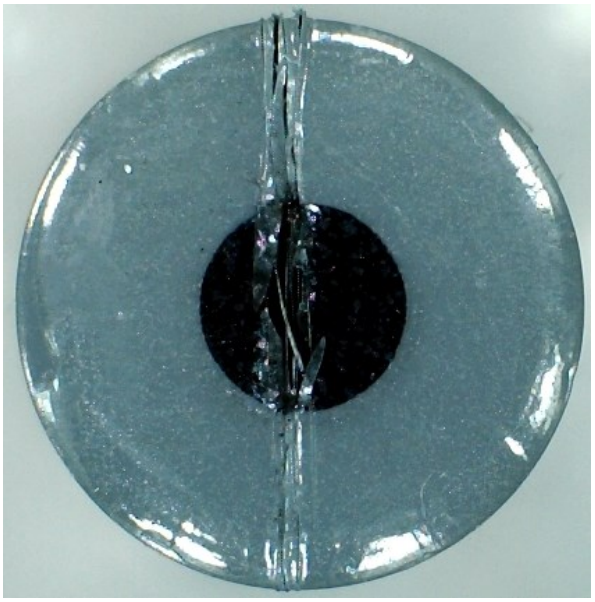

Replicate 2 after damaging ISM

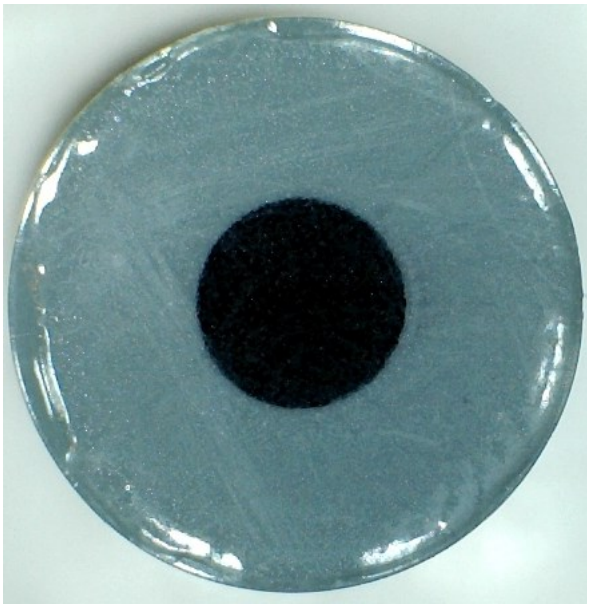

Replicate 5 before damaging ISM (control sample)

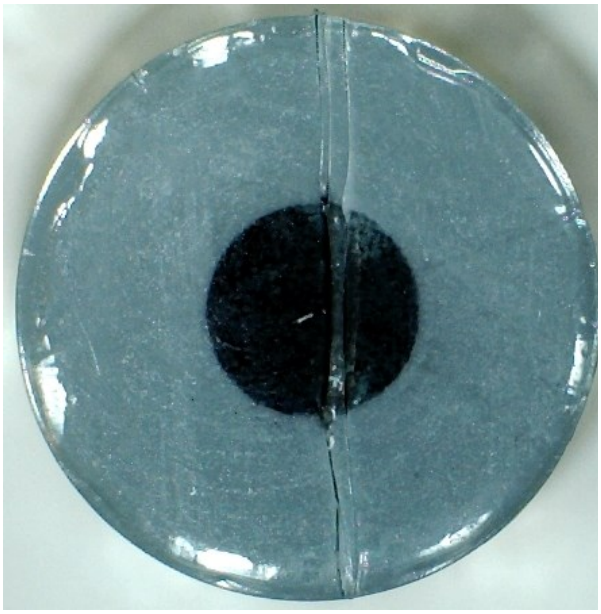

Replicate 5 after damaging ISM

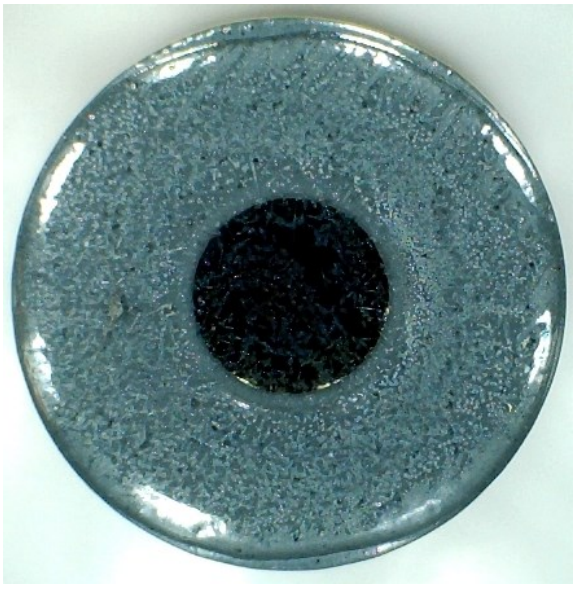

Replicate 6 before damaging ISM (control sample)

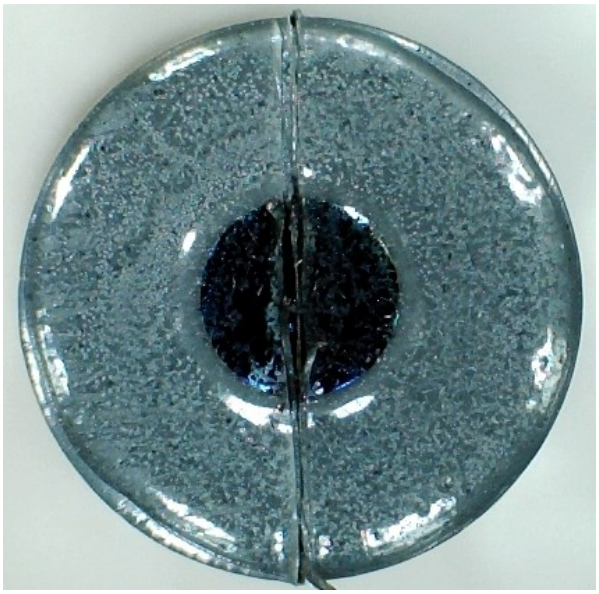

Replicate 6 after damaging ISM

Appendix D

Electrochemical Impedance Spectra recorded for Cl^--SC-ISEs after damaging the ISM. DC potential is open circuit potential (0.15V). Frequency range is 100 kHz to 10 mHz. Electrolyte = 0.1M KCl

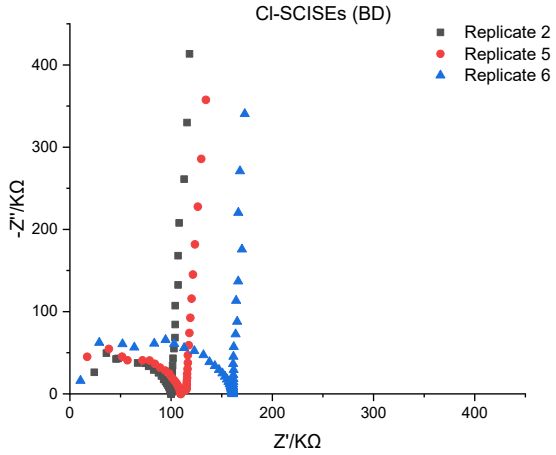

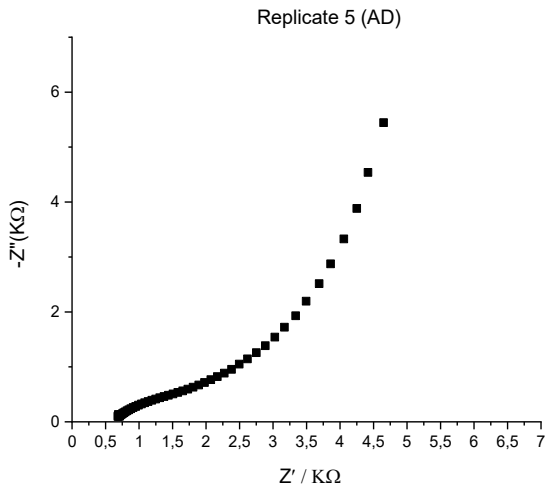

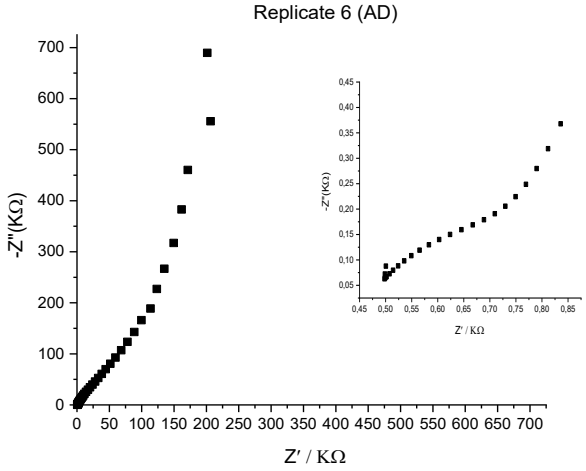

Appendix E

Chronopotentiometric responses recorded for chloride SC-ISEs in starting solution 0.001 M, 0.01 M KCl during stepwise 5 % and 10 % addition and in starting solution 0.1 M KCl during stepwise 10 % dilution in concentration before damaging (BD) and after damaging (AD) the ISM

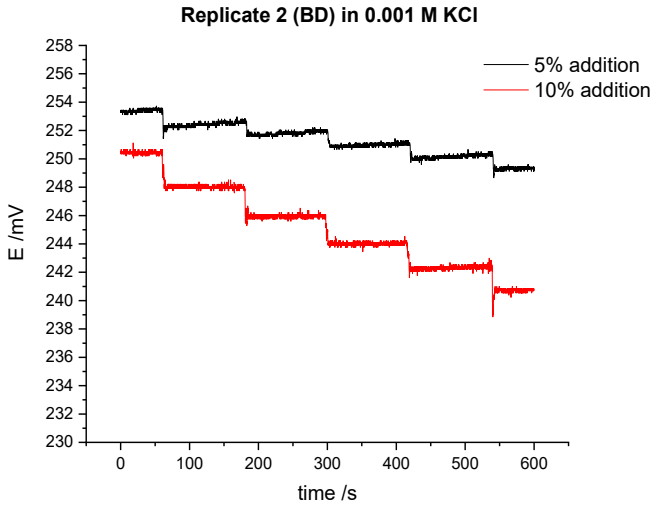

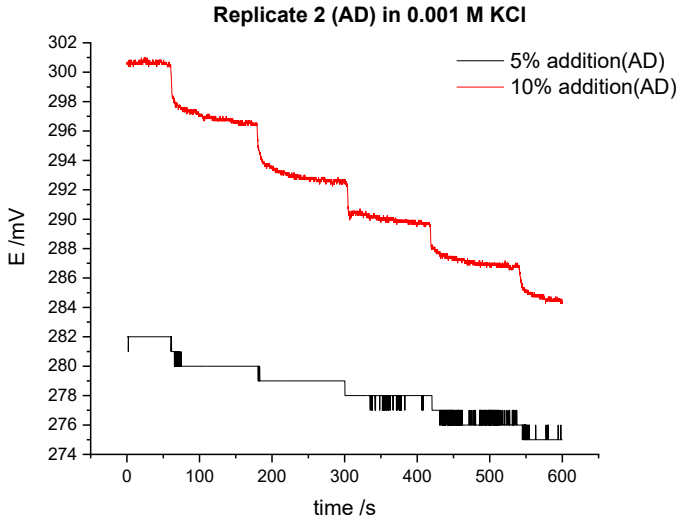

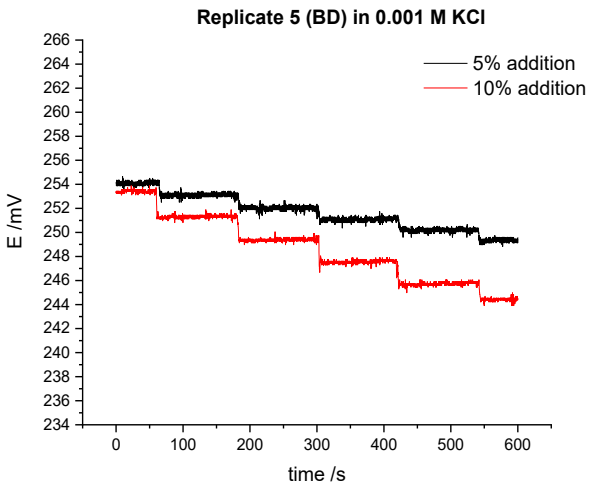

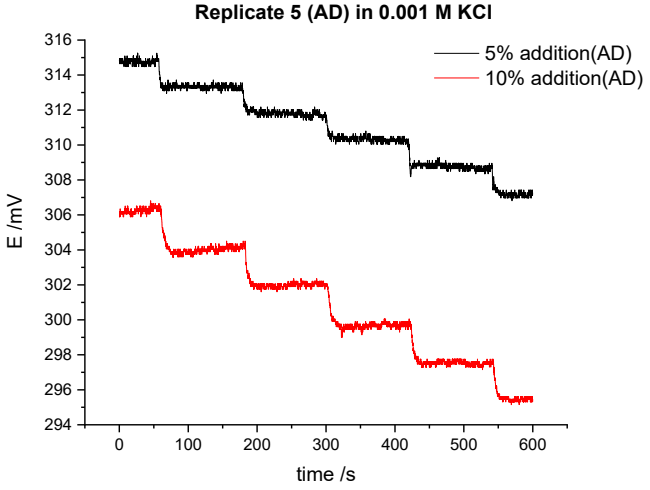

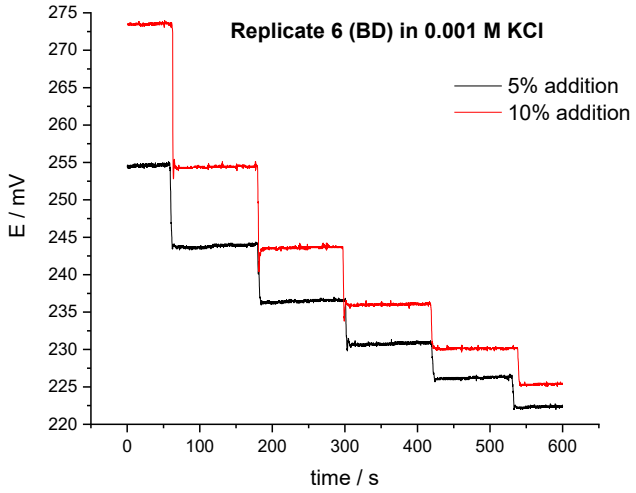
Replicate 6 (BD) in 0.001 M KCl
5% addition
10% addition
E / mV
time / s

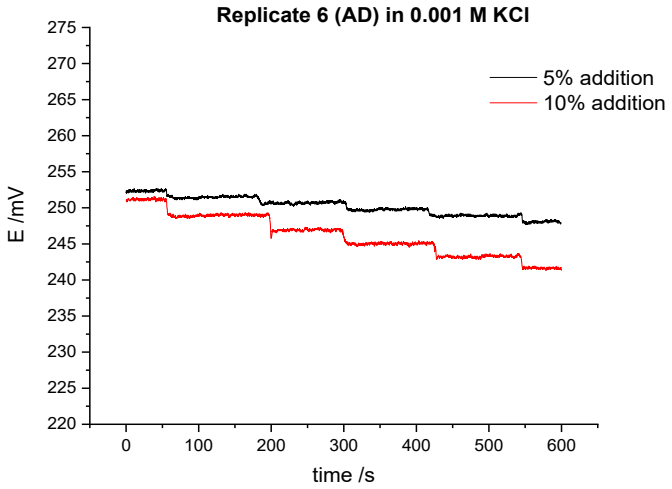
Replicate 6 (AD) in 0.001 M KCl
5% addition
10% addition
E /mV
time /s

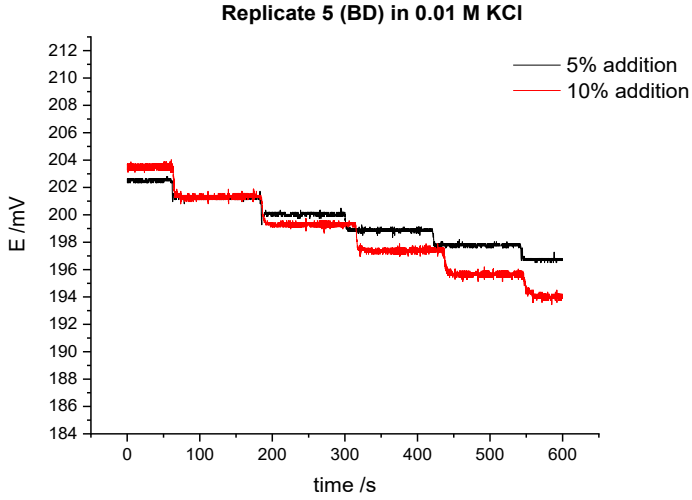
Replicate 5 (BD) in 0.01 M KCl
5% addition
10% addition
E /mV
time /s

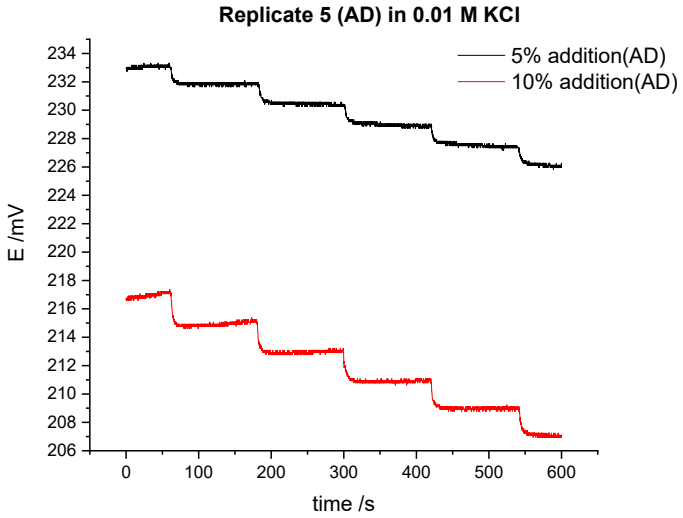
Replicate 5 (AD) in 0.01 M KCl
5% addition(AD)
10% addition(AD)
E /mV
time /s

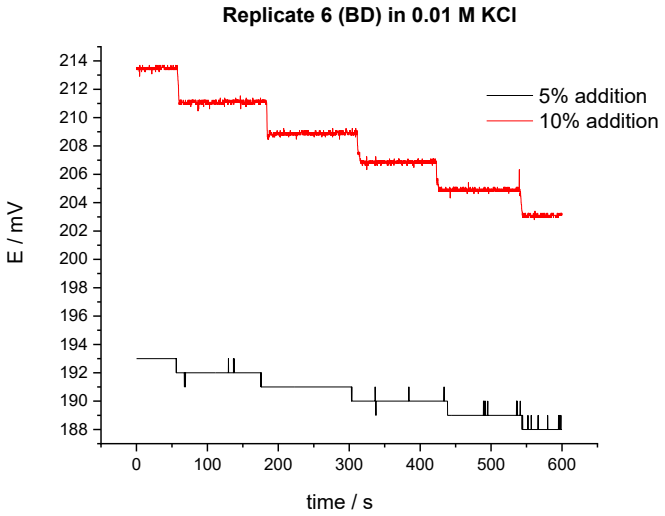
Replicate 6 (BD) in 0.01 M KCl
E / mV
time / s
5% addition
10% addition

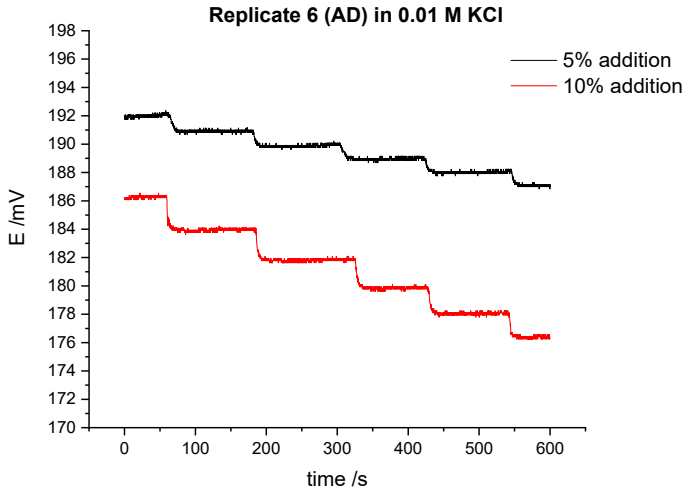
Replicate 6 (AD) in 0.01 M KCl
E /mV
time /s
5% addition
10% addition

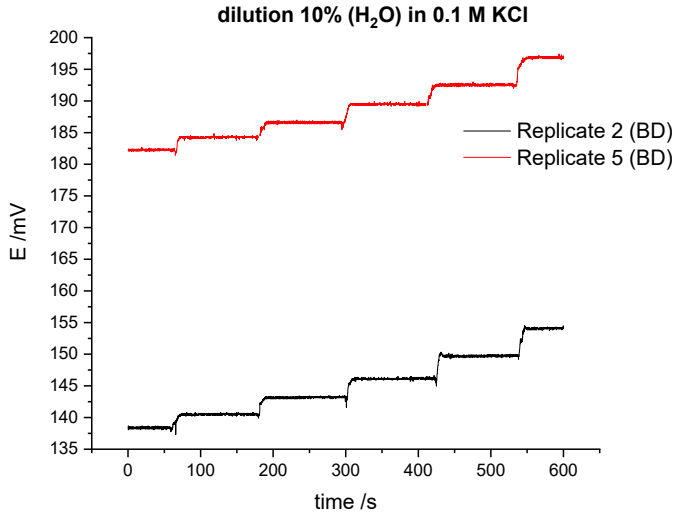
dilution 10% (H2O) in 0.1 M KCl
E /mV
time /s
Replicate 2 (BD)
Replicate 5 (BD)

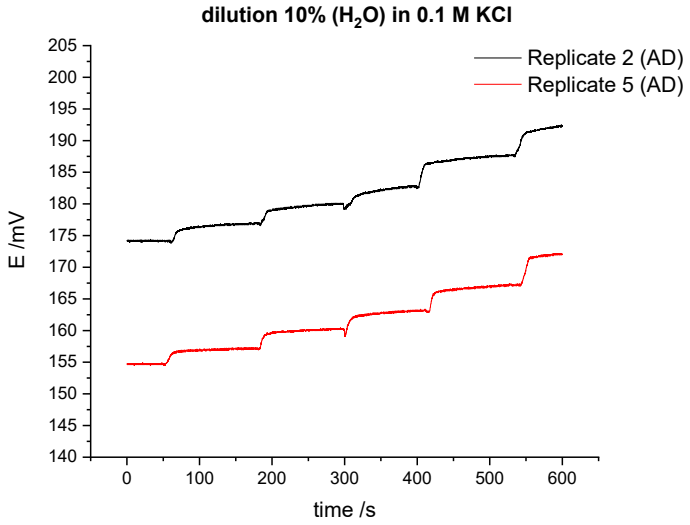
dilution 10% (H2O) in 0.1 M KCl
E /mV
time /s
Replicate 2 (AD)
Replicate 5 (AD)

Appendix F

Chronocoulometric responses recorded for chloride SC-ISEs in starting solution 0.001 M, 0.01 M KCl during stepwise 5 % and 10 % addition and in starting solution 0.1 M KCl during stepwise 10 % dilution in concentration before damaging (BD) and after damaging (AD) the ISM

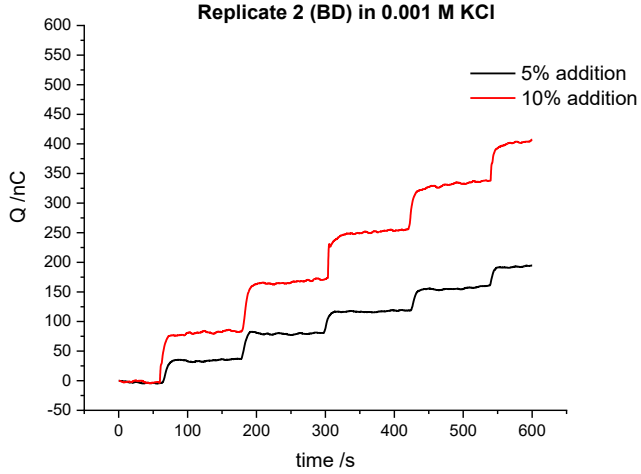

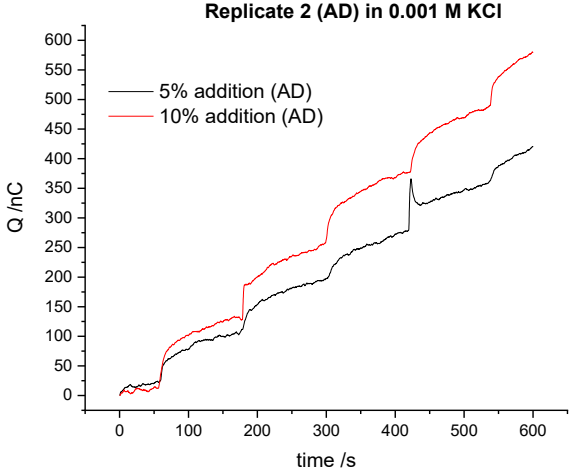

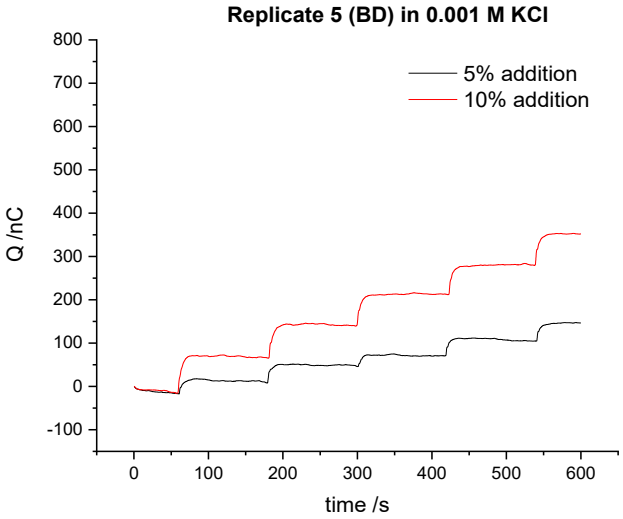

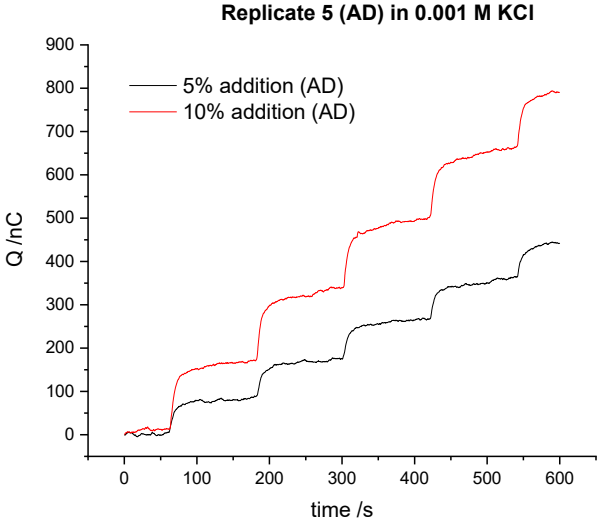

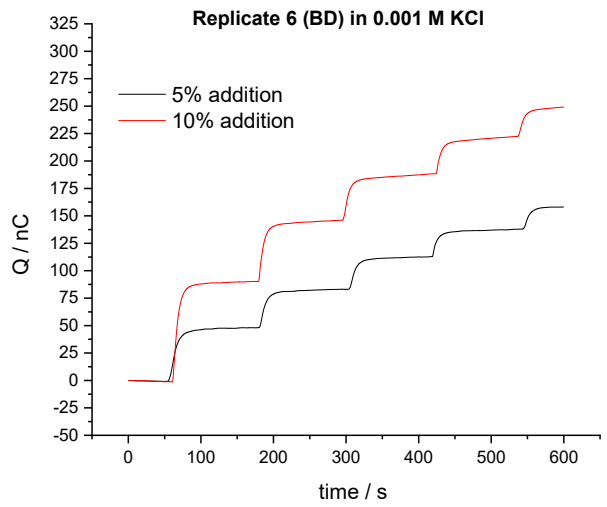
Replicate 6 (BD) in 0.001 M KCl
5% addition
10% addition
Q / nC
time / s

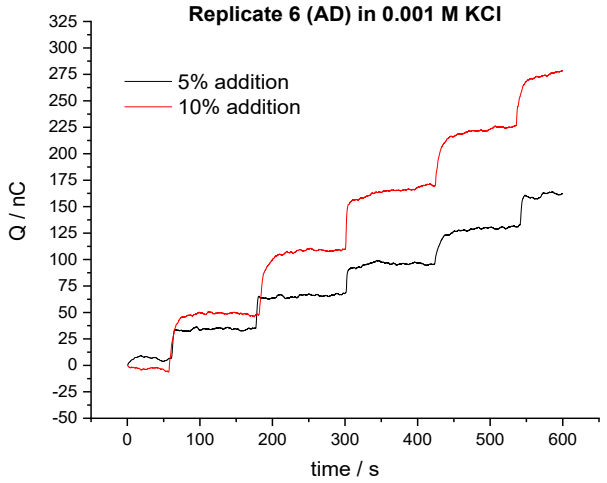
Replicate 6 (AD) in 0.001 M KCl
5% addition
10% addition
Q / nC
time / s

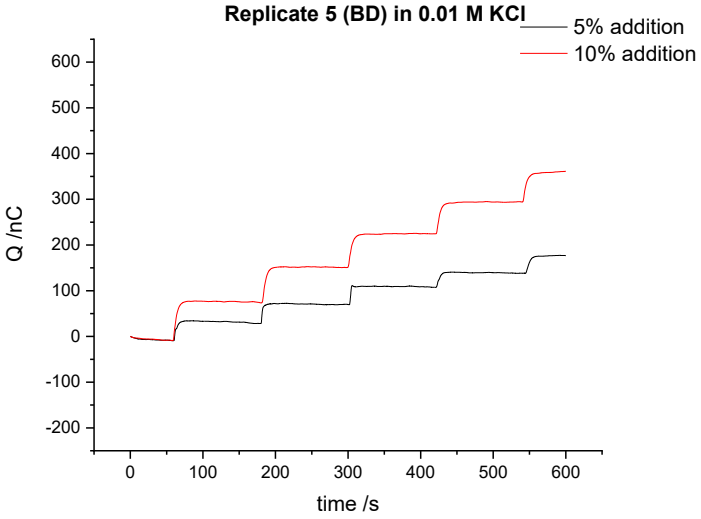
Replicate 5 (BD) in 0.01 M KCl
5% addition
10% addition
Q /nC
time /s

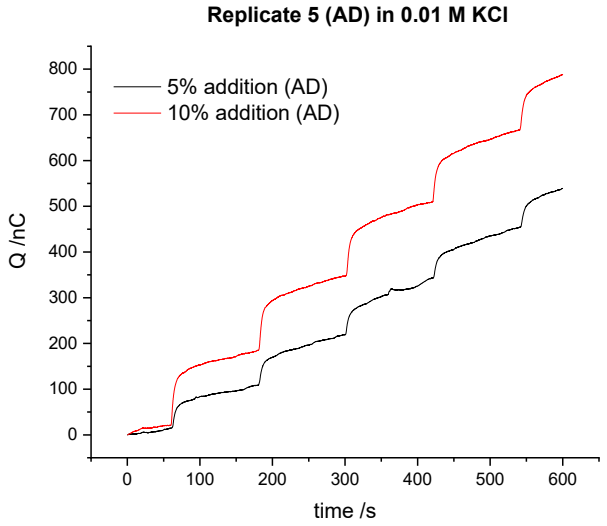
Replicate 5 (AD) in 0.01 M KCl
5% addition (AD)
10% addition (AD)
Q /nC
time /s

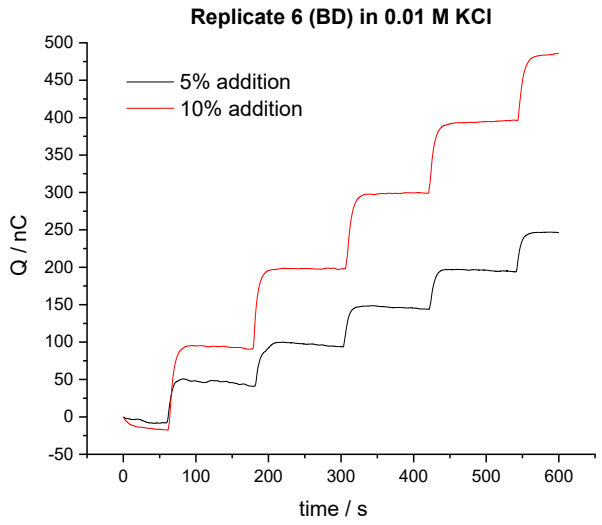
Replicate 6 (BD) in 0.01 M KCl
5% addition
10% addition
Q / nC
time / s

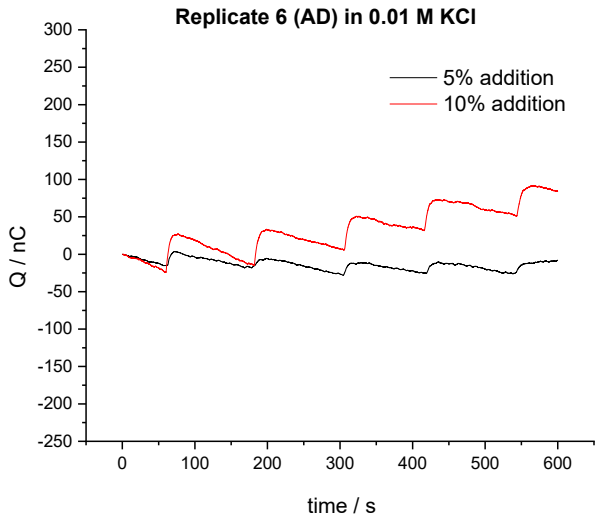
Replicate 6 (AD) in 0.01 M KCl
5% addition
10% addition
Q / nC
time / s

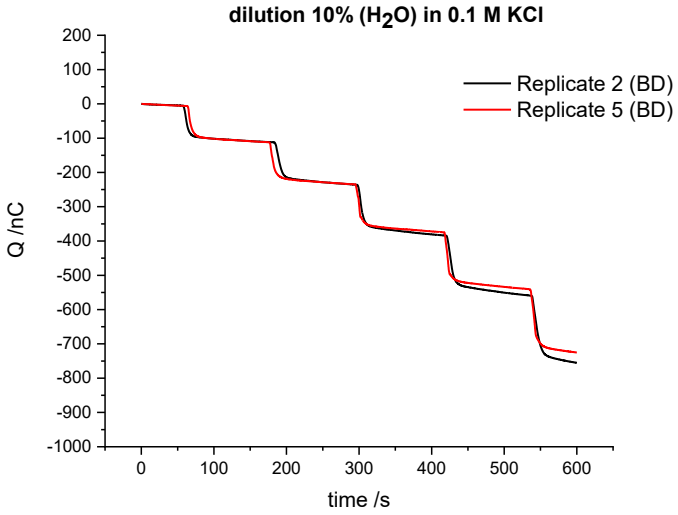
dilution 10% (H2O) in 0.1 M KCl
Replicate 2 (BD)
Replicate 5 (BD)
Q /nC
time /s

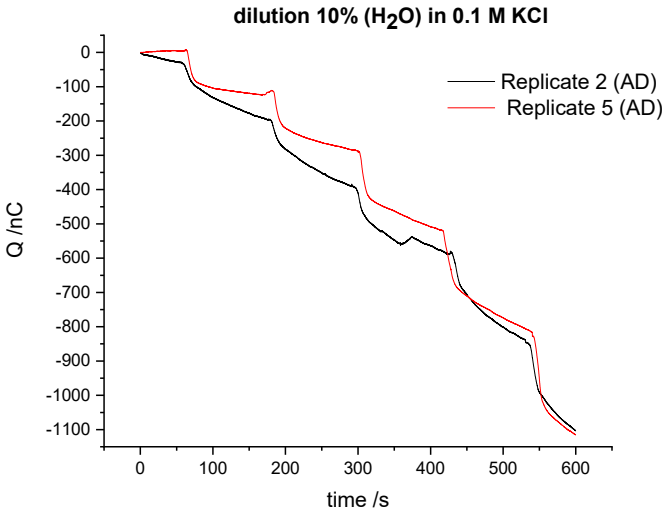
dilution 10% (H2O) in 0.1 M KCl
Replicate 2 (AD)
Replicate 5 (AD)
Q /nC
time /s

Appendix G

Chronoamperometric responses recorded for chloride SC-ISEs in starting solution 0.001 M, 0.01 M KCl during stepwise 5 % and 10 % addition and in starting solution 0.1 M KCl during stepwise 10 % dilution in concentration before damaging (BD) and after damaging (AD) the ISM

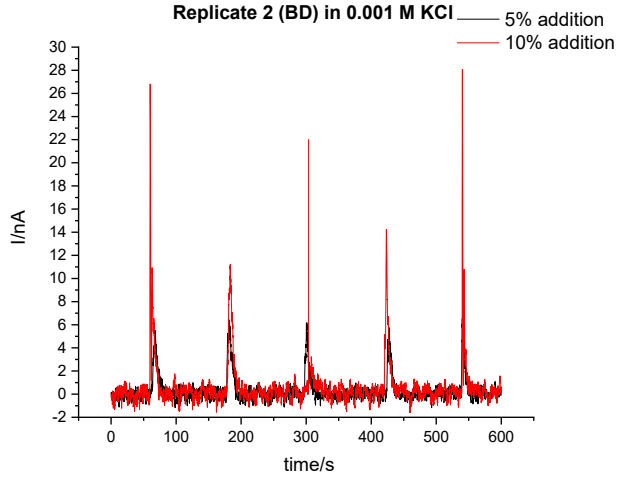

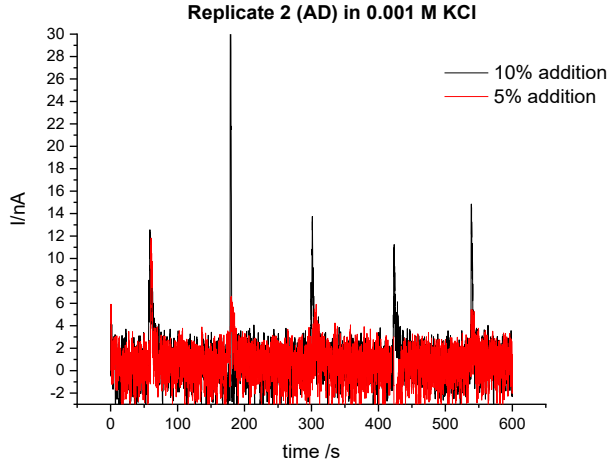

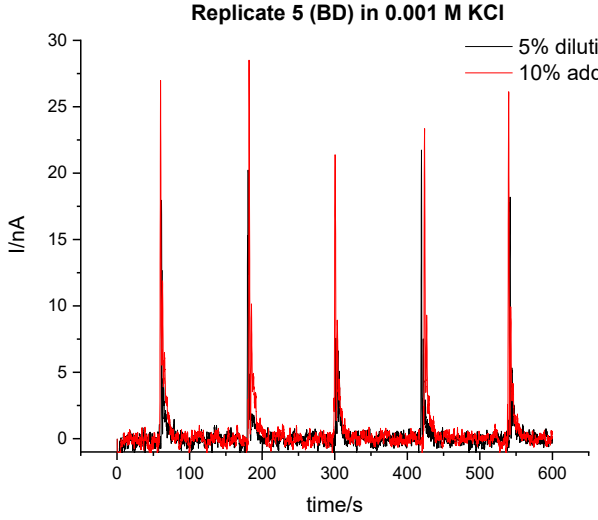

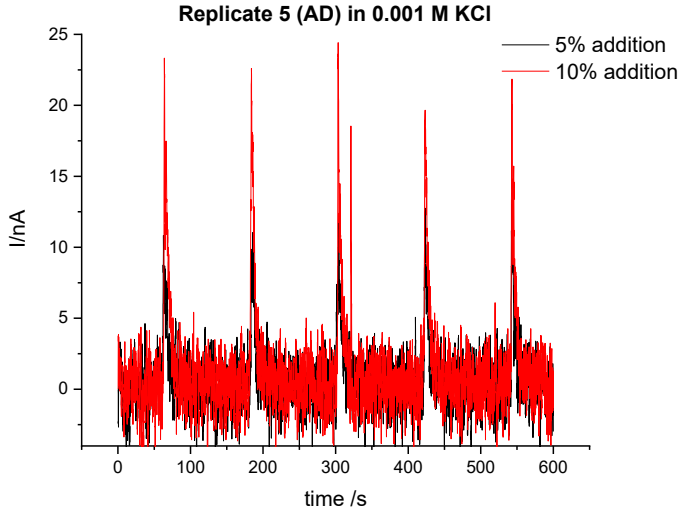

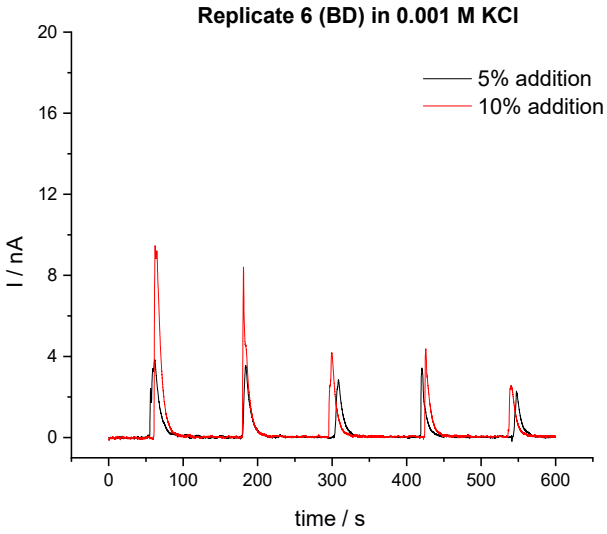
Replicate 6 (BD) in 0.001 M KCl
5% addition
10% addition
I / nA
time / s

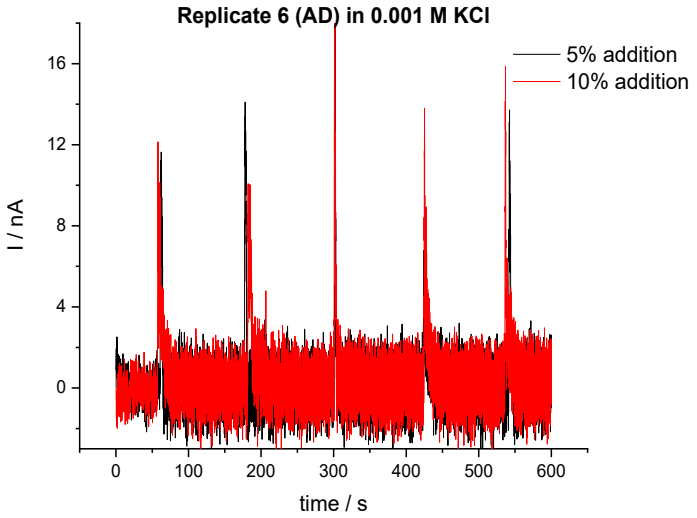
Replicate 6 (AD) in 0.001 M KCl
5% addition
10% addition
I / nA
time / s

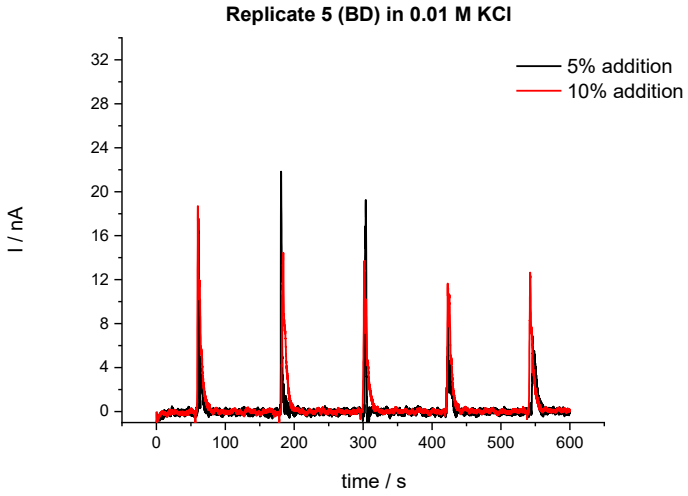
Replicate 5 (BD) in 0.01 M KCl
5% addition
10% addition
I / nA
time / s

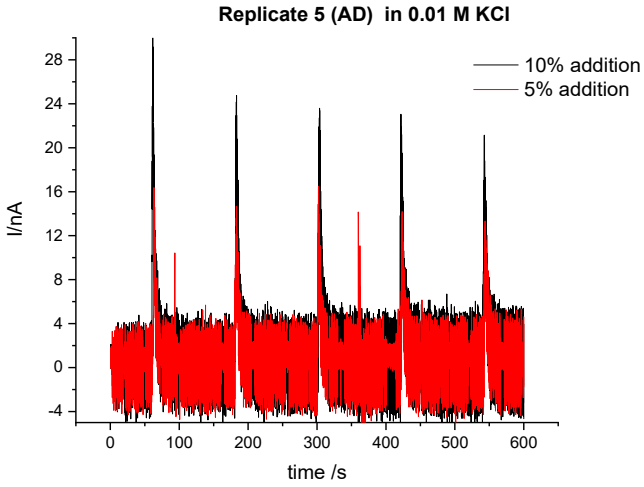
Replicate 5 (AD) in 0.01 M KCl
10% addition
5% addition
I/nA
time /s

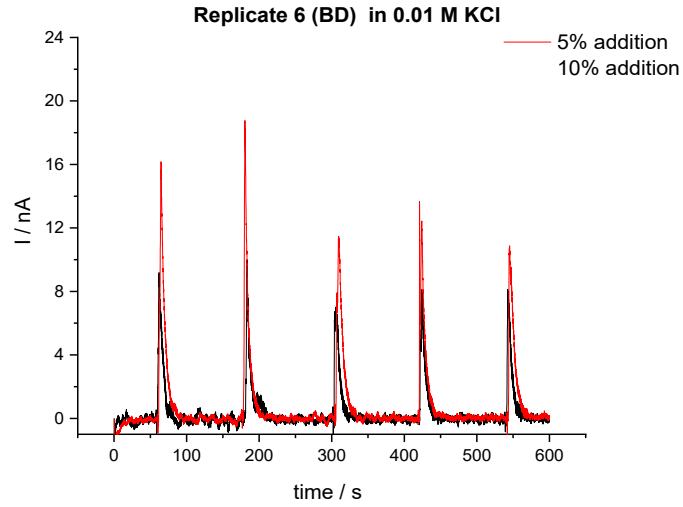
Replicate 6 (BD) in 0.01 M KCl
5% addition
10% addition
I / nA
time / s

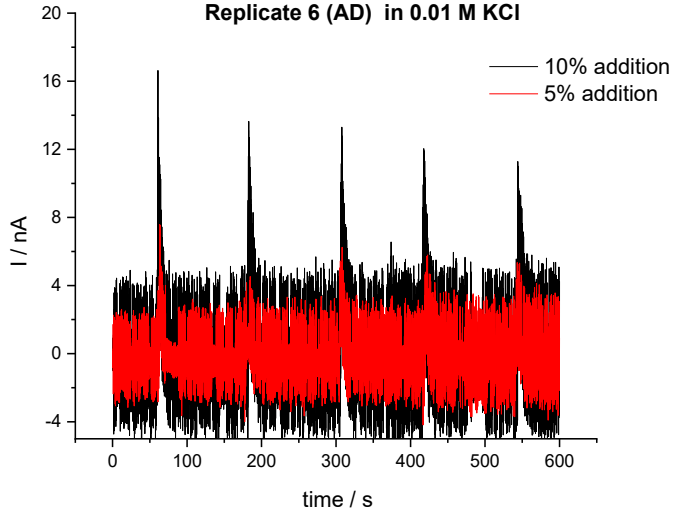
Replicate 6 (AD) in 0.01 M KCl
10% addition
5% addition
I / nA
time / s

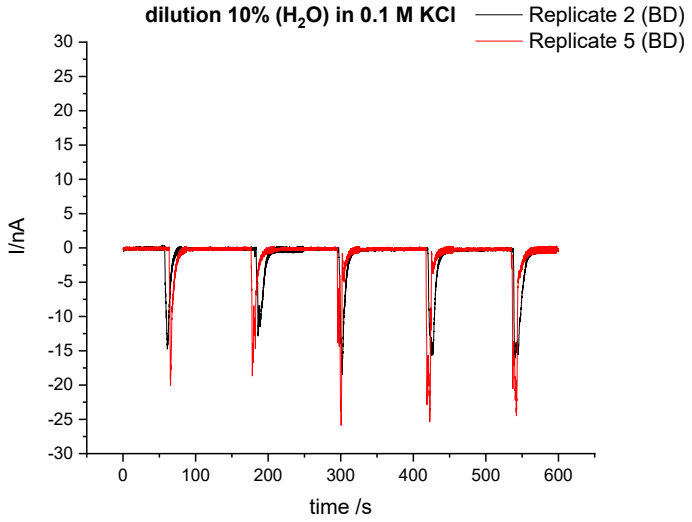
dilution 10% (H2O) in 0.1 M KCl
Replicate 2 (BD)
Replicate 5 (BD)
I/nA
time /s

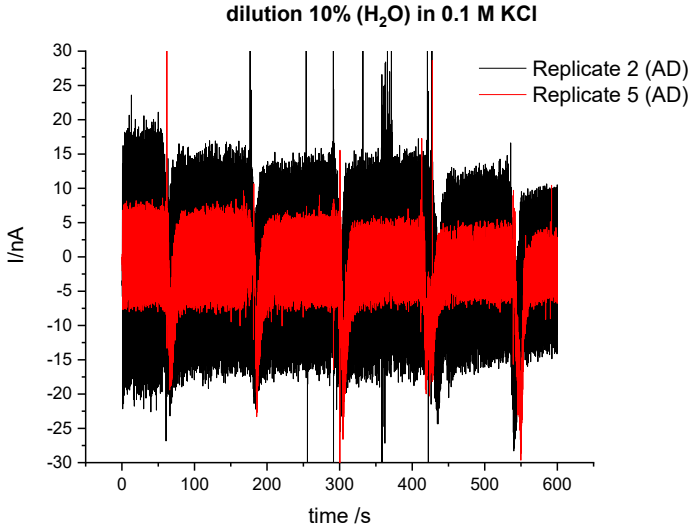
dilution 10% (H2O) in 0.1 M KCl
Replicate 2 (AD)
Replicate 5 (AD)
I/nA
time /s

Appendix H

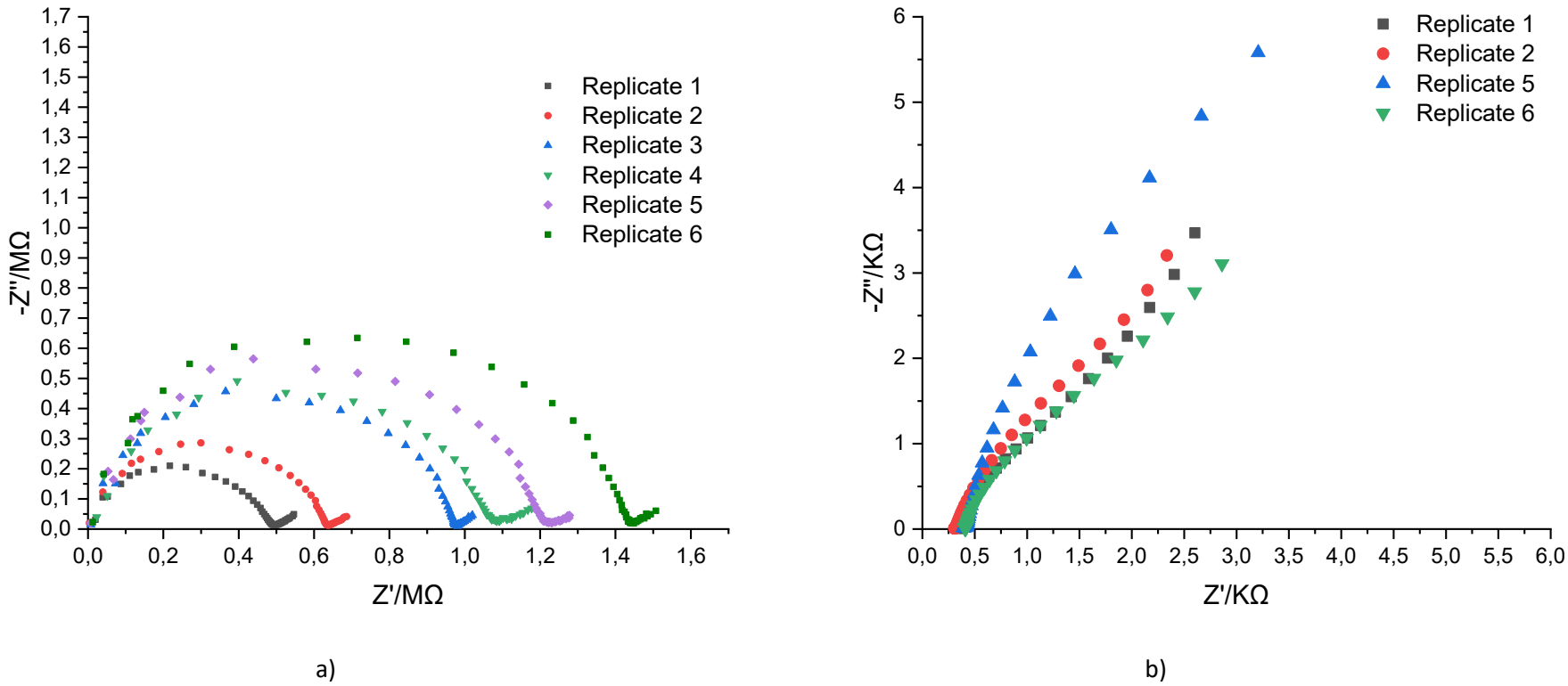

Electrochemical Impedance Spectra recorded for potassium SC-ISEs before (a) and after damaging the ISM (b). DC potential is open circuit potential (0.13V). The frequency range is 100 kHz to 10 mHz. Electrolyte = 0.1M KCl

Appendix I

Chronopotentiometric responses recorded for potassium SC-ISEs in starting solution 0.001 M and 0.01 M KCl during stepwise 10 % addition in concentration before damaging (BD) and after damaging (AD) the ISM with/without 0.1 M KCl as BGE

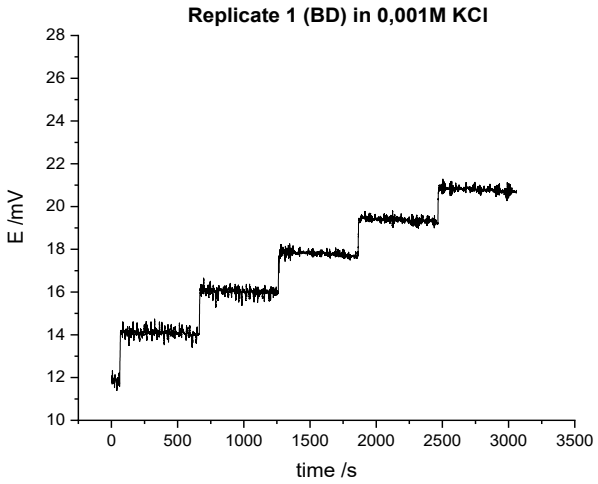

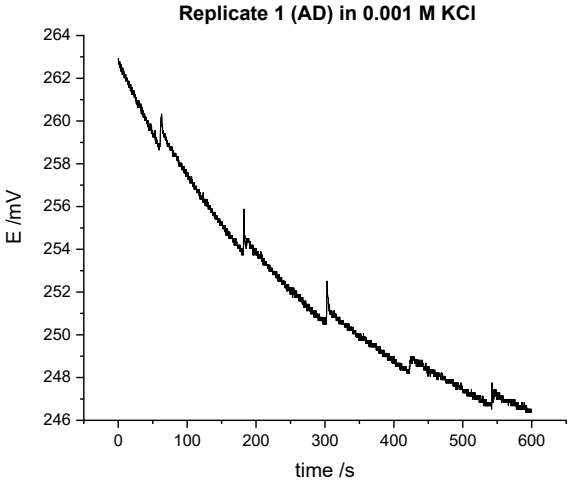

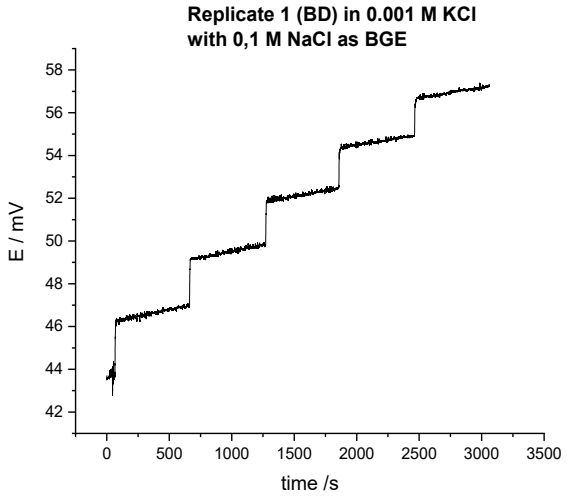

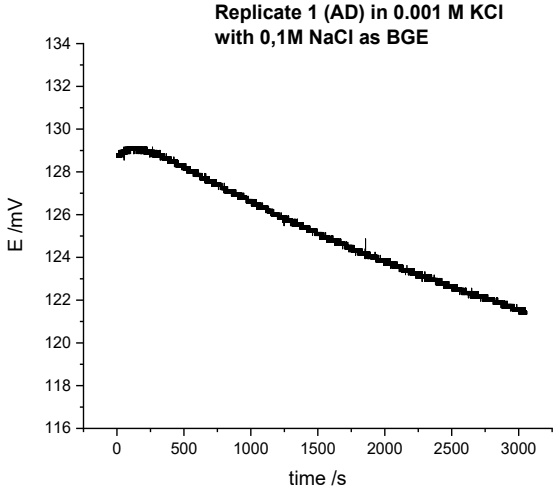

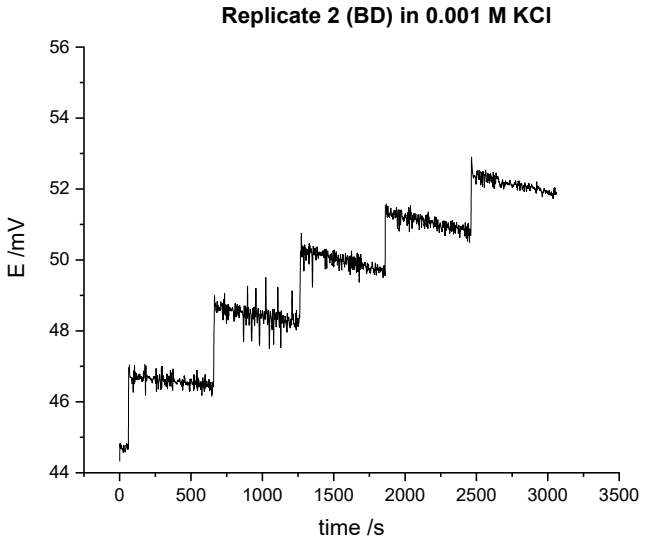
Replicate 2 (BD) in 0.001 M KCl
E /mV
time /s

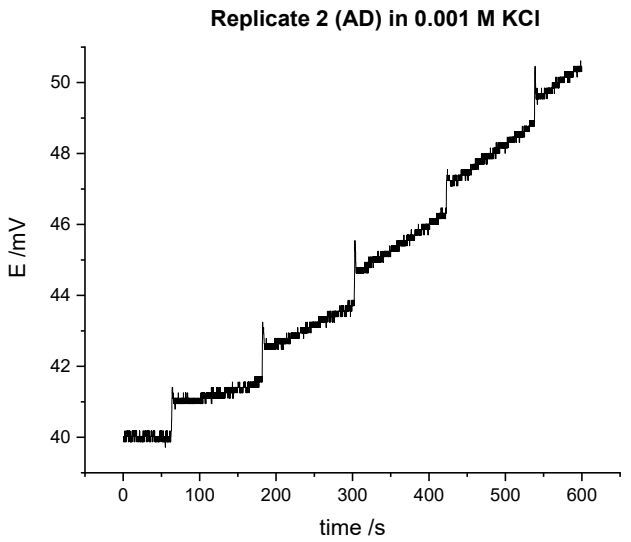
Replicate 2 (AD) in 0.001 M KCl
E /mV
time /s

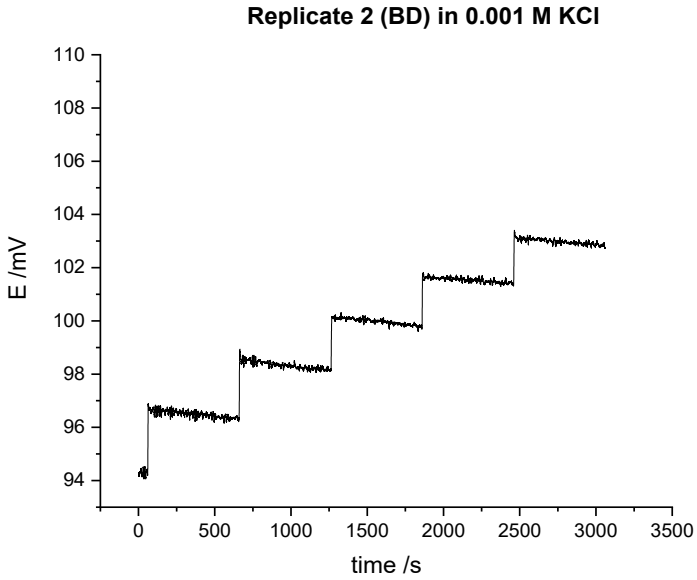
Replicate 2 (BD) in 0.001 M KCl
E /mV
time /s

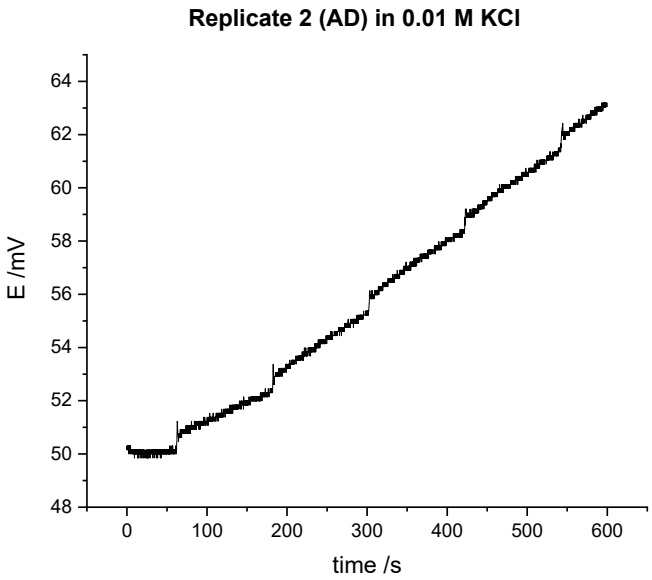
Replicate 2 (AD) in 0.01 M KCl
E /mV
time /s

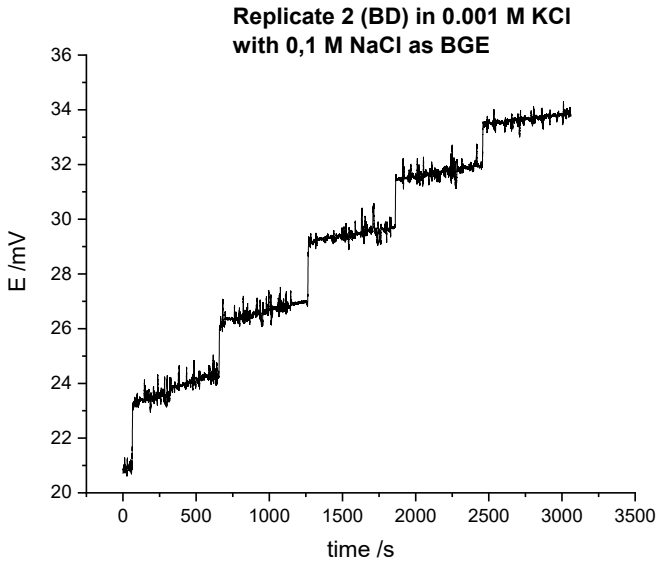
Replicate 2 (BD) in 0.001 M KCl
with 0,1 M NaCl as BGE
E /mV
time /s

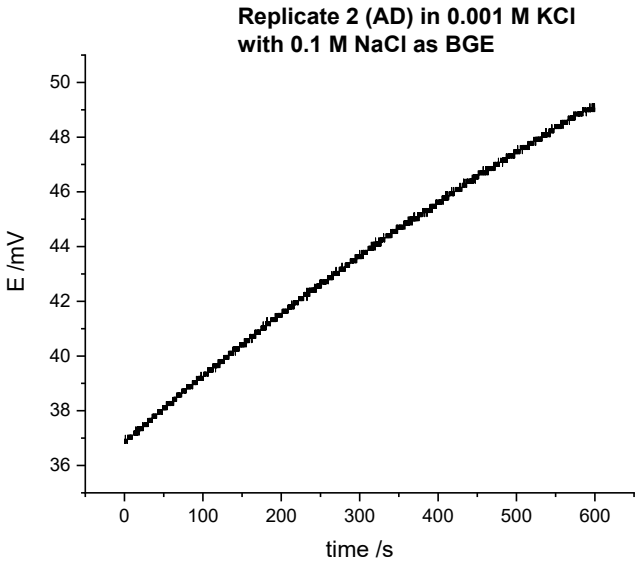
Replicate 2 (AD) in 0.001 M KCl
with 0.1 M NaCl as BGE
E /mV
time /s

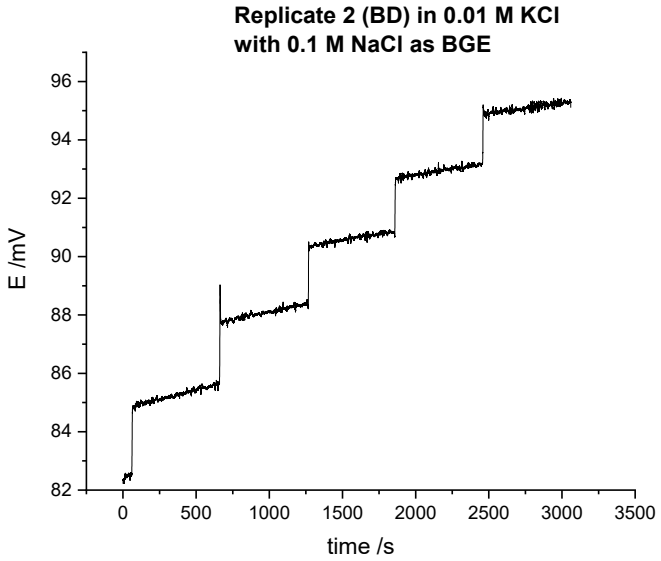
Replicate 2 (BD) in 0.01 M KCl
with 0.1 M NaCl as BGE
E /mV
time /s

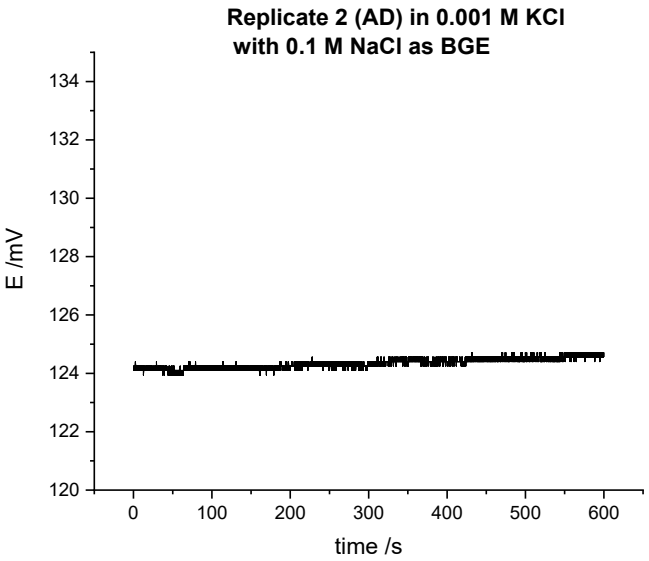
Replicate 2 (AD) in 0.001 M KCl
with 0.1 M NaCl as BGE
E /mV
time /s

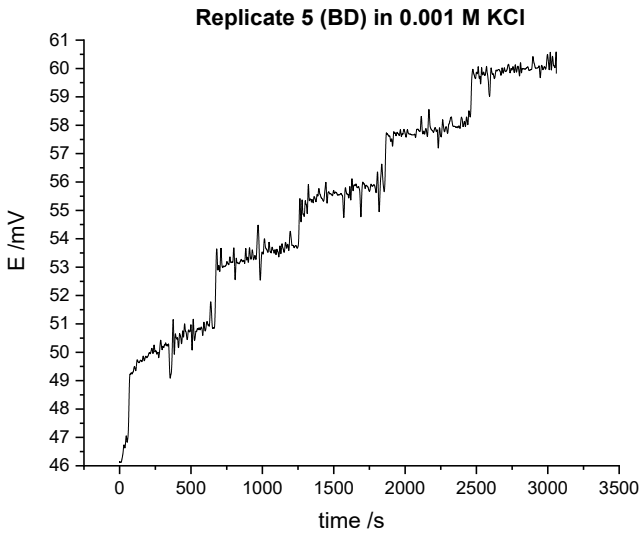
Replicate 5 (BD) in 0.001 M KCl
E /mV
time /s

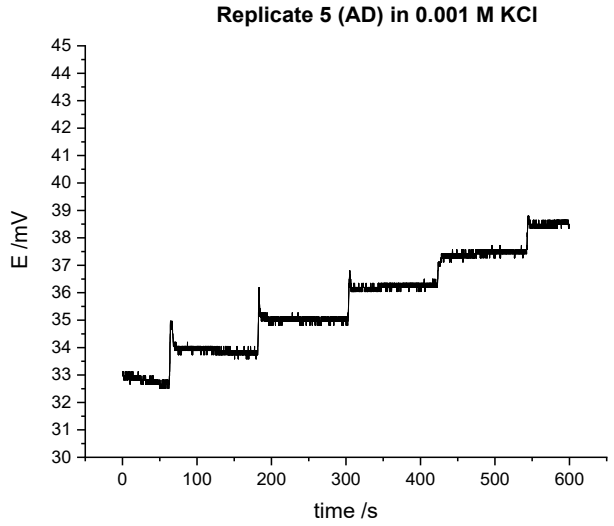
Replicate 5 (AD) in 0.001 M KCl
E /mV
time /s

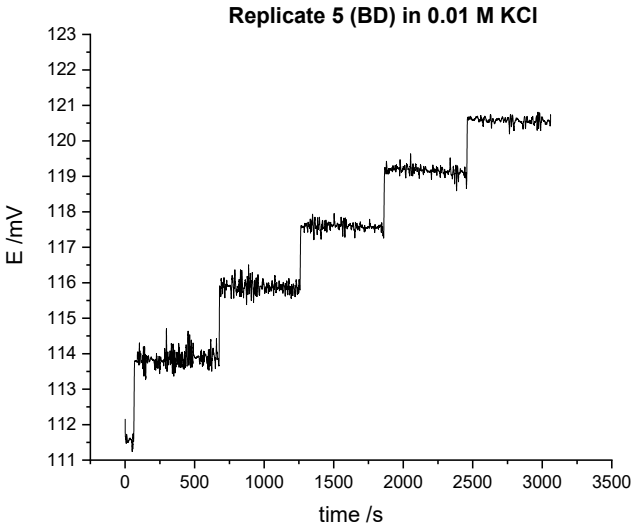
Replicate 5 (BD) in 0.01 M KCl
E /mV
time /s

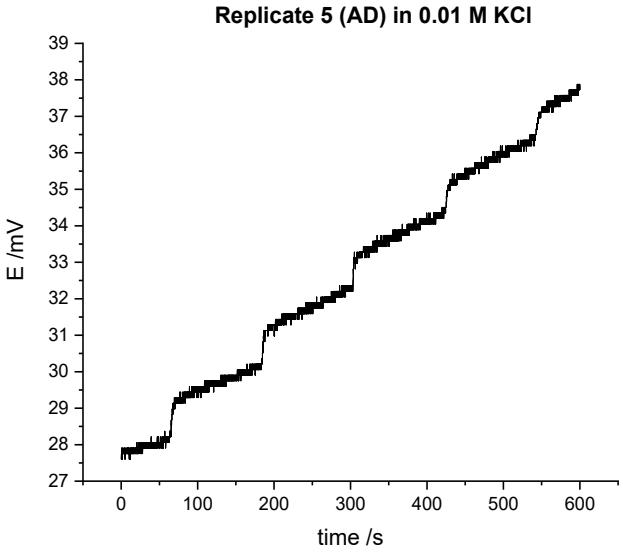
Replicate 5 (AD) in 0.01 M KCl
E /mV
time /s

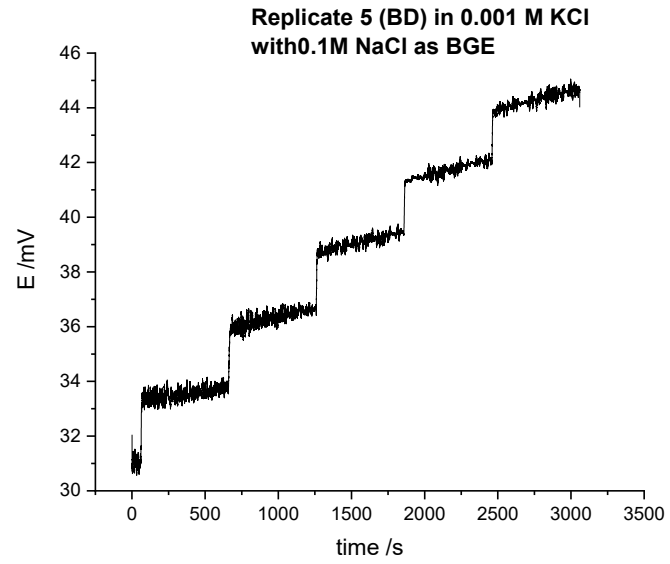
Replicate 5 (BD) in 0.001 M KCl
with0.1M NaCl as BGE
E /mV
time /s

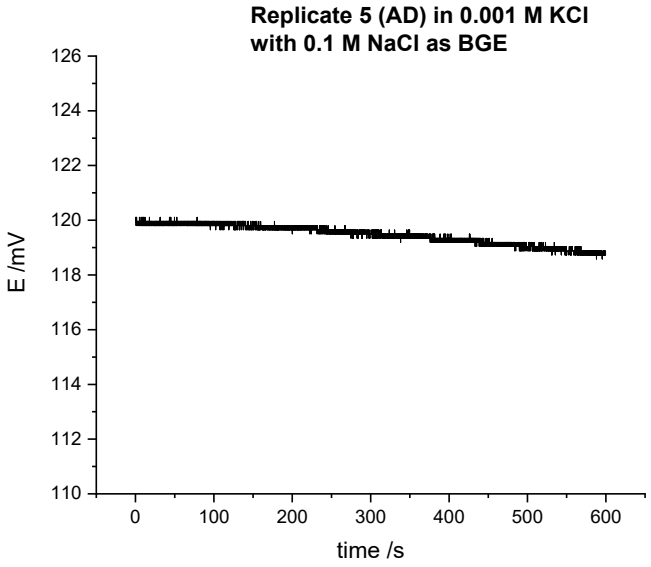
Replicate 5 (AD) in 0.001 M KCl
with 0.1 M NaCl as BGE
E /mV
time /s

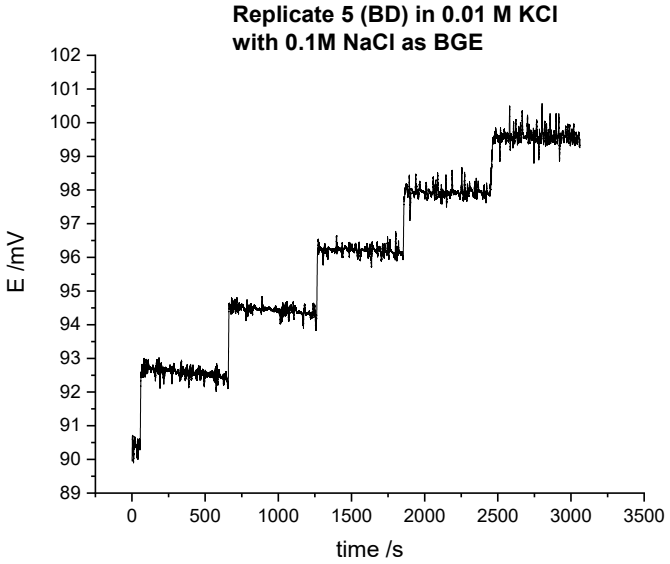
Replicate 5 (BD) in 0.01 M KCl
with 0.1M NaCl as BGE
E /mV
time /s

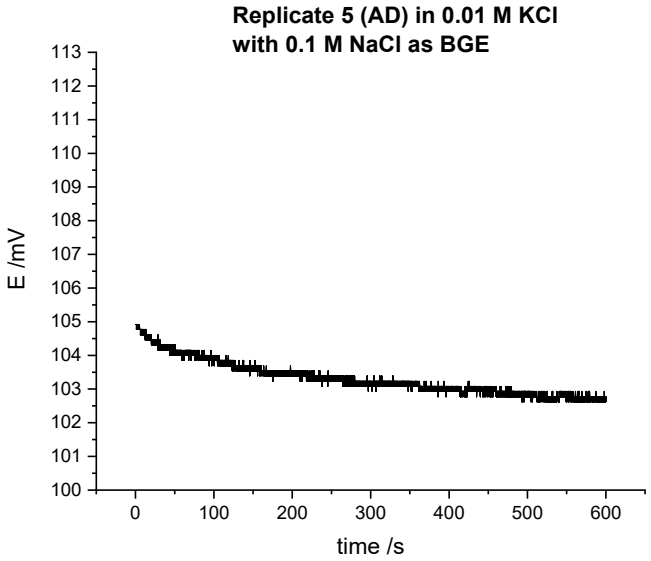
Replicate 5 (AD) in 0.01 M KCl
with 0.1 M NaCl as BGE
E /mV
time /s

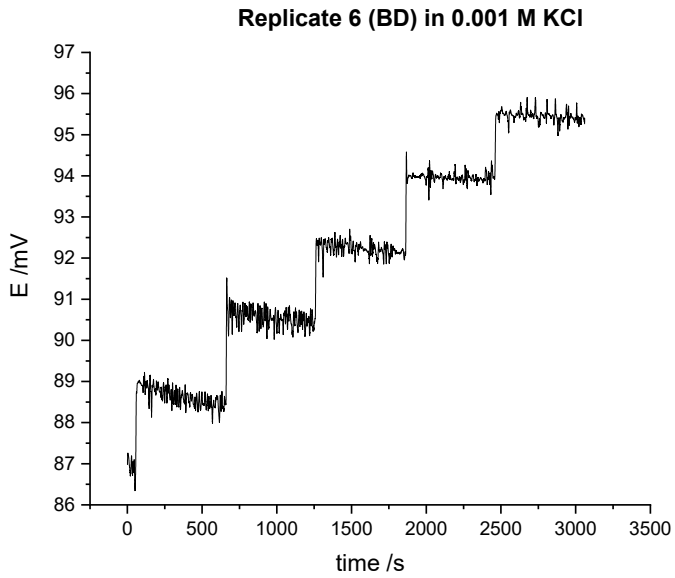
Replicate 6 (BD) in 0.001 M KCl
E /mV
time /s

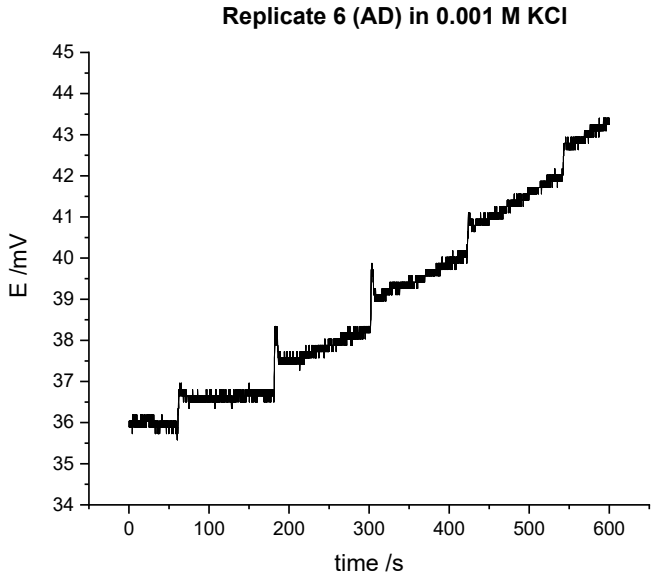
Replicate 6 (AD) in 0.001 M KCl
E /mV
time /s

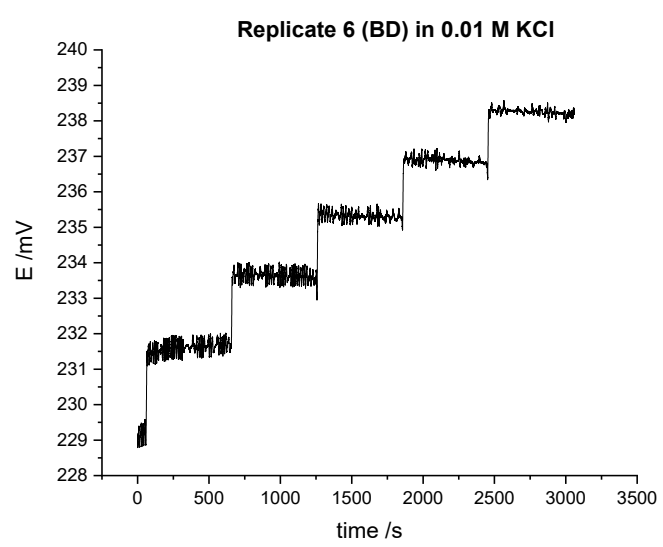
Replicate 6 (BD) in 0.01 M KCl
E /mV
time /s

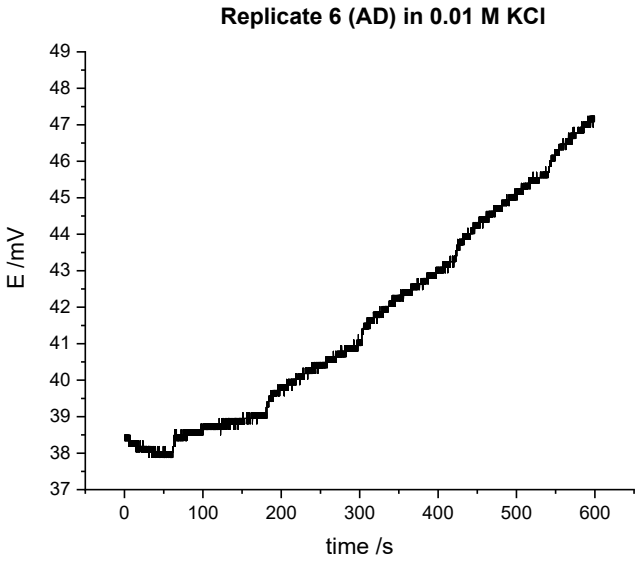
Replicate 6 (AD) in 0.01 M KCl
E /mV
time /s

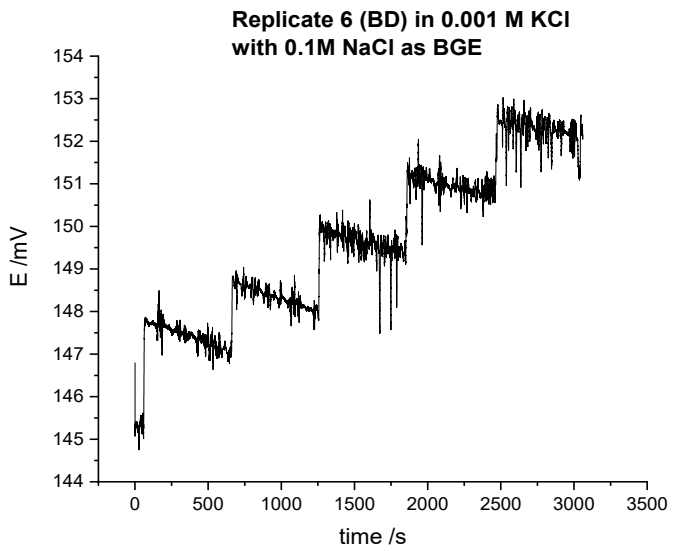
Replicate 6 (BD) in 0.001 M KCl
with 0.1M NaCl as BGE
E /mV
time /s

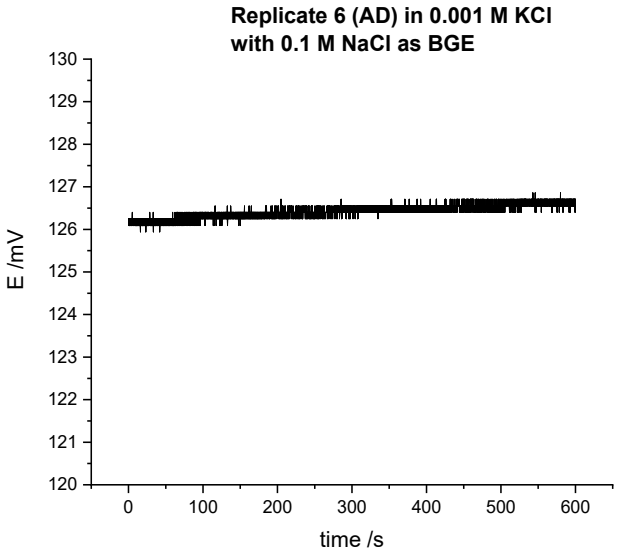
Replicate 6 (AD) in 0.001 M KCl
with 0.1 M NaCl as BGE
E /mV
time /s

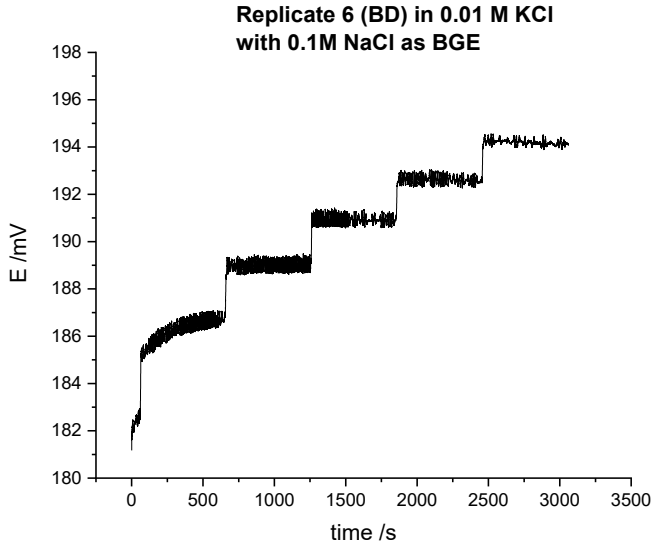
Replicate 6 (BD) in 0.01 M KCl
with 0.1M NaCl as BGE
E /mV
time /s

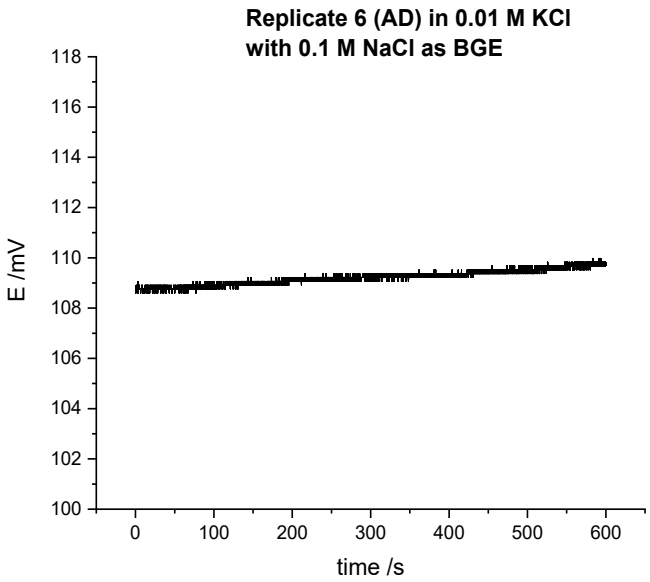
Replicate 6 (AD) in 0.01 M KCl
with 0.1 M NaCl as BGE
E /mV
time /s

Appendix J

Chronocoulometric responses recorded for potassium SC-ISEs in starting solution 0.001 M and 0.01 M KCl during stepwise 10 % addition in concentration before damaging (BD) and after damaging (AD) the ISM with/without 0.1 M KCl as BGE

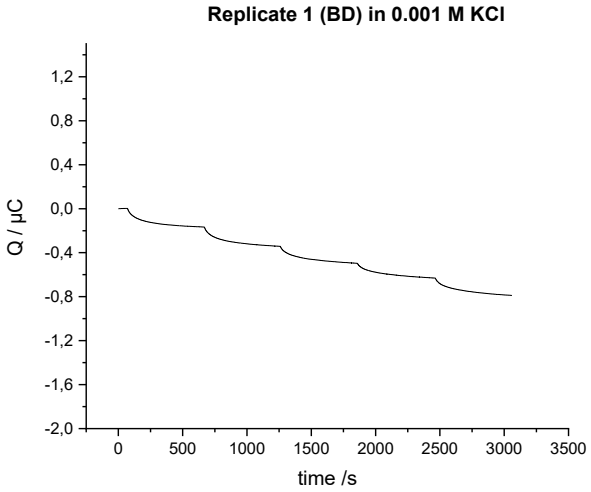

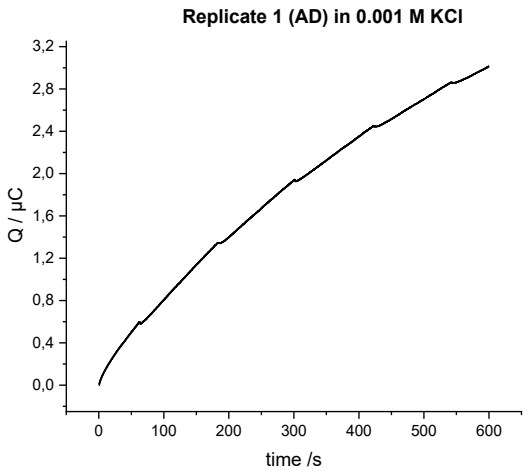

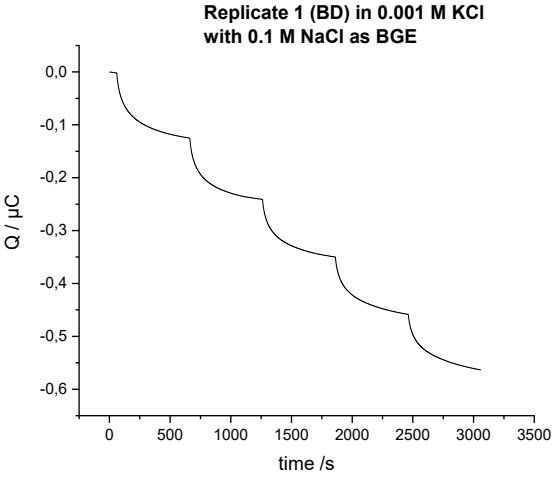

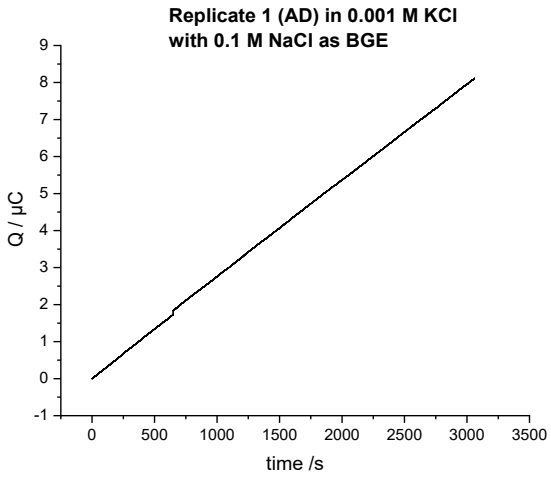

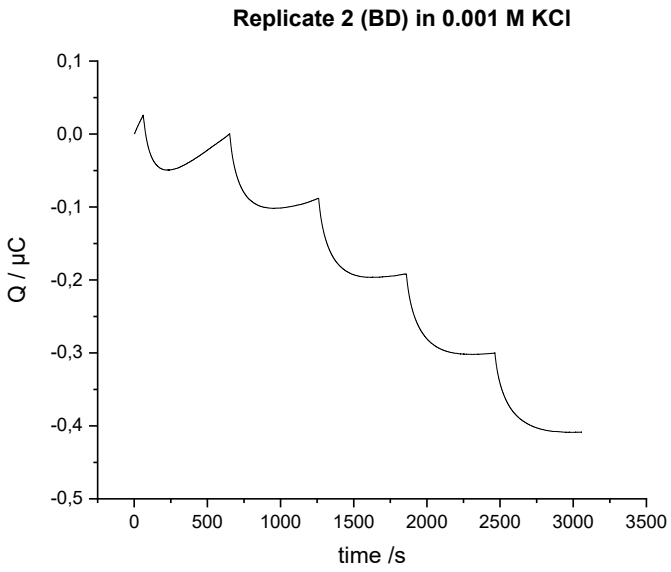
Replicate 2 (BD) in 0.001 M KCl
Q / µC
time /s
0,1
0,0
-0,1
-0,2
-0,3
-0,4
-0,5
0
500
1000
1500
2000
2500
3000
3500

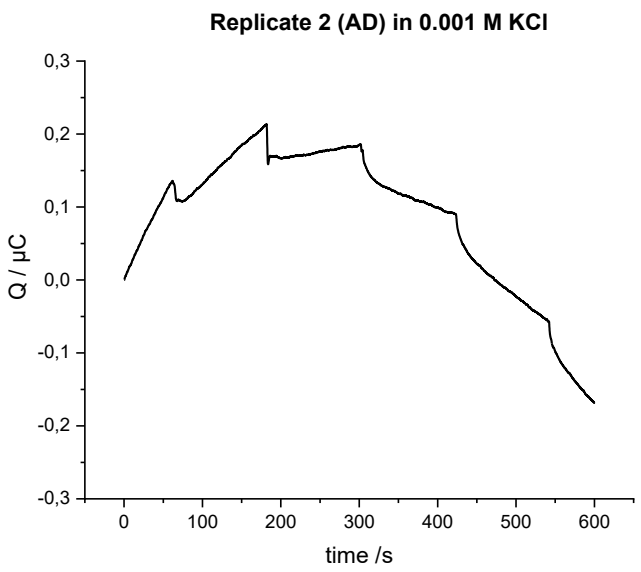
Replicate 2 (AD) in 0.001 M KCl
Q / µC
time /s
0,3
0,2
0,1
0,0
-0,1
-0,2
-0,3
0
100
200
300
400
500
600

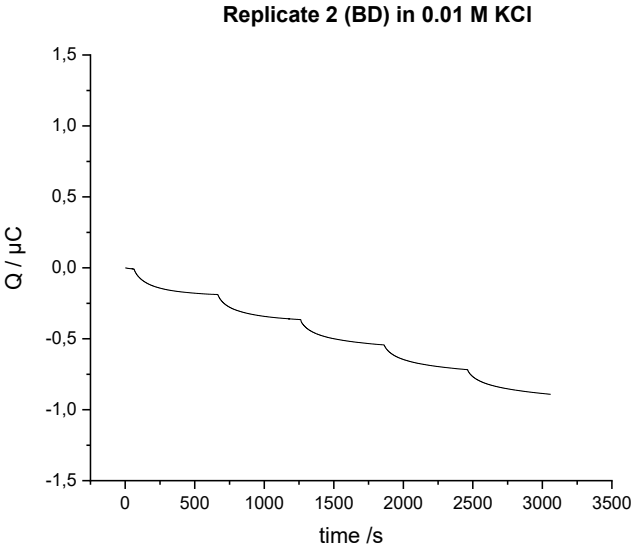
Replicate 2 (BD) in 0.01 M KCl
Q / µC
time /s
1,5
1,0
0,5
0,0
-0,5
-1,0
-1,5
0
500
1000
1500
2000
2500
3000
3500

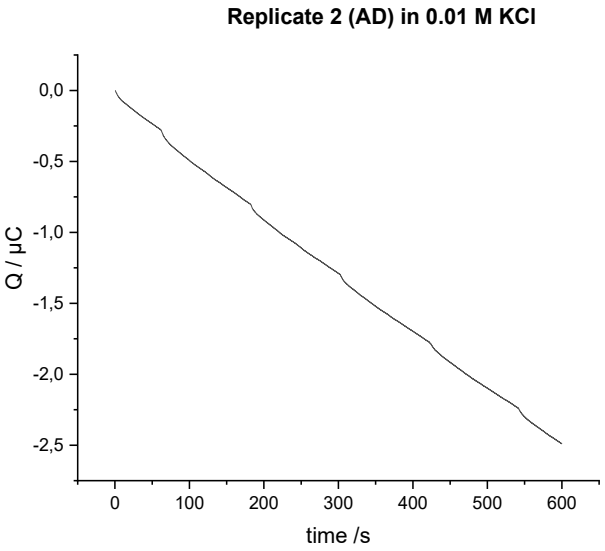
Replicate 2 (AD) in 0.01 M KCl
Q / µC
time /s
0,0
-0,5
-1,0
-1,5
-2,0
-2,5
0
100
200
300
400
500
600

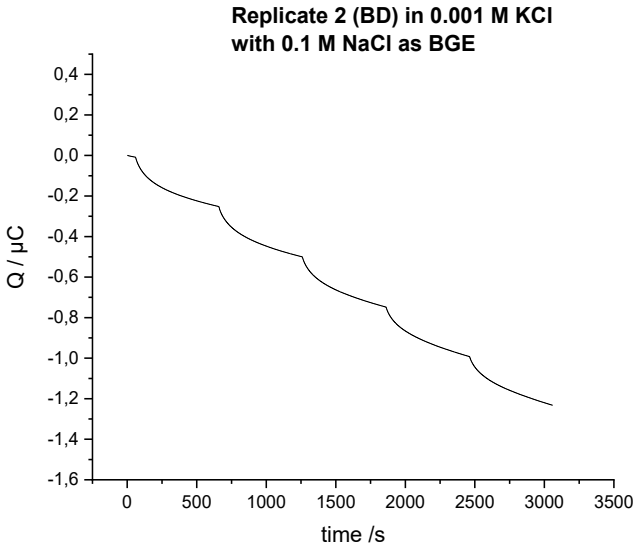
Replicate 2 (BD) in 0.001 M KCl
with 0.1 M NaCl as BGE
Q / µC
time /s

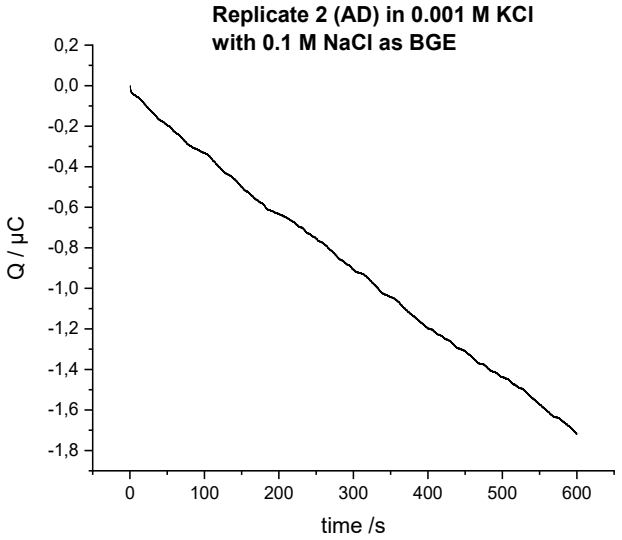
Replicate 2 (AD) in 0.001 M KCl
with 0.1 M NaCl as BGE
Q / µC
time /s

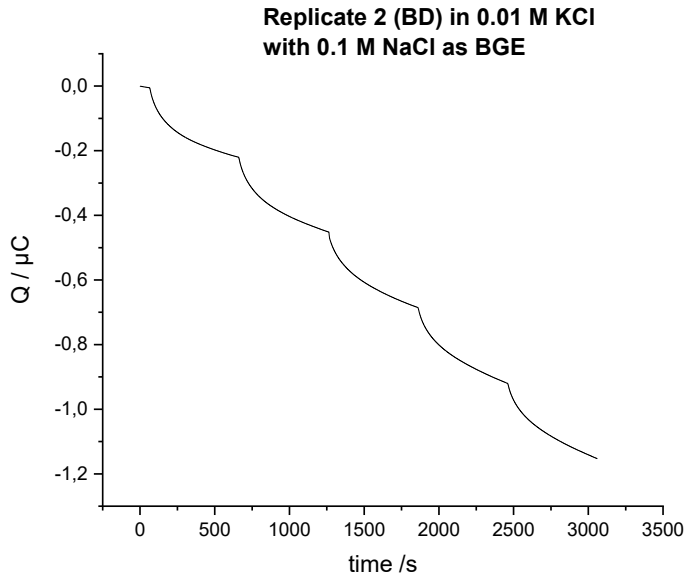
Replicate 2 (BD) in 0.01 M KCl
with 0.1 M NaCl as BGE
Q / µC
time /s

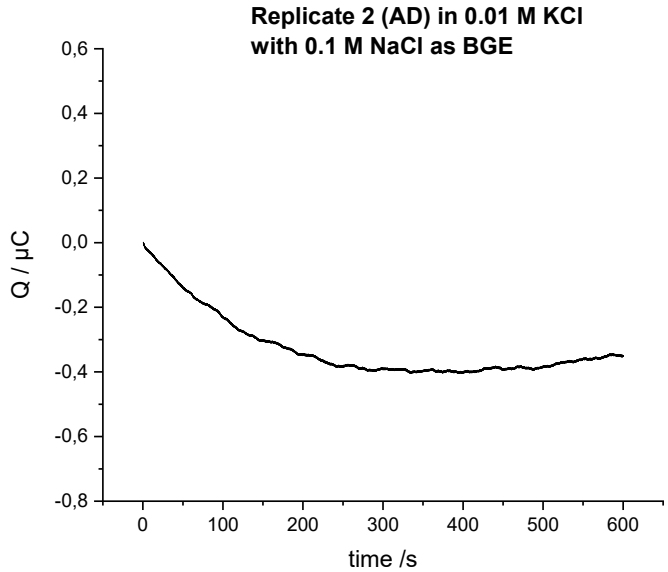
Replicate 2 (AD) in 0.01 M KCl
with 0.1 M NaCl as BGE
Q / µC
time /s

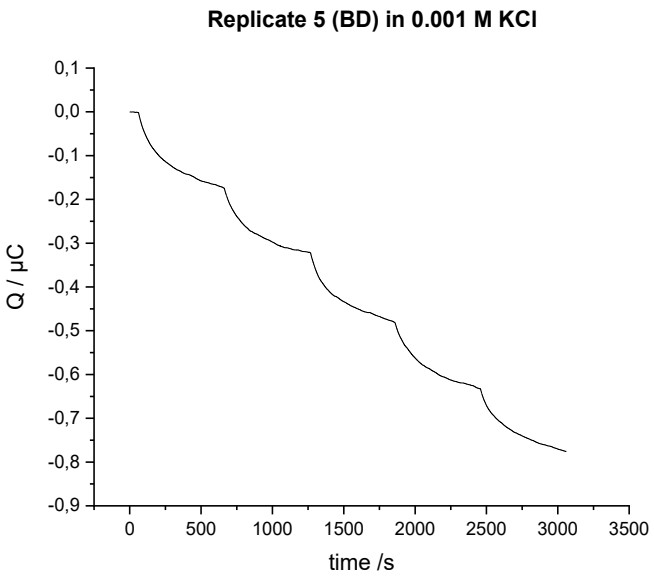
Replicate 5 (BD) in 0.001 M KCl
Q / µC
time /s

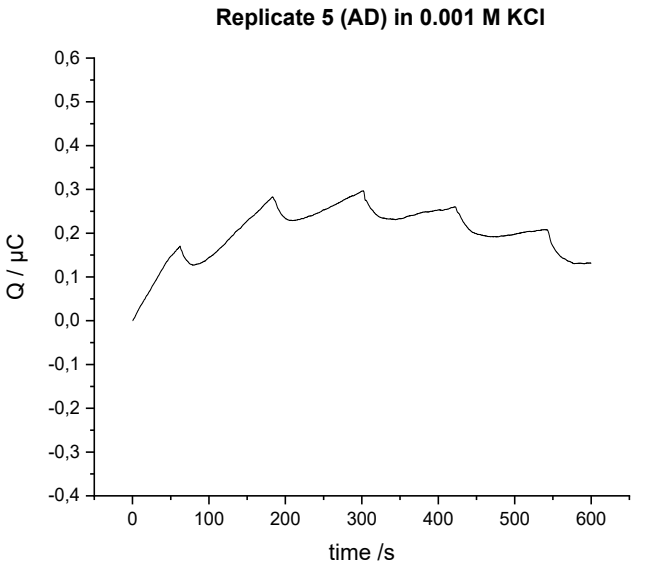
Replicate 5 (AD) in 0.001 M KCl
Q / µC
time /s

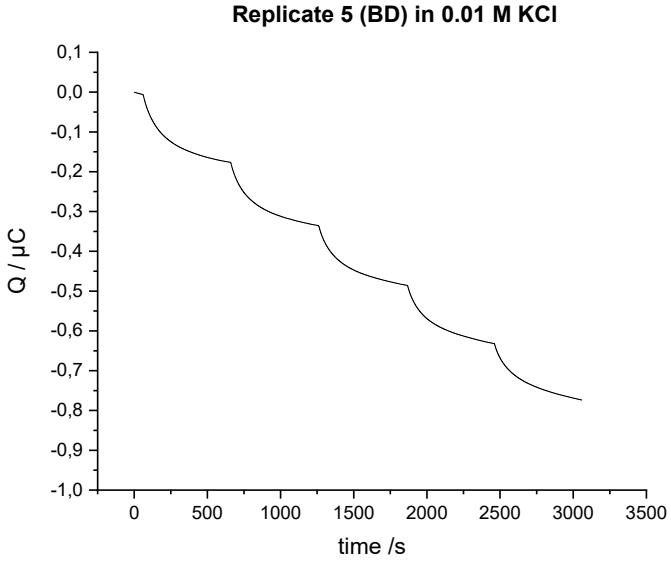
Replicate 5 (BD) in 0.01 M KCl
Q / µC
time /s

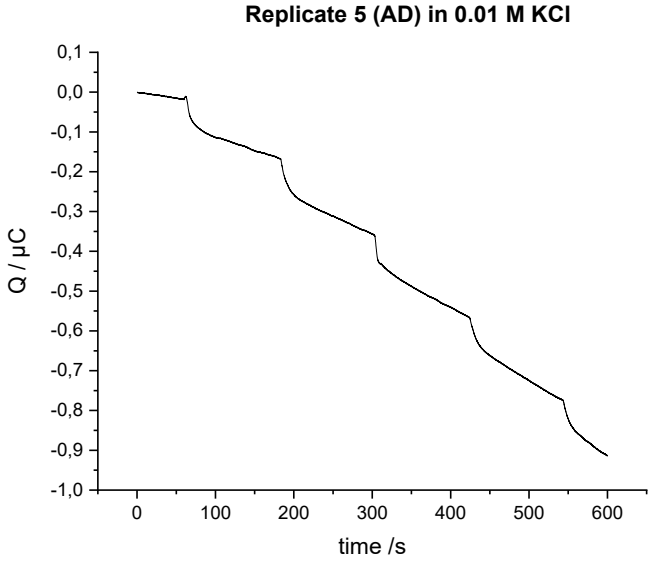
Replicate 5 (AD) in 0.01 M KCl
Q / µC
time /s

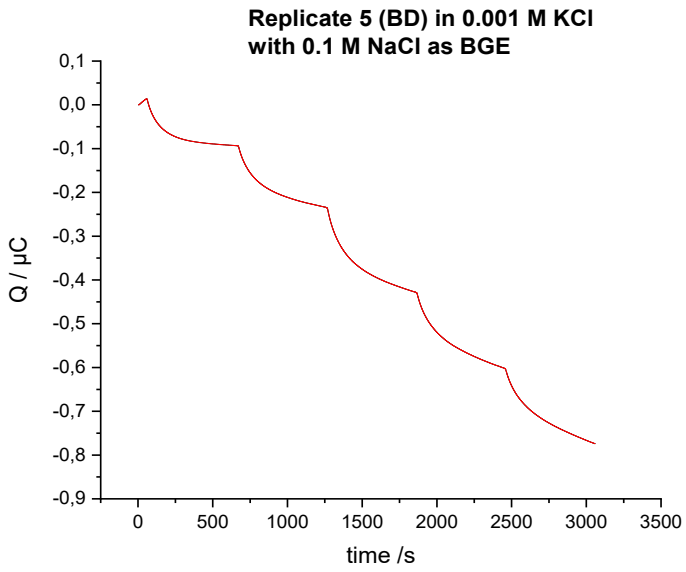
Replicate 5 (BD) in 0.001 M KCl
with 0.1 M NaCl as BGE
Q / µC
time /s

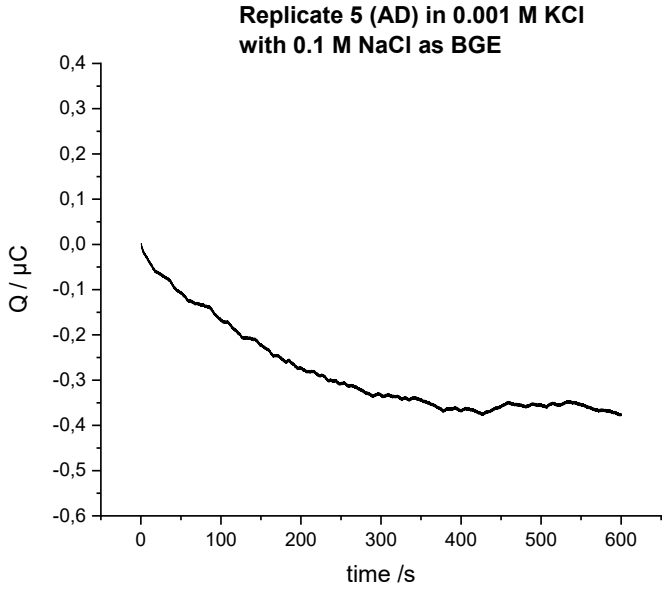
Replicate 5 (AD) in 0.001 M KCl
with 0.1 M NaCl as BGE
Q / µC
time /s

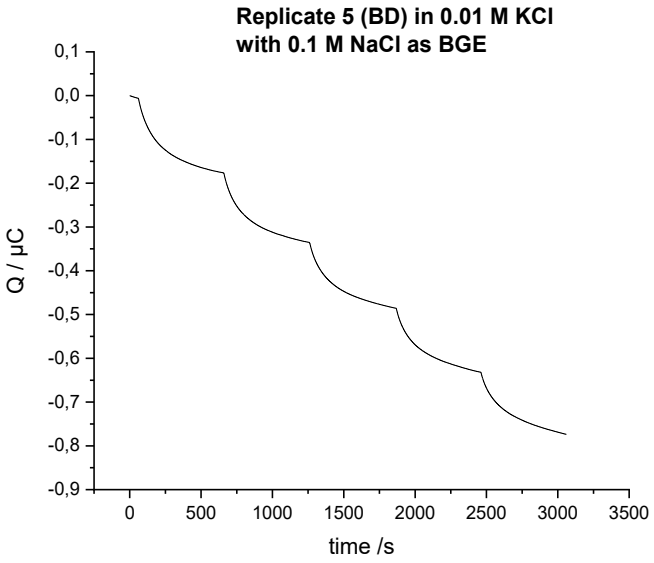
Replicate 5 (BD) in 0.01 M KCl
with 0.1 M NaCl as BGE
Q / µC
time /s

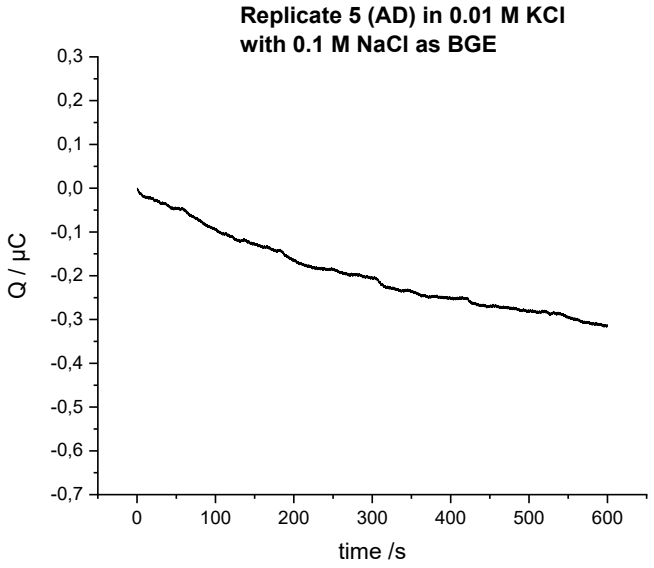
Replicate 5 (AD) in 0.01 M KCl
with 0.1 M NaCl as BGE
Q / µC
time /s

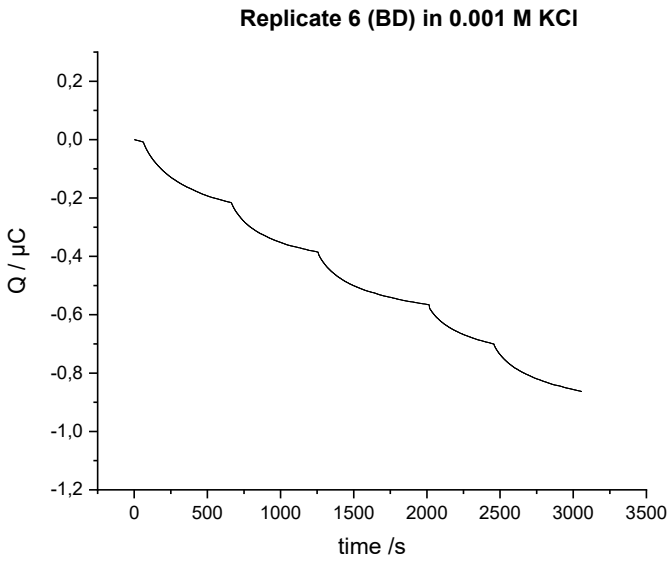
Replicate 6 (BD) in 0.001 M KCl
Q / µC
time /s
0,2
0,0
-0,2
-0,4
-0,6
-0,8
-1,0
-1,2
0
500
1000
1500
2000
2500
3000
3500

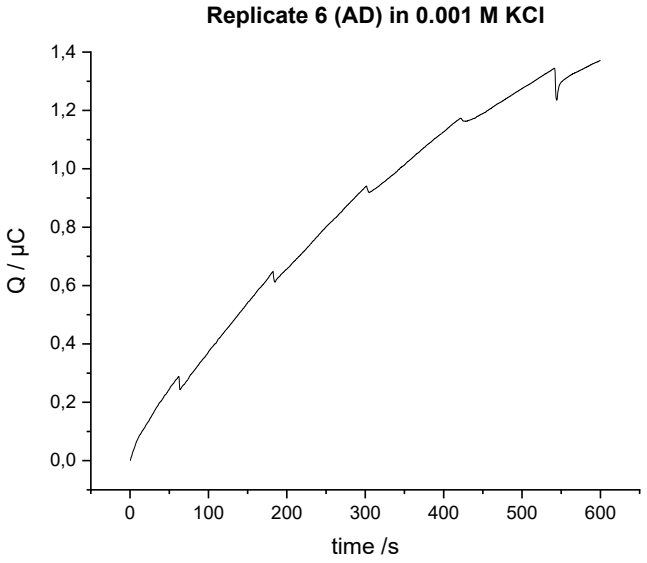
Replicate 6 (AD) in 0.001 M KCl
Q / µC
time /s
1,4
1,2
1,0
0,8
0,6
0,4
0,2
0,0
0
100
200
300
400
500
600

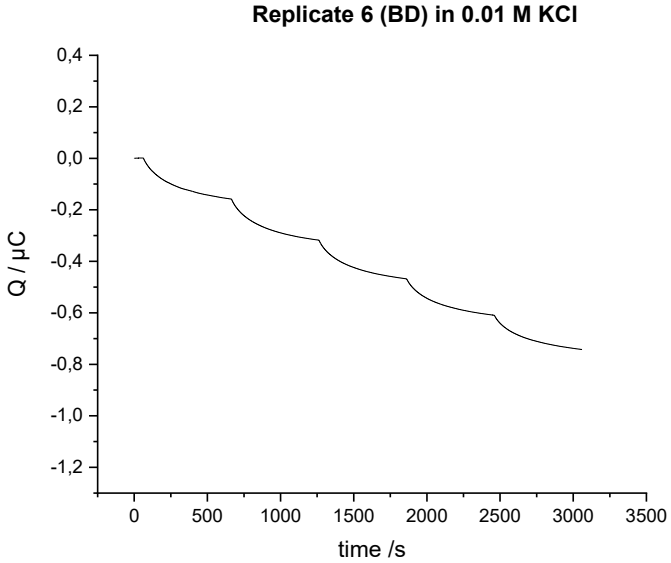
Replicate 6 (BD) in 0.01 M KCl
Q / µC
time /s
0,4
0,2
0,0
-0,2
-0,4
-0,6
-0,8
-1,0
-1,2
0
500
1000
1500
2000
2500
3000
3500

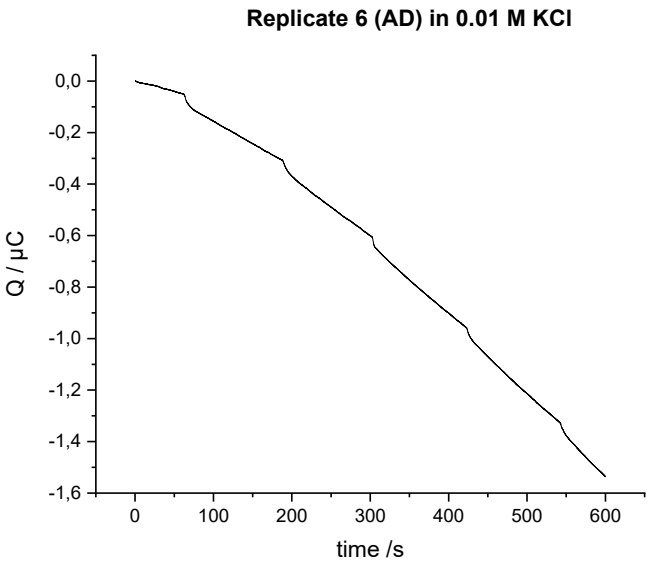
Replicate 6 (AD) in 0.01 M KCl
Q / µC
time /s
0,0
-0,2
-0,4
-0,6
-0,8
-1,0
-1,2
-1,4
-1,6
0
100
200
300
400
500
600

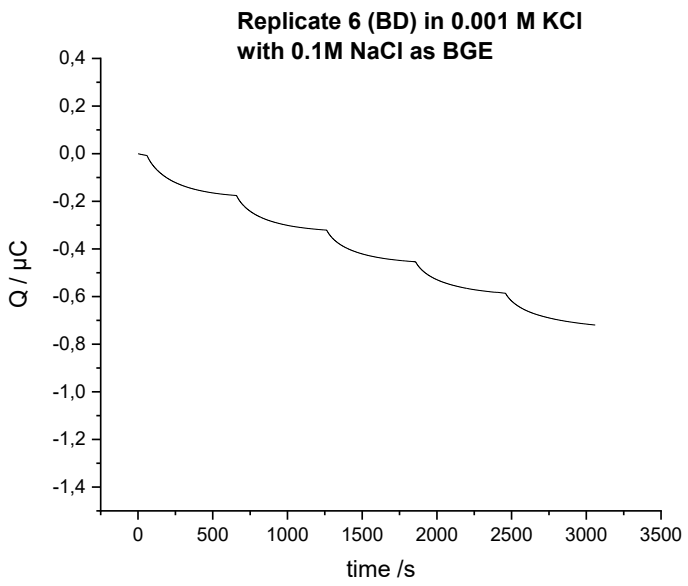
Replicate 6 (BD) in 0.001 M KCl
with 0.1M NaCl as BGE
Q / µC
time /s

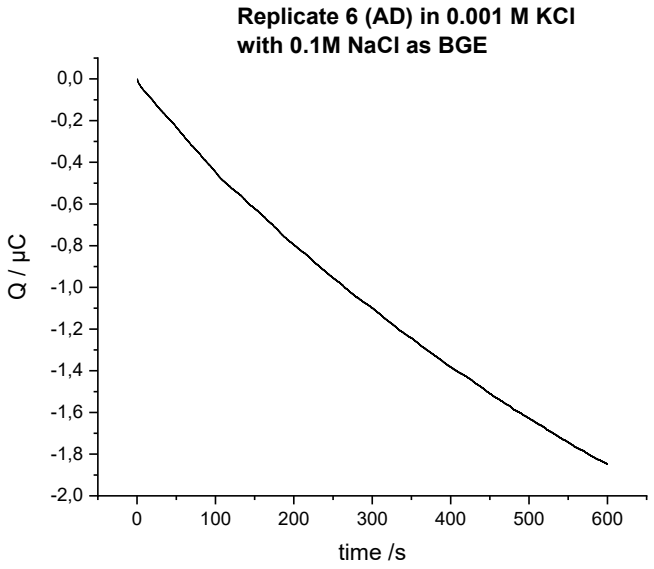
Replicate 6 (AD) in 0.001 M KCl
with 0.1M NaCl as BGE
Q / µC
time /s

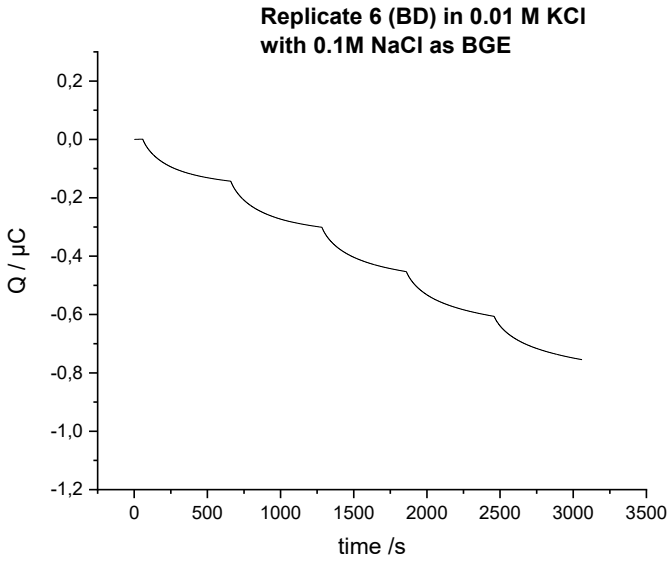
Replicate 6 (BD) in 0.01 M KCl
with 0.1M NaCl as BGE
Q / µC
time /s

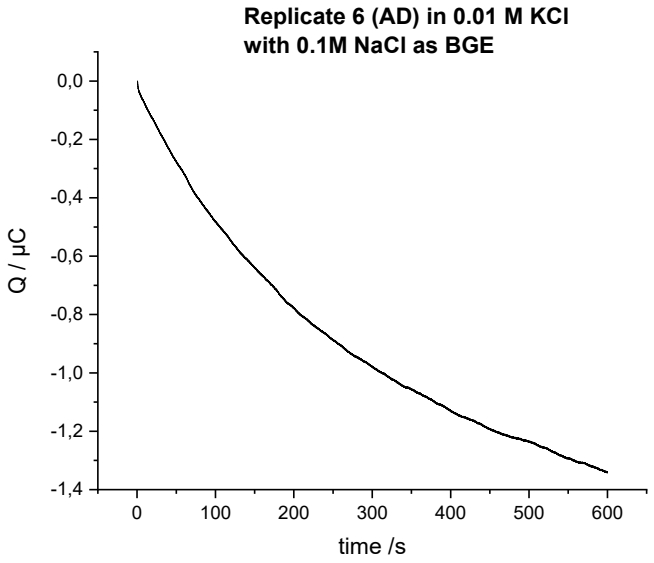
Replicate 6 (AD) in 0.01 M KCl
with 0.1M NaCl as BGE
Q / µC
time /s

Appendix K

Chronoamperometric responses recorded for potassium SC-ISEs in starting solution 0.001 M and 0.01 M KCl during stepwise 10 % addition in concentration before damaging (BD) and after damaging (AD) the ISM with/without 0.1 M KCl as BGE

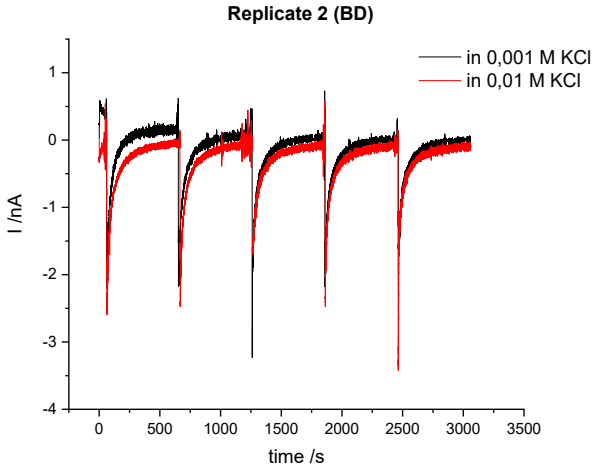

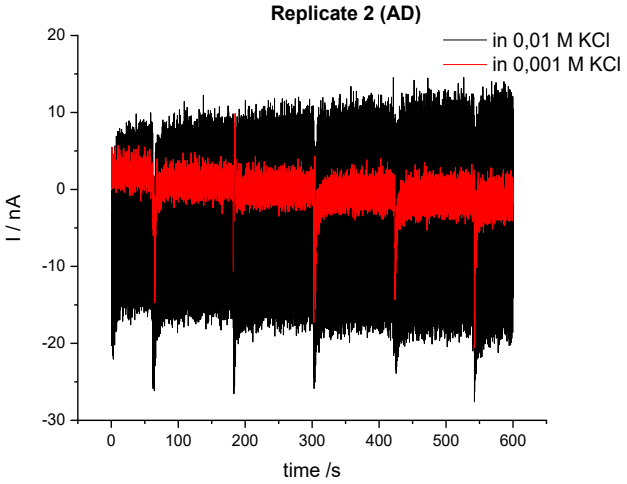

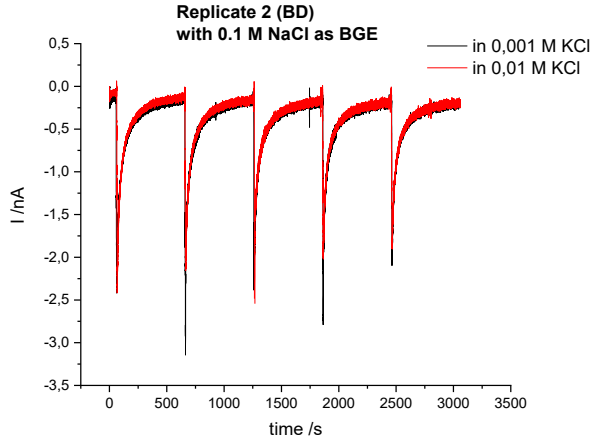

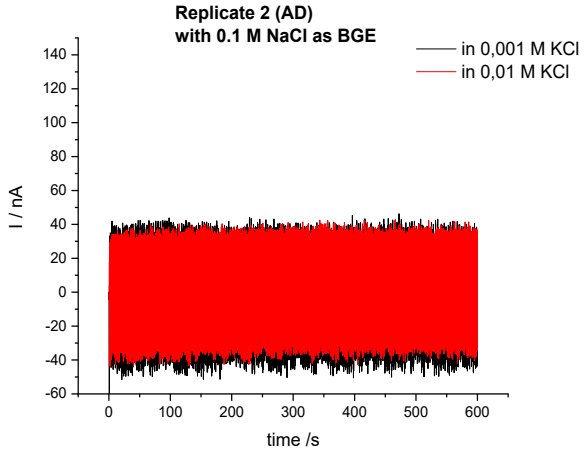

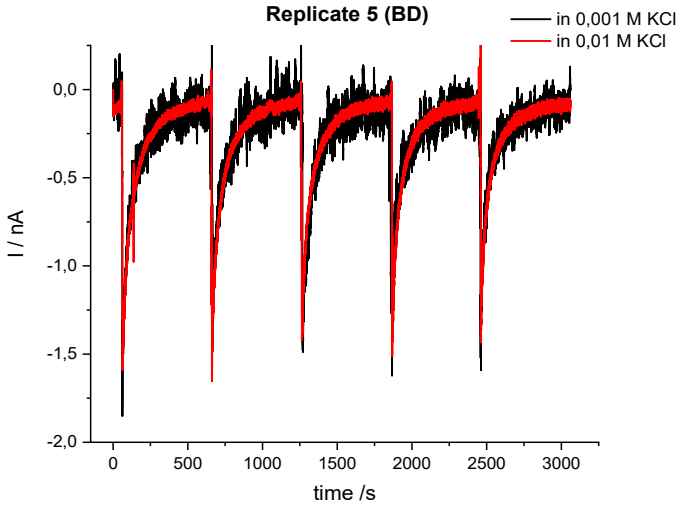
Replicate 5 (BD)
in 0,001 M KCl
in 0,01 M KCl
I / nA
time /s

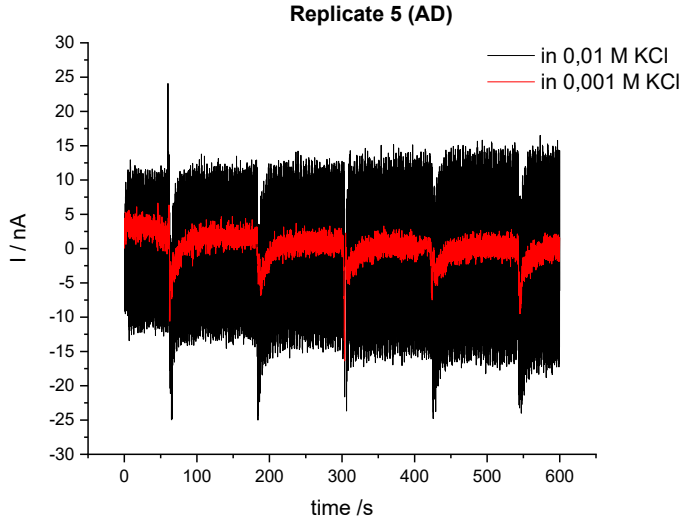
Replicate 5 (AD)
in 0,01 M KCl
in 0,001 M KCl
I / nA
time /s

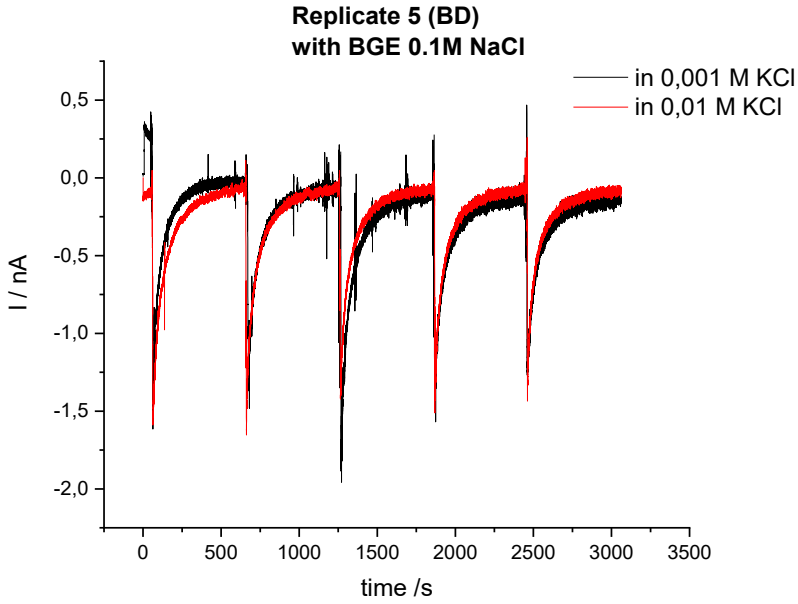
Replicate 5 (BD)
with BGE 0.1M NaCl
in 0,001 M KCl
in 0,01 M KCl
I / nA
time /s

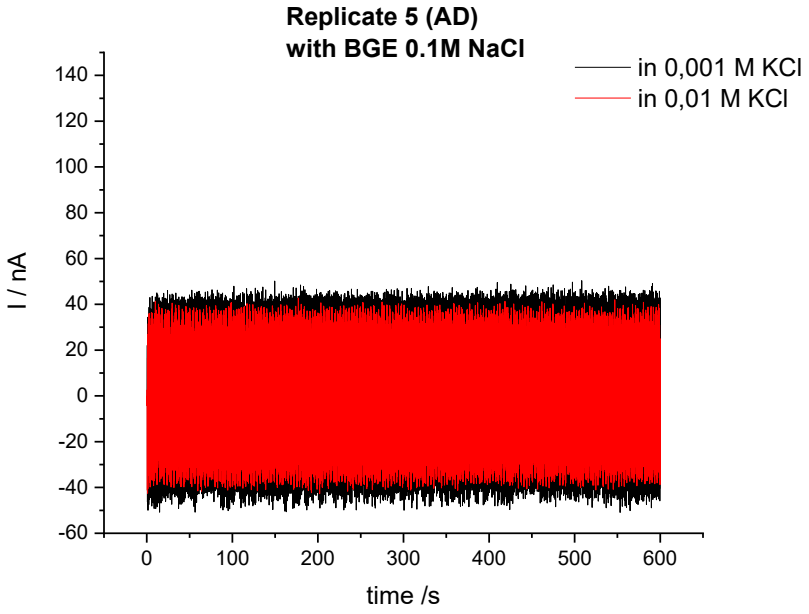
Replicate 5 (AD)
with BGE 0.1M NaCl
in 0,001 M KCl
in 0,01 M KCl
I / nA
time /s

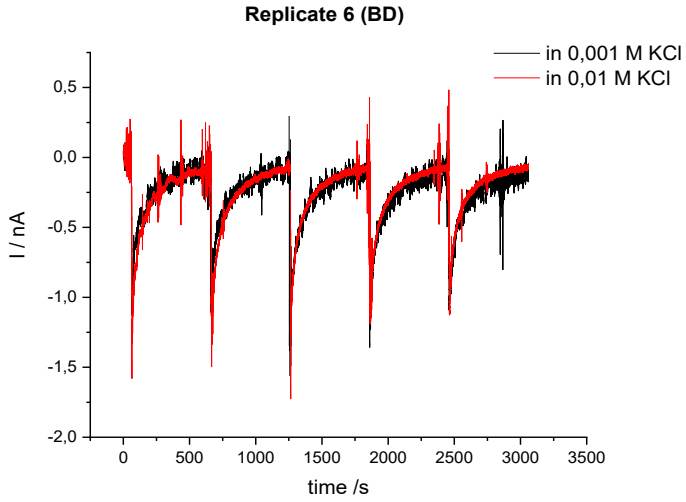
Replicate 6 (BD)
in 0,001 M KCl
in 0,01 M KCl
I / nA
time /s

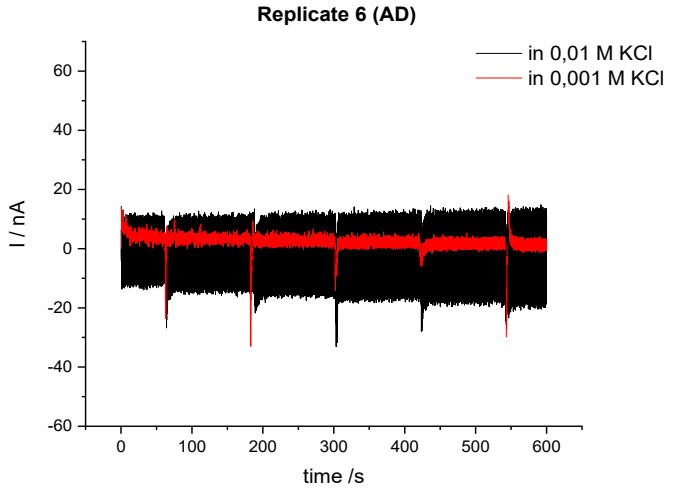
Replicate 6 (AD)
in 0,01 M KCl
in 0,001 M KCl
I / nA
time /s

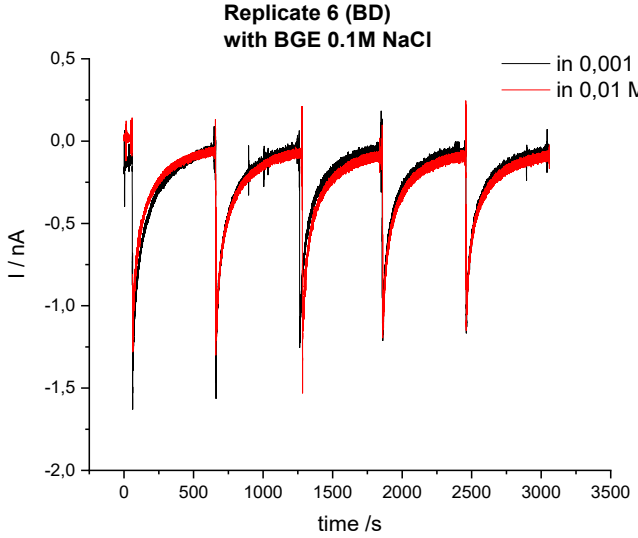
Replicate 6 (BD)
with BGE 0.1M NaCl
in 0,001 M KCl
in 0,01 M KCl
I / nA
time /s

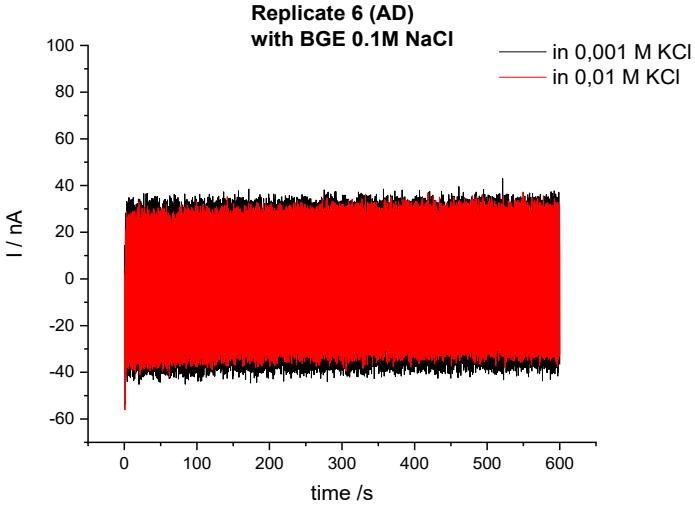
Replicate 6 (AD)
with BGE 0.1M NaCl
in 0,001 M KCl
in 0,01 M KCl
I / nA
time /s